DISS. ETH NO. 27756

MINIATURIZED IMPEDANCE-BASED PLATFORMS FOR PARALLELIZED AND REAL-TIME ASSESSMENT OF ANTISCHISTOSOMAL DRUG POTENCY

A thesis submitted to attain the degree of

DOCTOR OF SCIENCES of ETH ZURICH

(Dr. sc. ETH Zurich)

presented by

PAOLO SHAYAN RAVAYNIA

M.Sc. Biomedical Engineering, Politecnico di Milano

born on 07.03.1992

citizen of

Italy

accepted on the recommendation of

Prof. Dr. Andreas Hierlemann

Prof. Dr. Carlotta Guiducci

Dr. Mario Matteo Modena

2021

“The scientist is not a person who gives the right answers,
he is one who asks the right questions”
Claude Levi-Strauss

CONTENTS

ABSTRACT

This thesis presents the design, characterization and application of miniaturized impedance-based platforms for the long-term culture and continuous analysis of the larval stage of *Schistosoma mansoni,* a human parasitic, multicellular organism. Schistosomiasis is a neglected tropical disease caused by exposure to *Schistosoma* parasites, which affect hundreds of millions of people worldwide. For over 40 years, one drug, praziquantel, has been used for mass administration campaigns, and instances of decreasing efficacy have been recently reported. The standard method for antischistosomal drug discovery relies on manual visual evaluation of drug effects on living parasites *in vitro*, which is a slow, laborious and subjective procedure. The motivation of this work was to develop novel, reliable and automated technologies to speed up antischistosomal screening processes and to contribute filling the empty drug pipeline.

Microfabrication techniques provide a useful toolbox to build optimized *in vitro* culturing and testing environments. The combination of micro-structured chips and micro-fabricated electrode units enables to integrate electrical impedance measurements in the platforms, which can be used to perform a label-free and non-invasive analysis of target samples for drug screening applications.

In this thesis, two automated impedance-based platforms for the viability assessments of *S. mansoni* larvae during drug exposure are described:

1. A polydimethylsiloxane-based microwell chip with integrated co-planar platinum electrodes was developed for continuous impedance-based recordings of parasite motility, as a proxy of their viability. *S. mansoni* larvae were cultured on-chip and exposed to four established antischistosomal drugs for 48 hours. Real-time monitoring of dose-response relationships enabled to show the high and fast *in vitro* activity of the tested compounds.

2. An impedance-based platform featuring 128 polystyrene-based microwell units in parallel was implemented for analysis of large-scale drug libraries. The antischistosomal efficacy of 57 repurposed drugs was continuously analyzed in the system for 72 hours. The parallelized and continuous monitoring of parasite responses helped to reveal the rapid action and high potency of a small subset of drugs, which were then selected for follow-up *in vivo* tests.

The developed platforms represent a set of new tools for *in vitro* testing the activity of new compounds against *S. mansoni* larvae in an automated and parallelized manner. The realization of the chip using plastic materials facilitates high-volume production and renders the system widely applicable in academic and industrial screening settings. Finally, the modularity of the platforms, combined with the electrical impedance-based readout, offer great potential for further increasing the throughput and temporal resolution of the analysis, which are fundamental features to improve the standard screening process and to gain insights into drug dynamics.

SOMMARIO TESI

Questa tesi presenta la progettazione, la caratterizzazione e l'applicazione di piattaforme miniaturizzate basate su misure ad impedenza per la coltura a lungo termine e l'analisi di larve di *Schistosoma mansoni,* un parassita umano multicellulare. La schistosomiasi è una malattia tropicale causata dall'esposizione parassitaria al *Schistosoma*, che colpisce centinaia di milioni di persone in tutto il mondo. Da oltre 40 anni esiste un solo farmaco disponibile per le campagne di somministrazione di massa, il praziquantel, il quale ha già mostrato un'efficacia decrescente nel tempo. Inoltre, il metodo standard per la scoperta di farmaci antischistosomiali si basa tuttora sulla valutazione microscopica e manuale degli effetti del farmaco sui parassiti *in vitro*, che è una procedura lenta, laboriosa e soggettiva. La motivazione di questo lavoro era lo sviluppo di nuove tecnologie affidabili e automatizzate per accelerare i processi di selezione di farmaci antischistosomiali e contribuire all'identificazione di nuovi trattamenti, data la mancanza di medicinali alternativi.

Le tecniche di micro-fabbricazione forniscono uno strumento utile per costruire sistemi di coltura e misurazione ottimizzati. La combinazione di chip micro-strutturati ed elettrodi micro-fabbricati consente l'integrazione della misura di impedenza elettrica all'interno delle piattaforme, con le quali si possono eseguire analisi senza marcatori e non invasive dei campioni di interesse durante la selezione di nuovi farmaci.

In questa tesi vengono descritte due piattaforme automatizzate basate sulla analisi dell'impedenza per la misurazione della funzione vitale delle larve di *S. mansoni* esposte a diversi trattamenti:

1. È stato sviluppato un chip a base di micro-pozzetti utilizzando il polidimetilsilossano, il quale è stato integrato con elettrodi complanari in platino, per eseguire registrazioni continue di impedenza della motilità dei parassiti, come indicatore della loro funzione vitale. Le larve di *S. mansoni* sono state messe in coltura nel chip ed esposte a quattro noti farmaci antischistosomiali per 48 ore. Il monitoraggio in tempo reale delle relazioni dose-risposta ha consentito di mostrare l'elevata e rapida attività *in vitro* dei farmaci testati.
2. È stata implementata una piattaforma basata sulla misurazione di impedenza di 128 unità a micro-pozzetti, realizzati in polistirene, in parallelo per l'analisi di librerie di farmaci su larga scala. L'attività antischistosomiale di 57 farmaci, inizialmente identificati per altre patologie, è stata costantemente analizzata dal sistema per 72 ore.

Il monitoraggio parallelo e continuo delle risposte vitali dei parassiti ai trattamenti ha consentito di rilevare la veloce e alta efficacia di un sottogruppo di farmaci, che ha confermato la loro idoneità per ulteriori test *in vivo*.

Le piattaforme sviluppate rappresentano dei nuovi strumenti per misurare a lungo termine l'attività di nuovi farmaci *in vitro* contro le larve di *S. mansoni* in modo automatizzato e parallelizzato. La realizzazione del chip in plastica permette la produzione della nuova soluzione in grandi volumi e rende la sua applicazione ampiamente adatta in vari contesti accademici e industriali di processi di selezione di farmaci. Infine, la modularità della piattaforma combinata con la misurazione di impedenza elettrica mostra un grande potenziale nell'aumentare ulteriormente il volume e la risoluzione temporale dell'analisi, le quali sono caratteristiche fondamentali per migliorare il processo di selezione di antischistosomici e per ottenere maggiori informazioni sulla dinamica dei farmaci.

ACKNOWLEDGEMENTS

I would like to thank Prof. Andreas Hierlemann for giving me the opportunity to conduct my doctoral research at the Bio Engineering Laboratory. His precious support and guidance through the projects and collaborations contributed to all my scientific achievements, which were performed in a positive, stimulating and well-equipped work environment.

I am thankful to Prof. Carlotta Guiducci for being part of my thesis committee.

A special thanks goes to Dr. Mario Matteo Modena, who represents for me a model of supervision that every doctoral student needs to achieve successful outcomes. I enjoyed all our experiments, talks and engineering discussions, even the one we were of opposite ideas. Over these years, I could always count on his valuable input and encouragement, and all the results I made would not be possible without him.

I would like to thank Prof. Jennifer Keiser and all her group at the Swiss Tropical and Public Health Institute for the very pleasant collaboration on schistosomiasis projects.

It was a pleasure for me to work with Francesco Grassi and Estelle Grosjean, who contributed to the antischistosomal studies as a part of their student projects.

I would like to thank Dr. Fernando Cardes Garcia, who provided me important advice on the technological improvements and nice support during our snack break.

I would like to thank Dr. Carlo Cosimo Campa, as he carefully taught me complex biological phenomena and technical issues related to manuscript editing.

I would like to thank Silvia Ronchi, as she is my best Italian friend and college in Switzerland. We have helped each other continuously during the PhD studies and after many years we will surely continue to support for the new chapters of our life.

I also wanted to thank all the people of the BEL group for having a very good time during daily work, for organizing enjoyable experiences in our retreats and for the scientific discussions during meetings.

Thanks also go to all members of the D-BSSE facilities and administration, who were always very helpful with technical and organizational issues.

Finally, I am very grateful for the overall support of my parents, Mariuccia and Mahmoud, and their inexhaustible love throughout my life. Last but not the least, I cannot express how grateful I am to my girlfriend, Susanna, for her unending support and patience.

AUTHOR CONTRIBUTIONS

Stefan Biendl

Chapter 2-3: Participated in planning and performing the biological experiments and contributed to writing the manuscripts.

Matthias Alexander Dupuch

Chapter 2: Helped with the plastic coating of the fabricated microfluidic chips and contributed to the manuscript.

Francesco Grassi

Chapter 3: Analyzed the physicochemical properties of the active drugs, identified in the screening application, and contributed to the manuscript.

Prof. Dr. Andreas Hierlemann

Chapter 2-3: Coordinated and conceived the projects, revised and edited all chapters of this thesis.

Prof. Dr. Jennifer Keiser

Chapter 2-3: Helped through general consulting and editing of the manuscripts.

Dr. Flavio Christopher Lombardo

Chapter 2: Participated in planning and performing the biological experiments and contributed to writing the manuscript.

Dr. Mario Matteo Modena

Chapter 2-3: Conceived the impedance-based microfluidic chips that were presented in chapter 2 and 3. Provided ideas and contributed through consulting and guidance to all chapters of this thesis. He edited and revised all manuscripts.

Paolo Shayan Ravaynia

Chapter 2-3: Conceived, designed and developed all components of the impedance-based microfluidic chips and setup for reliable operation and drug-screening applications. Planned and performed all experiments, analyzed the data and wrote the manuscripts.

1. INTRODUCTION

1.1 Schistosomiasis

Schistosomiasis is a neglected tropical disease and human morbidity is associated with parasitic infections of the genus *Schistosoma*. Schistosome trematodes are infective flatworms with a unique life cycle involving sexual reproduction in mammalian hosts and asexual reproduction in snail intermediate hosts.[1] The disease is mainly caused by five schistosome species, namely *Schistosoma mansoni, S. japonicum, S. haematobium, S. mekongi, and S. intercalatum*, however the first three species account for 90% of human schistosomiasis cases.[2] Recent estimates show that more than 779 million people in 78 countries are at risk of contracting the disease and at least 290 million individuals have required preventive antischistosomal treatment.[3–5] Until now, the most afflicted countries are located in the region of sub-Saharan Africa, which is affected by around 50% of schistosomiasis infections and over 10,000 deaths per year.[2,6,7] The main reasons for schistosomal endemicity in these poor areas include the lack of safe water, proper hygiene and well-informed human behavior.[2]

Human schistosomiasis infections are mainly acquired by swimming or bathing in freshwater that is contaminated with the larval stage of *Schistosoma* flukes (cercariae). Once the cercariae come in contact with the human host, the parasites may penetrate the skin barrier, which activates a series of biochemical mechanisms causing them to shed their tail.[8] From this new stage, the schistosomula enter the blood circulation and, driven by the blood pressure, can reach the lungs, in which the larvae mature for up to 3 weeks. Hereafter, the schistosomula eventually migrate to the liver and, after 7 weeks, the larval parasites fully grow into a sexually dimorphic species and in adult pairs, which live in constant male-female copula and can persist for several years.[2,9]

The main cause of the disease is represented by the eggs that are released by the female adult schistosomes, mostly located in the liver. The number of secreted eggs range from few dozens to hundreds per day depending on the *Schistosoma* species and many of those eggs are eliminated through the intestine; however, the ones remaining embedded in the tissues are the cause of morbidity.[10,11] According to the Global Burden of Disease Study, schistosomiasis caused the loss of 1.4 million disability-adjusted life years in 2017.[12] If left untreated, in such long-term cases, the liver and intestine damages can be dramatic and lead to hepatic fibrosis and to an increased risk of bladder cancer.[6,13]

1.2 Current challenges in antischistosomal drug discovery

Schistosomiasis is a worldwide disease, which afflicts over 200 million individuals, and the antischistosomal treatment has been relying exclusively on a single drug, praziquantel, for more than 40 years.[14] After the abandonment of oxamniquine, another potent antischistosomal, due to the insurgency of parasite resistance, praziquantel has always been the drug of choice for administration campaigns, because of the low therapy costs, the well-known efficacy and the minor side effects.[15] Nowadays, hundreds of millions of doses of this compound are routinely distributed every year to treat schistosomiasis in human and veterinary medicine.[15] However, the widespread use of praziquantel, for both human endemic control and animal medicine, may imply an increased risk of resistance development due to the high evolutionary pressure posed on the *Schistosoma* parasites. Therefore, it has become essential to find novel alternative therapeutics against Schistosomiasis.

Currently, the drug discovery pipeline is dramatically empty and no vaccine is available, as a consequence of the low profit margins of neglected tropical diseases, the treatment of which, therefore, does not attract high investments from pharmaceutical companies.[16,17] Thus, the research for new antischistosomal vaccines or drugs relies predominantly on a handful of academic laboratories.[18] In the last ten years, global awareness of diseases has been increasing and non-profit public/private partnerships, such as Drugs for Neglected Diseases Initiative and Medicine for Malaria Venture, are being established in a number of academic settings for discovering, developing and facilitating the delivery of new/repurposed effective and affordable compounds.[19,20] However, the lack of high-throughput automated technologies delays the efficient screening of large compound libraries.

For several years, the gold standard for antischistosomal drug screening has been based on the phenotypic assessment of larval and adult schistosomes by microscopy-based visual scoring.[21] However, visual inspection does not facilitate medium or high throughput assays and suffers from operator bias, which makes the screening process slow and subjective. Moreover, it has been reported that only 20% of drug hits, identified by a specific laboratory, are then confirmed by other laboratories.[22,23]

The introduction of the more abundant and user-friendly larval-stage worms, or Newly Transformed Schistosomula (NTS), has pushed the development of alternatives to the standard drug screening method, but none of the implemented technologies has found widespread use. Antischistosomal drug screening systems, based on microthermal calorimetry, colorimetric assay, as well as computer-aided image recognition and photogram-image subtraction, have

been presented in literature.[24–26] Each of these approaches features relevant drawbacks and the lack of a unique technique adopted across the involved laboratories is the cause of conflicting results and fragmentation in the field. For the calorimetric assays, one of the main limitations is the high number of needed parasites, which renders this method difficult to be used in high-throughput applications.[24] In the case of colorimetric experiments, the need of expensive dyes limits its use in low-resource academic settings.[25,27] For the computer-aided phenotypic analysis of schistosomula, the screening requires high computational power and sophisticated algorithms and/or devices that can be costly and difficult to implement widely.[26] Therefore, to accelerate antischistosomal drug discovery, novel automated drug-screening systems are urgently required to achieve high throughput and real-time drug activity measurements, small sample volumes, and low-cost and easy-to-use equipment.

1.3 Miniaturized analysis systems

Miniaturized culturing systems have been optimized over several years with the goal of improving diagnostics, providing scalability for increased throughput, automating simple or complex *in vitro* biological assays, reducing sample volumes and decreasing experimental costs.[28] Micro Total Analysis Systems (μTAS), also denoted lab-on-chip methodologies, are based on the design and fabrication of micro-structured environments including micro-separators, micro-reactors and microfluidics, and serve a large variety of biological and biochemical assays.[29,30] In addition, the fact that a large number of microsystems feature precise spatial and temporal control of single cells and small multicellular organisms has made those platforms attractive for cell- and organ-based screening applications in comparison to conventional techniques.[31,32]

Moreover, the introduction of simple fabrication methods, such as the soft-lithography process using polydimethylsiloxane (PDMS), a soft and optically transparent biocompatible elastomer, rendered the implementation of novel μTAS more appealing to a broad range of bioengineering laboratories, which fueled the development of various custom-made designs.[33,34] However, a main drawback of PDMS is the ad/absorption of small hydrophobic substances, such as small biomolecules and drugs, from the liquid phase. To overcome biases in evaluating outcomes of drug dose-response assays, several PDMS surface treatments have been developed depending on the applications.[35,36] To overcome the absorption limitations of PDMS, well-characterized platforms can be fabricated using thermoplastic materials, such as polystyrene. Polystyrene is frequently adopted to produce micro-scale chip design with high reproducibility, high throughput and at low costs (in high volume applications) by using, e.g., injection molding.[37,38]

Over the years, the application of micro-devices has also gained increasing importance for investigations of multicellular parasitic worms, such as *Caenorhabditis elegans* nematodes, under precisely controlled conditions *in vitro,* which yielded fundamental results in parasite pharmacology and physiology. Several microfluidic platforms were developed to investigate the worm behavior and sensory responses related to mechanosensitivity, chemosensitivity and light sensitivity.[39–41] Novel on-chip approaches for accurate immobilization, imaging and sorting of single adult worms and larvae have been implemented.[42]

The detection method of most μTAS relies on light and fluorescence microscopy to optically analyze cells and/or organisms and to identify biological mechanisms.[43] This technique involves the use of a label, such as a fluorophore, to stain specific biomolecules or units of interest. Although fluorescence imaging can provide a plethora of information on cell behavior, this methodology can be limited by the occurrence of phototoxic effects upon frequent imaging, which restrict its use for long-term monitoring, and may require complex image analysis.[44] Therefore, the integration of label-free electrical detection methods on chip can provide an independent output that is complementary to conventional imaging procedures, features a better temporal resolution and enhances information on the dynamic behavior of cells or organisms.

1.4 Electrical impedance spectroscopy

The development of miniaturized systems also enables the use of electrical impedance spectroscopy (EIS) to quantify multi-parameter characteristics of single-cell and small multicellular organisms in real-time. EIS is a non-invasive technique for measuring the dielectric properties of a sample of interest as a function of frequency.[45] This technique can provide information on cell/organism size, membrane resistance and capacitance, and cytoplasmic conductivity.[46] Impedance measurements can be therefore used to detect variations of these features over time caused by the activity of test drug molecules. In addition, EIS readout has the advantage to be easily automated and parallelized in multiple microwells enabling incremental upscaling and increasing of throughput.

By applying the Coulter principle of cell counting to the microfluidic field, more advanced devices, called impedance microfluidic cytometers, have been implemented since the 1990s.[47] The first devices were realized by integrating a pair of gold electrodes within an epoxy-based microfluidic channel to perform AC multi-frequency measurements on single cells.[47,48] In the later work of Gawad *et al.*, a differential impedance detection was carried out using a cytometer featuring three co-planar electrodes on a glass substrate and a microfluidic channel made in PDMS, in which erythrocytes and ghost cells were flown for cell sorting.[49] By adopting

parallel facing electrodes, several micro-cytometers were developed to analyze and differentiate various cell types, such as yeast, bacteria and leukocytes.[50–52]

Moreover, electrical cell-substrate impedance sensing (ECIS) systems were realized to monitor the changes in AC impedance of 2-D cellular layers using interdigitated planar electrodes deposited at the bottom of a culture dish.[53] Such platforms provided continuous information on proliferation, viability and cytotoxicity effects of cells, which were cultured over the planar electrodes for long-term periods.[54,55] In the study of Nguyen *et al.*, the ECIS methodology was also adopted to investigate single cancer cell migration in 3-D matrices within a microfluidic chip.[56]

EIS detection was also used as a label-free technique to characterize the effects of compounds on the morphology, size, and viability of 3-dimensional cellular models, such as microtissues.[57] The integration of impedance-based readouts in microfluidic devices, like hanging-drop networks or chips based on gravity-driven perfusion, has been successfully demonstrated for investigating multiple microtissue spheroids in an automated manner.[58,59]

Microfluidic platforms with embedded electrodes were also implemented to perform whole-organism drug screening of *C. elegans*, to guide the movement of worms by the application of localized electric fields and to identify their developmental stages by impedance characterization.[60–62] The xCelligence system, a commercial device featuring interdigitated microelectrodes at the bottom of a 96-well plate, was presented as an impedance-based tool for measuring the motility of adult schistosomes and drug effects on helminths.[63] Recently, Chawla *et al.* developed an integrated microfluidic platform for an end-point viability assessment of schistosomula parasites under drug exposure using an impedance-based motility analysis.[64] Nevertheless, no EIS micro-system has been reported so far, which is capable of monitoring the viability of *Schistosoma mansoni* larvae over extended time and in an automated fashion for medium- or high-throughput drug-screening applications.

1.5 Scope and structure of the thesis

This thesis focuses on the development, characterization, and application of miniaturized impedance-based systems that enable the long-term culturing and automated viability detection of *S. mansoni* larvae exposed to test compounds. First, a PDMS-based microwell platform design with integrated impedance readout was developed and validated for continuous measurements of dose-response relationships of established antischistosomal drugs. Second, by realizing this platform completely in plastics, the throughput of impedance-based NTS analysis was increased, and the continuous monitoring of antischistosomal efficacy of large compound collections became possible. The thesis conclusion highlights the main results of the developed platforms and includes a brief outlook, in which the next potential development steps for the system are described.

The thesis contains two journal articles:

1. Parallelized Impedance-Based Platform for Continuous Dose-Response Characterization of Antischistosomal Drugs. Ravaynia, P. S., Lombardo, F. C., Biendl, S., Dupuch, M. A., Keiser, J., Hierlemann, A., Modena, M. M. Adv. Biosys. 2020, 4, 1900304.
2. Real-time and Automated Monitoring of Antischistosomal Efficacy of a Pandemic Compound Collection for Drug Discovery. Ravaynia, P. S., Biendl, S., Grassi, F., Keiser, J., Hierlemann, A., Modena, M. M. In preparation for submission.

1.6 Summary of major results

Long-term evaluation of Schistosomula parasite viability by impedance-based detection

The current screening of antischistosomal drugs is limited by the low throughput and potential subjectivity of the visual assessment of schistosomula phenotypes. To overcome these drawbacks, an impedance-based platform for automated and unbiased detection of the viability of *S. mansoni* larvae over 32 independent units following drug treatment was developed. By testing multiple concentrations of praziquantel, oxethazaine, mefloquine and methiothepine on chip, the platform enabled the continuous and parallelized characterization of drug-induced schistosomula behavior and the extraction of dose-response relationships during more than 48 hours. Such characterization is essential for selecting promising antischistosomals that feature high activity and fast kinetics.

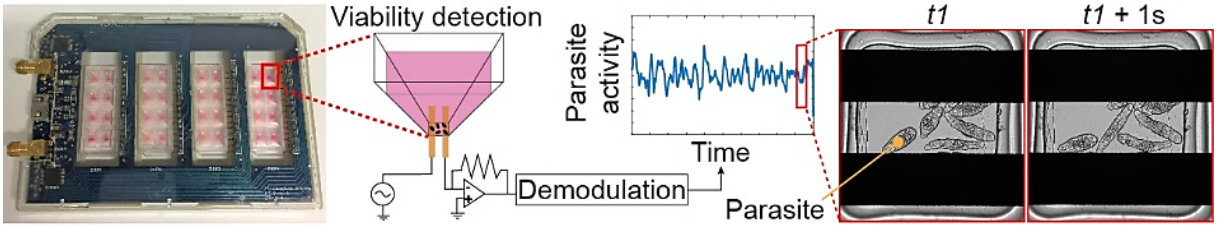

Continuous and high-throughput monitoring of antischistosomal pharmacodynamics

For an under-funded neglected disease as schistosomiasis, drug library repurposing represents an important source for the identification of novel therapeutics, however high-throughput screening systems are urgently needed to speed up antischistosomal drug discovery. Thus, a new impedance-based plastic platform was implemented to enable reliable and large-scale schistosomula monitoring for the screening of compound collections. By simultaneously recording up to 128 conditions using a single instrument, the parallelized device enabled the continuous evaluation of the antischistosomal activity of 57 selected compounds from the Pandemic Response Box library over 72 hours in an automated manner and provided insights into their pharmacodynamics. The system thus allows for an informed selection of novel potent and fast-acting drugs.

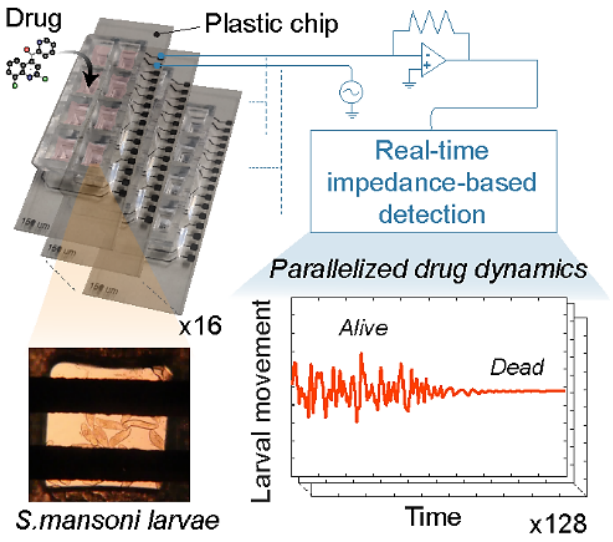

1.7 References

[1] D. P. McManus, D. W. Dunne, M. Sacko, J. Utzinger, B. J. Vennervald, X.-N. Zhou, *Nat. Rev. Dis. Prim.* **2018**, *4*, 13.

[2] B. Gryseels, K. Polman, J. Clerinx, L. Kestens, *Lancet* **2006**, *368*, 1106.

[3] J. Utzinger, E. K. N'Goran, C. R. Caffrey, J. Keiser, *Acta Trop.* **2011**, *120*, S121.

[4] L. G. Song, X. Y. Wu, M. Sacko, Z. D. Wu, *Parasitol. Res.* **2016**, *115*, 4071.

[5] L. A. Tchuem Tchuenté, D. Rollinson, J. R. Stothard, D. Molyneux, *Infect. Dis. Poverty* **2017**, *6*, 1.

[6] D. G. Colley, A. L. Bustinduy, W. E. Secor, C. H. King, *Lancet* **2014**, *383*, 2253.

[7] C. H. King, *PLoS Negl. Trop. Dis.* **2017**, *11*, 2.

[8] J. McKerrow, J. Salter, *Trends Parasitol.* **2002**, *18*, 193.

[9] B. G. M. Jamieson, *Schistosoma*, CRC Press, **2017**.

[10] D. P. McManus, D. W. Dunne, M. Sacko, J. Utzinger, B. J. Vennervald, X. N. Zhou, *Nat. Rev. Dis. Prim.* **2018**, *4*, 1.

[11] T. Elbaz, G. Esmat, *J. Adv. Res.* **2013**, *4*, 445.

[12] C. H. King, A. P. Galvani, *Lancet* **2018**, *391*, 307.

[13] M. S. Tucker, L. B. Karunaratne, F. A. Lewis, T. C. Freitas, Y. san Liang, *Schistosomiasis*, **2013**.

[14] M. A. Verjee, **2019**, 153.

[15] A. Ross, M. Inobaya, R. Olveda, T. Chau, D. Olveda, *Res. Rep. Trop. Med.* **2014**, 65.

[16] M. S. Tucker, F. A. Lewis, J. D. Driver, W. O. Granath, *J. Parasitol.* **2014**, *100*, 778.

[17] A. Ricciardi, M. Ndao, *J. Biomol. Screen.* **2015**, *20*, 6.

[18] J. Keiser, *Parasitology* **2010**, *137*, 589.

[19] E. Chatelain, J. R. Ioset, *Drug Des. Devel. Ther.* **2011**, 175.

[20] S. Nwaka, A. Hudson, *Nat. Rev. Drug Discov.* **2006**, *5*, 941.

[21] B. Ramirez, Q. Bickle, F. Yousif, F. Fakorede, M.-A. Mouries, S. Nwaka, *Expert Opin.*

Drug Discov. **2007**, *2*, S53.

[22] G. Panic, M. Vargas, I. Scandale, J. Keiser, *PLoS Negl. Trop. Dis.* **2015**, *9*, e0003962.

[23] N. R. Mansour, R. Paveley, J. M. F. Gardner, A. S. Bell, T. Parkinson, Q. Bickle, *PLoS Negl. Trop. Dis.* **2016**, *10*, 1.

[24] T. Manneck, O. Braissant, Y. Haggenmuller, J. Keiser, *J. Clin. Microbiol.* **2011**, *49*, 1217.

[25] G. Panic, D. Flores, K. Ingram-Sieber, J. Keiser, *Parasites and Vectors* **2015**, *8*, 1.

[26] R. A. Paveley, N. R. Mansour, I. Hallyburton, L. S. Bleicher, A. E. Benn, I. Mikic, A. Guidi, I. H. Gilbert, A. L. Hopkins, Q. D. Bickle, *PLoS Negl. Trop. Dis.* **2012**, *6*, 1.

[27] C. Lalli, A. Guidi, N. Gennari, S. Altamura, A. Bresciani, G. Ruberti, *PLoS Negl. Trop. Dis.* **2015**, *9*, e0003484.

[28] J. Wu, M. Dong, C. Rigatto, Y. Liu, F. Lin, *npj Digit. Med.* **2018**, *1*, 1.

[29] S. Achinas, J. I. Heins, J. Krooneman, G. J. W. Euverink, *Micromachines* **2020**, *11*, DOI 10.3390/MI11090853.

[30] P. Neužil, S. Giselbrecht, K. Länge, T. J. Huang, A. Manz, *Nat. Rev. Drug Discov.* **2012**, *11*, 620.

[31] J. El-Ali, P. K. Sorger, K. F. Jensen, *Nature* **2006**, *442*, 403.

[32] U. Marx, T. B. Andersson, A. Bahinski, M. Beilmann, S. Beken, F. R. Cassee, M. Cirit, M. Daneshian, S. Fitzpatrick, O. Frey, C. Gaertner, C. Giese, L. Griffith, T. Hartung, M. B. Heringa, J. Hoeng, W. H. De Jong, H. Kojima, J. Kuehnl, M. Leist, A. Luch, I. Maschmeyer, D. Sakharov, A. J. A. M. Sips, T. Steger-Hartmann, D. A. Tagle, A. Tonevitsky, T. Tralau, S. Tsyb, A. Van De Stolpe, R. Vandebriel, P. Vulto, J. Wang, J. Wiest, M. Rodenburg, A. Roth, *ALTEX* **2016**, *33*, 272.

[33] D. E. W. Patabadige, S. Jia, J. Sibbitts, J. Sadeghi, K. Sellens, C. T. Culbertson, *Anal. Chem.* **2016**, *88*, 320.

[34] X. M. Zhao, *J. Mater. Chem.* **1997**, *7*, 1069.

[35] H. Sasaki, H. Onoe, T. Osaki, R. Kawano, S. Takeuchi, *Sensors Actuators B Chem.* **2010**, *150*, 478.

[36] J. B. You, B. Lee, Y. Choi, C. S. Lee, M. Peter, S. G. Im, S. S. Lee, *Biotechniques* **2020**, *69*, 47.

[37] P. M. Van Midwoud, A. Janse, M. T. Merema, G. M. M. Groothuis, E. Verpoorte, *Anal. Chem.* **2012**, *84*, 3938.

[38] E. Berthier, E. W. K. Young, D. Beebe, *Lab Chip* **2012**, *12*, 1224.

[39] S. Johari, V. Nock, M. M. Alkaisi, W. Wang, *Mater. Sci. Forum* **2012**, *700*, 182.

[40] K. E. McCormick, B. E. Gaertner, M. Sottile, P. C. Phillips, S. R. Lockery, *PLoS One* **2011**, *6*, DOI 10.1371/journal.pone.0025710.

[41] J. N. Stirman, M. Brauner, A. Gottschalk, H. Lu, *J. Neurosci. Methods* **2010**, *191*, 90.

[42] N. A. Bakhtina, J. G. Korvink, *RSC Adv.* **2014**, *4*, 4691.

[43] N. M. M. Pires, T. Dong, U. Hanke, N. Hoivik, *Sensors (Switzerland)* **2014**, *14*, 15458.

[44] D. R. Rines, D. Thomann, J. F. Dorn, P. Goodwin, P. K. Sorger, *Cold Spring Harb. Protoc.* **2011**, *6*, 1026.

[45] F. Kremer, A. Schönhals, *Broadband Dielectric Spectroscopy*, **2003**.

[46] L. L. Crowell, J. S. Yakisich, B. Aufderheide, T. N. G. Adams, *Micromachines* **2020**, *11*, DOI 10.3390/mi11090832.

[47] Y. Xu, X. Xie, Y. Duan, L. Wang, Z. Cheng, J. Cheng, *Biosens. Bioelectron.* **2016**, *77*, 824.

[48] H. E. Ayliffe, a B. Frazier, R. D. Rabbitt, *IEEE J. Microelectromechanical Syst.* **1999**, *8*, 50.

[49] S. Gawad, L. Schild, P. Renaud, *Lab Chip* **2001**, *1*, 76.

[50] N. Haandbæk, S. C. Bürgel, F. Rudolf, F. Heer, A. Hierlemann, *ACS Sensors* **2016**, *1*, 1020.

[51] N. Haandbæk, O. With, S. C. Bürgel, F. Heer, A. Hierlemann, *Lab Chip* **2014**, *14*, 3313.

[52] D. Holmes, D. Pettigrew, C. H. Reccius, J. D. Gwyer, C. Van Berkel, J. Holloway, D. E. Davies, H. Morgan, *Lab Chip* **2009**, *9*, 2881.

[53] J. Wegener, C. R. Keese, I. Giaever, *Exp. Cell Res.* **2000**, *259*, 158.

[54] C. Xiao, J. H. T. Luong, *Toxicol. Appl. Pharmacol.* **2005**, *206*, 102.

[55] J. Martinez-Serra, A. Ggutierrez, S. Muñoz-Ccapó, M. Nnavarro-Palou, T. Rros, J. C. Aamat, B. Lopez, T. F. Marcus, L. Fueyo, A. G. Suquia, J. Gines, F. Rrubio, R. Rramos, J. Besalduch, *Onco. Targets. Ther.* **2014**, *7*, 985.

[56] T. A. Nguyen, T. I. Yin, D. Reyes, G. A. Urban, *Anal. Chem.* **2013**, *85*, 11068.

[57] D. Kloß, R. Kurz, H. G. Jahnke, M. Fischer, A. Rothermel, U. Anderegg, J. C. Simon, A. A. Robitzki, *Biosens. Bioelectron.* **2008**, *23*, 1473.

[58] Y. R. F. Schmid, S. C. Bürgel, P. M. Misun, A. Hierlemann, O. Frey, *ACS Sensors* **2016**, *1*, 1028.

[59] S. C. Bürgel, L. Diener, O. Frey, J. Y. Kim, A. Hierlemann, *Anal. Chem.* **2016**, *88*, 10876.

[60] S. R. Lockery, S. E. Hulme, W. M. Roberts, K. J. Robinson, A. Laromaine, T. H. Lindsay, G. M. Whitesides, J. C. Weeks, *Lab Chip* **2012**, *12*, 2211.

[61] J. A. Carr, A. Parashar, R. Gibson, A. P. Robertson, R. J. Martin, S. Pandey, *Lab Chip* **2011**, *11*, 2385.

[62] Z. Zhu, W. Chen, B. Tian, Y. Luo, J. Lan, D. Wu, D. Chen, Z. Wang, D. Pan, *Sensors Actuators, B Chem.* **2018**, *275*, 470.

[63] G. Rinaldi, A. Loukas, P. J. Brindley, J. T. Irelan, M. J. Smout, *Int. J. Parasitol. Drugs Drug Resist.* **2015**, *5*, 141.

[64] K. Chawla, M. M. Modena, P. S. Ravaynia, F. C. Lombardo, M. Leonhardt, G. Panic, S. C. Bürgel, J. Keiser, A. Hierlemann, *ACS Sensors* **2018**, *3*, 2613.

2. PARALLELIZED IMPEDANCE-BASED PLATFORM FOR CONTINUOUS DOSE-REPONSE CHARACTERIZATION OF ANTISCHISTOSOMAL DRUGS

Paolo S. Ravaynia[1], Flavio C. Lombardo[2,3], Stefan Biendl[2,3], Matthias A. Dupuch[4], Jennifer Keiser[2,3], Andreas Hierlemann[1] and Mario M. Modena[1]

[1] ETH Zurich, Dept. of Biosystems Science and Engineering, Bio Engineering Laboratory, Basel, Switzerland and

[2] Swiss Tropical and Public Health Institute, Department of Medical Parasitology and Infection Biology, Basel, Switzerland

[3] University of Basel, Basel, Switzerland

[4] ETH Zurich, Dept. of Mechanical and Process Engineering, Micro and Nanosystems, Zurich, Switzerland

Published in Advanced Biosystems, 2020

doi: 10.1002/adbi.201900304

2.1 Abstract

Schistosomiasis is an acute and chronic disease caused by tropical parasitic worms of the genus Schistosoma, which parasitizes annually over 200 millions of people worldwide. Screening of antischistosomal compounds is hampered by the low throughput and potential subjectivity of the visual evaluation of the parasite phenotypes, which affects the current drug assays. Here, an impedance-based platform, capable of assessing the viability of S. mansoni schistosomula exposed to drugs, is presented. This automated and parallelized platform enables unbiased and continuous measurements of dose-response relationships for more than 48 hours. The platform performance is established by exposure of schistosomula to three test compounds, praziquantel, oxethazaine and mefloquine, which are known to affect the larvae phenotypes. The system is thereafter used to investigate the response of schistosomula to methiothepine, an antipsychotic compound, which causes complex drug-induced effects. Continuous monitoring of the parasites reveals transient behavioral phenotypes and allows for extracting temporal characteristics of dose-response curves, which are essential for selecting drugs that feature high activity and fast kinetics of action. These measurements demonstrate that impedance-based detection provides a wealth of information for the *in vitro* characterization of candidate antischistosomals and represents a promising tool for the identification of new lead compounds.

2.2 Introduction

Efficient and reliable screening methods are an essential tool for the discovery of novel drug candidates. The demand for improving the identification of promising compounds is particularly high in the field of neglected tropical diseases (NTDs), where funding and commercial investments are typically low.[1,2] Among the frequently occurring NTDs, schistosomiasis is a tropical disease caused by worms of the genus *Schistosoma*, which infect over 200 million people worldwide, predominantly children living in poor rural areas of Sub-Saharan Africa.[3,4] If left untreated, the infection slowly develops into a debilitating chronic disease, which leads to fibrosis of the liver, intestines and/or bladder, anemia, urogenital cancers and, eventually, death.[4] Despite the high prevalence of schistosomiasis, the current anthelmintic drug discovery pipeline is alarmingly unproductive.[5] For over 40 years, praziquantel has been the treatment of choice for schistosomiasis and has been widely used as chemotherapeutic agent in mass drug-administration campaigns.[3] Hundreds of millions of treatments are administered to children and populations at risk each year,[6] raising a significant potential public-health threat due to the emergence of praziquantel drug resistance.[5,7,8] In addition, reported cases of reduced efficacy of praziquantel have been associated with multiple rounds of mass drug administration, highlighting the need for new antischistosomal drugs.[9]

Compound libraries of pharmaceutical and academic organizations offer a potential source for identification of candidate therapeutics. However, the large number of drugs that need to be tested requires the use of medium- or high-throughput assays to implement an efficient and cost-effective screening.[10,11] In addition to drug efficacy, information on pharmacodynamics would allow to select lead candidates. High activity, fast action and low toxicity represent key parameters for the selection of promising leads during the *in vitro* screening process.[10,12,13] Despite these requirements, the current gold standard for antischistosomal drug screening is based on worm phenotypic evaluation using operator-based microscopy, which is limited in throughput, labor-intensive and subjective. Therefore, the development of advanced screening methods for the identification of new promising lead compounds is of high importance and priority.

In the last years, the more abundant *S. mansoni* larval-stage worms, or Newly Transformed Schistosomula (NTS), have been used for the preselection of lead compounds prior to testing in adult parasites and to overcome the limitations related to the handling of adult worms for large-scale screenings.[14,15] The advent of NTS-based screenings has set the stage for the development of automated and higher-throughput systems, and several screening methods have

been explored. Microcalorimetry was found to be a useful tool to thoroughly analyze drug effects on adult and larval stage helminths in real-time, however it requires a large number of NTS per sample (at least 400).[16,17] An alternate approach based on an image-based automated microscopy system was described as a label-free method to evaluate helminth viability based on morphology and motility.[18,19] Nonetheless, it has not been adopted for systematic dose-response assays and real-time monitoring, as the high computational burden and the low level of parallelization limit its use for routine analysis. The impedance-based xCelligence system, which detects parasite viability in a 96-well plate format, has been applied to adult-stage *S. mansoni* but not to the highly abundant NTS.[20] In summary, no drug screening system, which can automatically measure NTS viability and continuously assess dose-response effects, is currently available.

To address these current limitations, a first version of an *in vitro* impedance-based microfluidic assay for drug screening on NTS has been developed.[21] Electrical impedance spectroscopy (EIS) is a non-invasive and label-free technique for investigating the dielectric properties of a sample and its potential variations within a specific frequency range.[22,23] We previously demonstrated that the confinement of NTS in small sensing regions and the use of electrodes featuring dimensions comparable to those of the parasite larvae enable to assess NTS motility by means of EIS, and that this motility characterization may be a good indicator of NTS viability in drug screening applications.[21] However, the rather complex microfluidic structures ultimately limited the analysis throughput, the measurements still required considerable sample handling by an operator, and the system did not allow for long-term culturing and real-time detection of drug-induced effects.

In this paper, we present a parallelized impedance-based platform to continuously assess dose-response effects of drugs on NTS. The electrical-impedance microwell (EIM) platform includes 32 analysis units to allow for simultaneous execution of several measurement replicates and to increase throughput. To achieve high sensitivity of the detection method without physical confinement of the parasites in channels of sub-millimeter dimensions, we used sensing electrodes with dimensions comparable to the NTS size, which resulted in a sensing volume of ~25 nL or ~100 µm height, given the well dimensions. This configuration enabled the use of a large medium reservoir over the sensing region to achieve long-term culturing of the parasites without affecting the detection characteristics of the system with respect to NTS motility. In addition, the chip design features simple loading of the parasites, which are driven into the nanoliter sensing volume by sedimentation. To validate our platform, we first measured the

NTS response to three antischistosomal compounds, oxethazaine, praziquantel and mefloquine, which have already been shown to cause different phenotypical behaviors *in vitro*, i.e., they reduce parasite motility, stimulate hyperactivity or induce both effects, respectively.[24–28] As a case study, we then analyzed the activity of an antipsychotic drug, methiothepine, which belongs to the emerging class of tricyclic compounds and serotonin modulators, which have been investigated as potential therapeutic agents against schistosomiasis.[24,29] The obtained results indicate that the EIM platform can provide continuous dose-dependent viability and activity patterns of NTS on-chip and can be a suitable component for antischistosomal drug screening.

2.3 Results

2.3.1 EIM platform function and operation

The overall concept of the EIM platform is illustrated in **Figure 1**. To provide continuous impedance-based recordings of parasite motility in parallel to optical inspection, the analysis unit was fabricated from two transparent components: a PDMS (polydimethylsiloxane) microwell and a glass slide patterned with platinum electrodes. Each culture unit was loaded with 60 µL of NTS suspension (~10-15 NTS per 60 µL) by using a pipette (Figure 1A II). The NTS rapidly (~1 min) settled to the bottom of the microwell (chamber) on the patterned glass substrate. Each microwell was equipped with a pair of coplanar electrodes for detecting NTS motility by measuring conductivity variations that were caused by parasite movements between the electrodes. To measure the signal fluctuations upon NTS activity and movements, an AC voltage was applied to the left co-planar electrode, and the current flowing through the sensing volume was then measured at the right electrode and converted to voltage through a trans-impedance amplifier (Figure 1A III). Motile and non-motile parasites were evaluated separately in the device to detect differences in the voltage signal during 1-min acquisition. Because of the parasite movements, the high-pass-filtered signal output of motile NTS exhibits clear fluctuations around zero (Figure 1A IV), while non-motile NTS do not cause signal variations, and the trace only shows the readout background noise (in the µV range, Figure S1, Supporting Information).

To assign a motility value as a function of signal fluctuations in a time window of 60 seconds, we computed the signal power in a bandwidth of 1-3 Hz. Figure 1B shows an example of the separation between the normalized signal power generated by motile and non-motile NTS, evaluated every 15 minutes during 1 hour. The signal power measured with alive and motile parasites (-13.1 ± 1.1 dBµ, ~0.05 a.u.) was, therefore, constantly two orders of magnitude higher than the signal power obtained from the non-motile counterpart (-34.7 ± 0.6 dBµ, in the range of 0.0005 a.u.), which evidences the robust recognition and differentiation of worm motility by using our platform.

The motility of the parasites was also qualitatively evaluated by visual inspection under an inverted microscope, as the chip was optically transparent and openings were included in the chip holder. The sequence of bright-field images clearly shows the contraction/extension movements of the alive NTS in between the electrode pair, while non-motile NTS do not move or change position (Figure 1C). The microscopy observations correlated with the impedance-

based recordings and confirmed that the impedance signal fluctuations arose from the parasite movements.

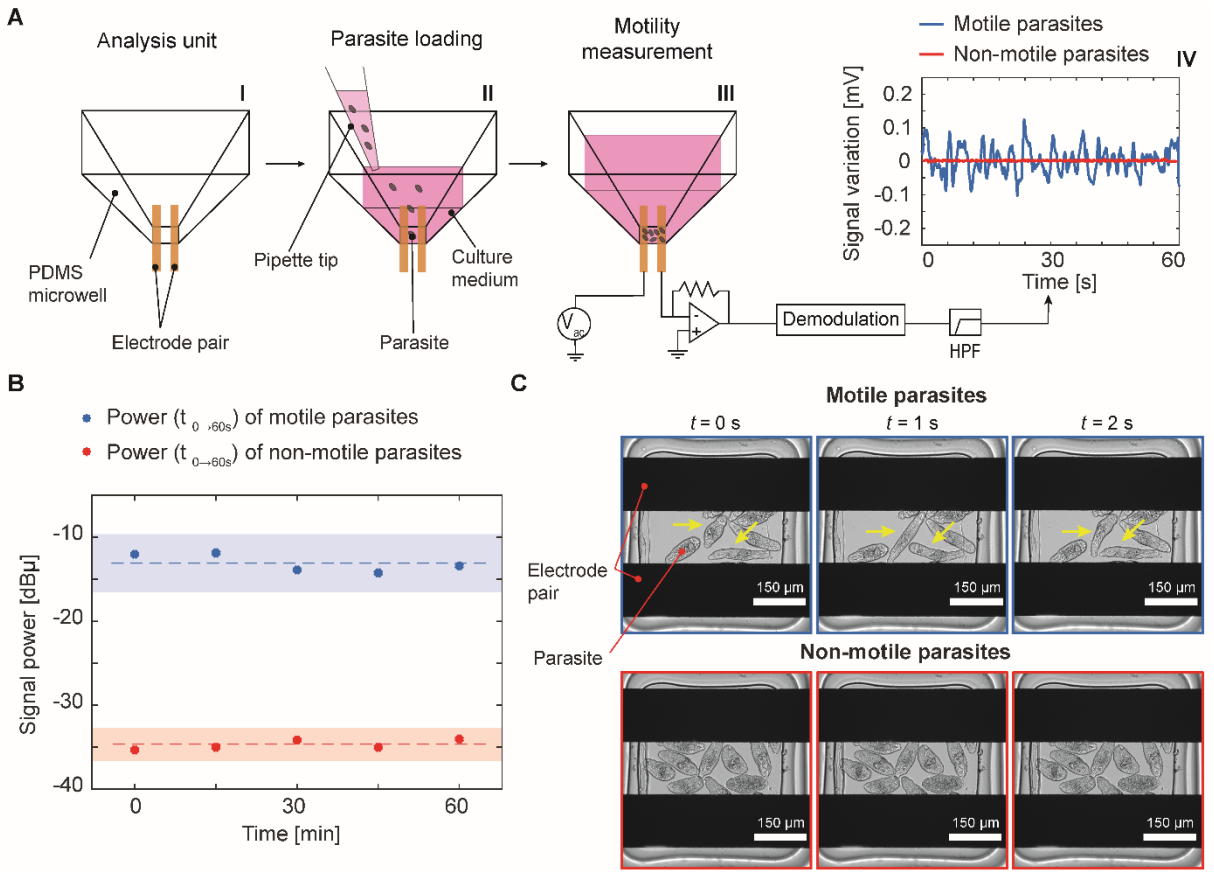

Figure 1. Detection of NTS parasite motility by the EIM platform. **A** The analysis unit of the EIM platform consists of an inverted-pyramid-shape PDMS part, aligned with a pair of platinum electrodes (I). After loading and sedimentation of the schistosomula in the inverted-pyramid-shape PDMS well (II), the impedance-based motility measurement of NTS was carried out (III). Signal fluctuations, caused by impedance variations between the electrodes owing to larvae movements, were acquired using a 500 kHz sinusoidal excitation. The graph shows an example of 60s of signal recordings for both, motile and non-motile parasites (IV). The signal was filtered using a 0.2 Hz high-pass filter to remove the signal baseline. **B** The power of the signals acquired from motile and non-motile NTS parasites was calculated in a bandwidth of 1-3 Hz during a time window of 1 minute and measured every 15 min. The dotted line indicates the mean value of the signal power for motile (blue) and non-motile (red) NTS. The shaded areas show ± 3 standard deviations. The power unit refers to 10^{-6} a.u. **C** Bright-field microscopy images of motile and non-motile NTS parasites in the analysis units. The yellow arrows indicate parasites that contract and elongate between frames.

2.3.2 Higher-throughput EIM platform design

The higher-throughput EIM platform was designed to achieve parallelized and automated monitoring of the motility of NTS exposed to different test conditions. The platform included three components (**Figure 2A**): 1) a custom-made PCB (printed circuit board) for signal routing; 2) four analysis chips; 3) a device holder to accommodate the chips and provide connections between the PCB and the electrode pads on the chips. All these parts were designed

according to a 96-well-standard format to ensure compatibility with standard lab equipment and automated imaging and analysis tools. The PCB enabled the multiplexing of the analog input/output signals of the impedance spectroscopy unit to any of the 32 parasite chambers. The PCB featured two analog multiplexers to separately switch the 32 input and output electrodes, spring-contact connectors for interfacing with the fluidic chips, a mini-HDMI plug to connect to the controller board outside of the incubator, and two analog SMA connectors to the input/output ports of the impedance spectroscope. The chips were inserted in a 3D-printed device holder with four insertion sites. Each chip included a top PDMS layer, containing the microfluidic structures that defined the 8 analysis units (microwell) and a bottom glass slide patterned with 16 co-planar platinum electrodes. To prevent absorption of small hydrophobic molecules from the solution into the PDMS during the drug assays, all chips were coated with a parylene-C layer (Figure S2-S3, Supporting Information).[30] Moreover, the microwells were arranged at 9 mm pitch to allow for loading of the parasites and of the medium by means of a standard multichannel pipette to simplify platform operation. Each analysis unit was shaped as an inverted pyramid to bring the parasites down to the micro-sensing area (450 x 450 μm^2) through sedimentation and to provide enough medium volume (60 µL) for multi-day experiments. Despite the considerable liquid volume over the sensing area, the electrode dimensions limited the sensing volume to the first 100 µm in height, which corresponds to the approximate size of the NTS (~50 x 100 μm^2) (Figure S4, Supporting Information). The overall sensing volume (~25 nL) was defined to enable testing with ~10-15 NTS per condition, which represents a ~10 fold reduction in sample consumption with respect to standard visual evaluation methods.[12]

The automated multiplexing in the platform allowed to simultaneously record from up to 32 analysis units. From an electrical point of view, each sample can be described as a variable impedance Z_s, representing the NTS suspension between the electrodes, in series with two double-layer capacitances, C_{dl}, which form at the interface between the electrodes and the medium (Figure 2B). The variations of Z_s over time were caused by the movement of the NTS in between the electrodes, while the Z_s average value depended on the solution conductivity and on the number of parasites between the electrodes. A multiplexing and switching architecture was used to route the output of the lock-in amplifier to each of the 32 parasite chamber units. Correspondingly, a de-multiplexing stage was used to route the output signals of each chamber to the input of the trans-impedance amplifier (TIA). The frequency of the sinusoidal carrier signal (500 kHz) was selected to enable fast multiplexing and to minimize the signal attenuation in the EIM platform (~-32 dBV, Figure S5, Supporting Information). The switching interval

and the selection of the electrode pairs were defined by a custom-made Python script, which interfaced to a microcontroller (MCU, on the controller board) that controlled the de/multiplexers on the PCB. To achieve continuous and quasi-parallel impedance measurements of the NTS in the 32 chambers, we performed short recordings (1 ms) at each electrode pair and fast switching (1.5 µs) between all the units in a round-robin fashion, which resulted in an effective sampling frequency of ~32 Hz per chamber unit.

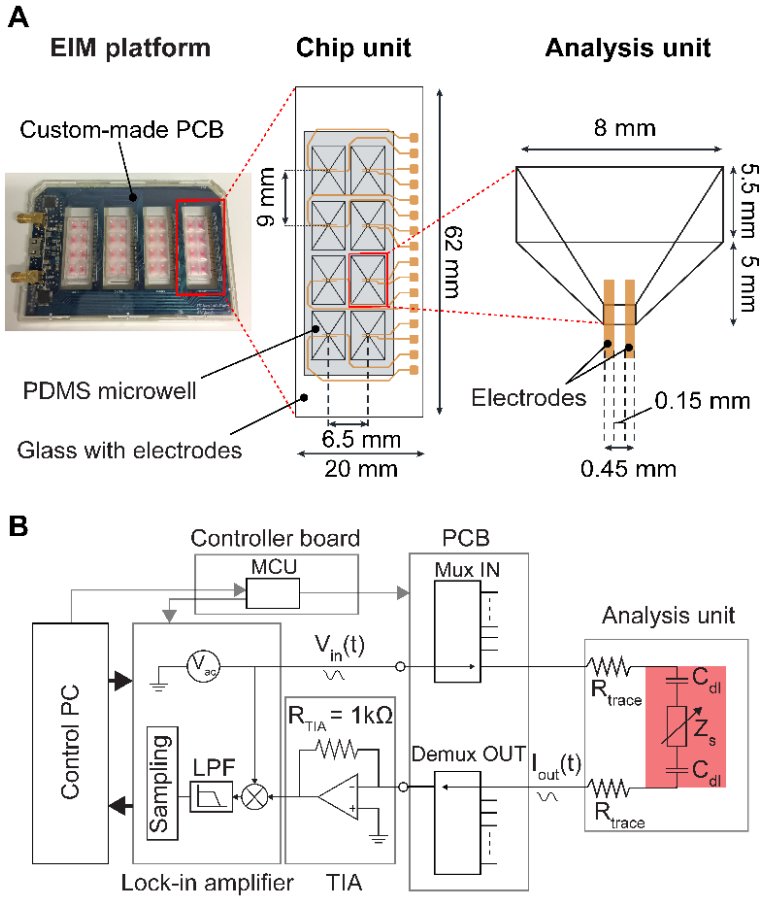

Figure 2. Design of the EIM platform. **A** The EIM platform can accommodate up to 4 chip units, which were placed on a custom-made PCB. A single chip (highlighted with dashed red line) hosted 8 PDMS analysis units that were plasma-bonded to a glass substrate featuring platinum electrodes. The PDMS cavity featured an inverted-pyramid shape to promote sedimentation of the parasites to the sensing volume over the coplanar electrodes. **B** The electrical equivalent circuit of the experimental setup, which included a lock-in amplifier for generating the AC stimulation signal (V_{in}), a custom-made PCB for routing the AC signal to the selected analysis unit and a trans-impedance amplifier (TIA) for current-to-voltage conversion. The voltage signal was sampled by the lock-in amplifier and recorded. A controller board featuring a microcontroller (MCU) was used for synchronizing the switching between the analysis units and the lock-in amplifier.

2.3.3 Monitoring of parasite motility under drug dosage

To validate the ability of the EIM platform to detect NTS motility and to discriminate between different schistosomula movement characteristics, we measured the signal fluctuations caused

by the parasites following incubation with two compounds, known to affect schistosomula phenotypes. We selected oxethazaine, a fast-acting *in vitro* compound that reduces parasite motility,[24] and praziquantel, which, although mostly effective against adult parasites, is known to have an excitatory effect on NTS *in vitro*.[26] The parasites were exposed to different concentrations of these test compounds, and we tested our impedance-based motility readout. As controls, we measured also the motility of NTS under standard medium conditions and in medium containing the drug vehicle (DMSO). The parasite larvae were first loaded in the chips under standard medium condition using a multichannel pipette. We then performed impedance measurements of all the chambers during 1 hour to evaluate the motility of the untreated parasites and to confirm their initial viability (**Figure 3A**). After baseline acquisition, the different drug concentrations were added to the chamber units and NTS motility was recorded over time. This procedure enabled us to normalize the power of the signal fluctuations to the power of the first 1-hour window for each condition and to extract a motility index. This normalization also allowed for comparing measurements from chambers with different numbers of parasites, as the absolute signal power depends on the number of loaded parasites.

Our platform allowed to differentiate the inhibitory and excitatory effects, induced by the two test compounds (Figure 3B). After addition of oxethazaine (t = 0 h) at all concentrations tested, the NTS exhibited a considerable decrease in motility, compared to the vehicle control condition, during 48 hours of continuous measurements. The reduction of NTS motility showed a drug-dose dependence: the motility index for 6 µM oxethazaine reached zero (i.e., no motility) in 12 hours, whereas the 3 µM condition required about 24 hours to achieve the same effect. The highest drug concentration, 12 µM, inhibited the larvae movement within the first 15 minutes upon addition of the compound. Contrarily, praziquantel showed a drastic increase in NTS motility, which is in line with the phenotypical evaluations of drug effects reported in literature.[25,26] Higher motility index values (~ 1.5) were obtained for 1.5 µM and 3 µM of praziquantel. After reaching a peak of the motility index, all the drug-dose curves exhibited a gradual decrease in motility and approached the vehicle-control behavior in about 18 hours. Moreover, the effect of both drugs was also confirmed in a 96 well-plate by the standard visual method (Movie S1-S2, Supporting Information).

By focusing on the first 2 hours of the motility detection for both compounds, we evaluated the sensitivity of the platform in discriminating motility changes caused by different drug concentrations (Figure 3C). To observe drug-induced rapid variations of NTS behavior, the motility index was computed for 1-min windows every 15 min during the entire recording. We

achieved a robust discrimination of the effects induced by 3 µM, 6 µM and 12 µM of oxethazaine after 75 min compared to the 0.5% (v/v) DMSO and 1.5 µM oxethazaine conditions. For praziquantel, we observed a significant increase in motility after 30 min for all tested concentrations in comparison to the vehicle-control condition.

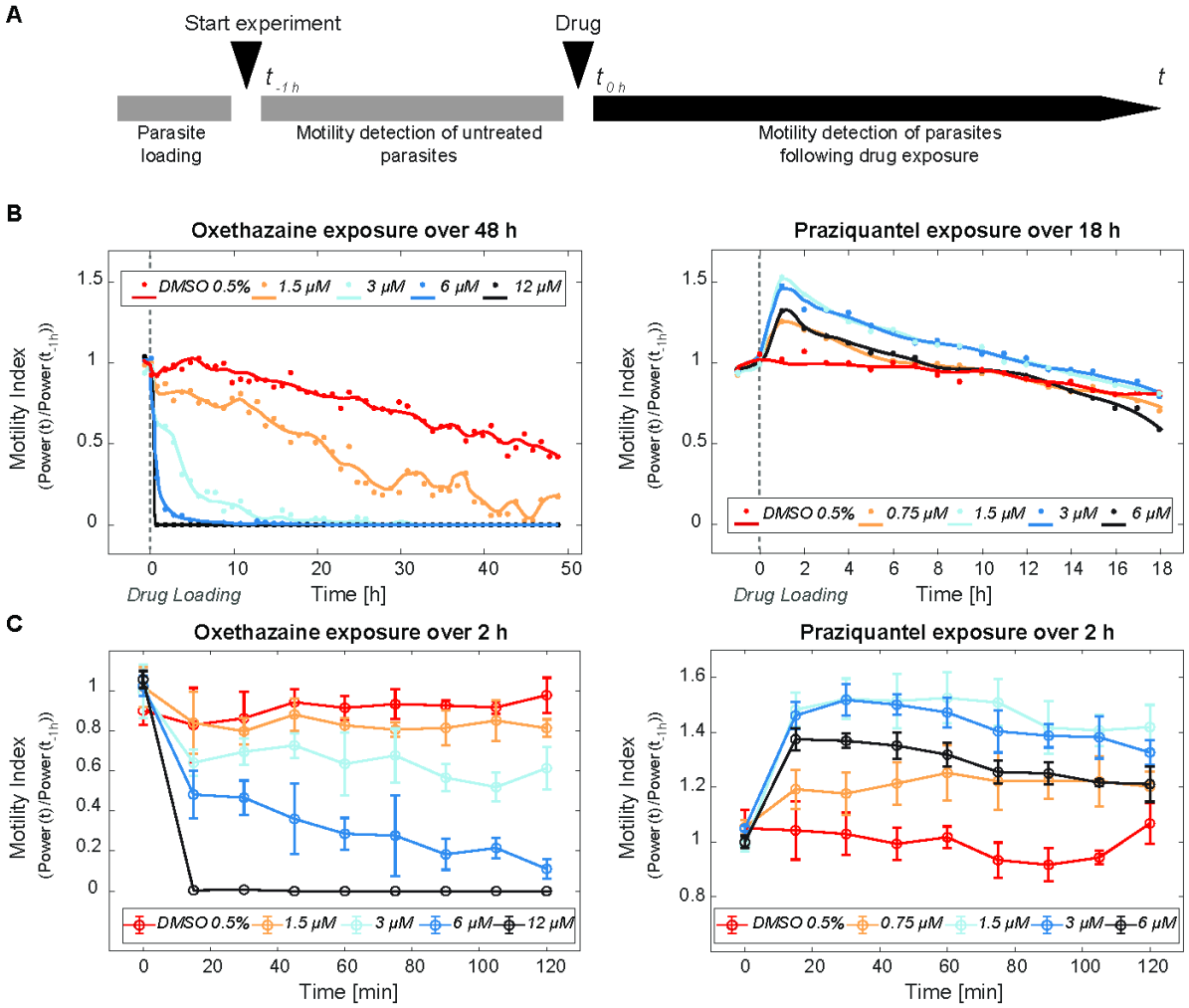

Figure 3. Measurements of drug-induced NTS parasite motility via impedance-based recording. **A** The flow diagram shows the main steps for performing an impedance-based drug assay. First, 30 µL of NTS solutions were loaded into all analysis-unit chambers. After 1 hour of impedance-based motility detection, the measurement was stopped and additional 30 µL of drug solution were dispensed into each chamber. Afterwards, the impedance detection was restarted and recordings of drug-induced motility variations continued until the end of the assay. **B** The graphs show the variations in the motility index of the vehicle-control sample (exposed to 0.5% v/v DMSO) and of NTS exposed to four different concentrations of oxenthazaine (left) and praziquantel (right). For clarity, one point per hour is displayed, and each point indicates the mean value of the motility index determined from three analysis units. Five trend lines were superimposed to the points to guide the eye for the different tested conditions. **C** The motility graphs of the first 2 hours of recording for both, oxenthazaine and praziquantel. Each point represents the mean value of the motility index simultaneously measured with three analysis units, while the error bars represent the standard error of the mean.

2.3.4 Long-term dose-response drug analysis

To evaluate the performance of our platform in continuously assessing NTS viability and generating real-time dose-response curves, we exposed the parasite larvae for 48 hours to six serially diluted concentrations (1.5, 3, 6, 12, 25, 50 µM) of two compounds, oxethazaine and mefloquine, which are known for their antischistosomal activity *in vitro*.[24,28] The impedance-based parasite viability was calculated by normalizing the motility index of each drug condition to the motility index of the vehicle control at each time point along two days of drug exposure.

By measuring parasite viability exposed to oxethazaine via the EIM platform, no signal fluctuations were detected for the NTS incubated with the highest drug concentrations (12 µM, 25 µM and 50 µM) after 30 minutes, indicating that the NTS were dead (**Figure 4A**). For the same time point, the viability upon dosage of 6 µM was already reduced to ~0.5, which indicates that a significant fraction of the NTS population has deceased or lost its motility. After 17 hours, only the parasites exposed to 1.5 µM showed a viability above 0.5 (0.54 ± 0.05), which further decreased to ~0.2 (0.2 ± 0.19) at 48 hours of incubation with the drug. By testing the activity of mefloquine on the NTS, we obtained dose-response curves along time that evidenced a lower potency compared to oxethazaine. After 3 hours, only the parasites exposed to 50 µM were dead, whereas those exposed to 25 µM showed a viability slightly below 0.5 (0.39 ± 0.21). Towards the end of the drug assay (39 h), only the parasites exposed to 6 µM displayed a viability of 0.37 ± 0.19, which further decreased to 0.15 ± 0.08 at 48 hours. Parasites exposed to drug concentrations lower than 6 µM were viable and showed a high level of motility during the entire assay.

We used the viability calculations to extract IC_{50} values of oxethazaine and mefloquine (Figure 4B). IC_{50} corresponds to the drug concentration at which the larvae were compromised in their activity and moving 50% less. Sigmoid fits (shown in Figure 4A) were used to calculate the IC_{50} values over time. The IC_{50} values obtained from the impedance-based viability measurements showed that oxethazaine featured an IC_{50} of 6.1 ± 0.76 µM at 30 minutes incubation. The IC_{50} value rapidly decreased and reached 2.02 ± 0.16 µM after 12 hours of drug exposure. Between 24 and 48 hours, the IC_{50} did not change significantly anymore (1.51 ± 0.21 µM and 1.45 ± 0.34 µM, respectively). In the case of mefloquine, the impedance-based estimations evidenced an IC_{50} of 24 ± 1.42 µM after 3 hours of exposure, which decreased linearly to 8.51 ± 1.07 µM during 24 hours of incubation. Finally, the IC_{50} calculated at 48 h using the EIM platform was 5.05 ± 0.21 µM.

The parasite viability was also evaluated using the standard visual scoring method at 24 and 48 hours in a 96-well plate to validate the IC_{50} estimations obtained with the EIM platform (Movie S1-S3, Supporting Information). The IC_{50} concentrations of oxethazaine obtained from the visual evaluation were 1.39 ± 0.06 µM after 24 hours and 1.23 ± 0.04 µM after 48 hours. In the case of mefloquine, the IC_{50} estimations from the visual method were 2.28 ± 0.22 µM at 24 h, and 2.03 ± 0.16 µM at 48 h. The visual-score-based evaluations were in good accordance and within the same order of magnitude as the results obtained with the impedance-based method (Figure S6, Supporting Information).

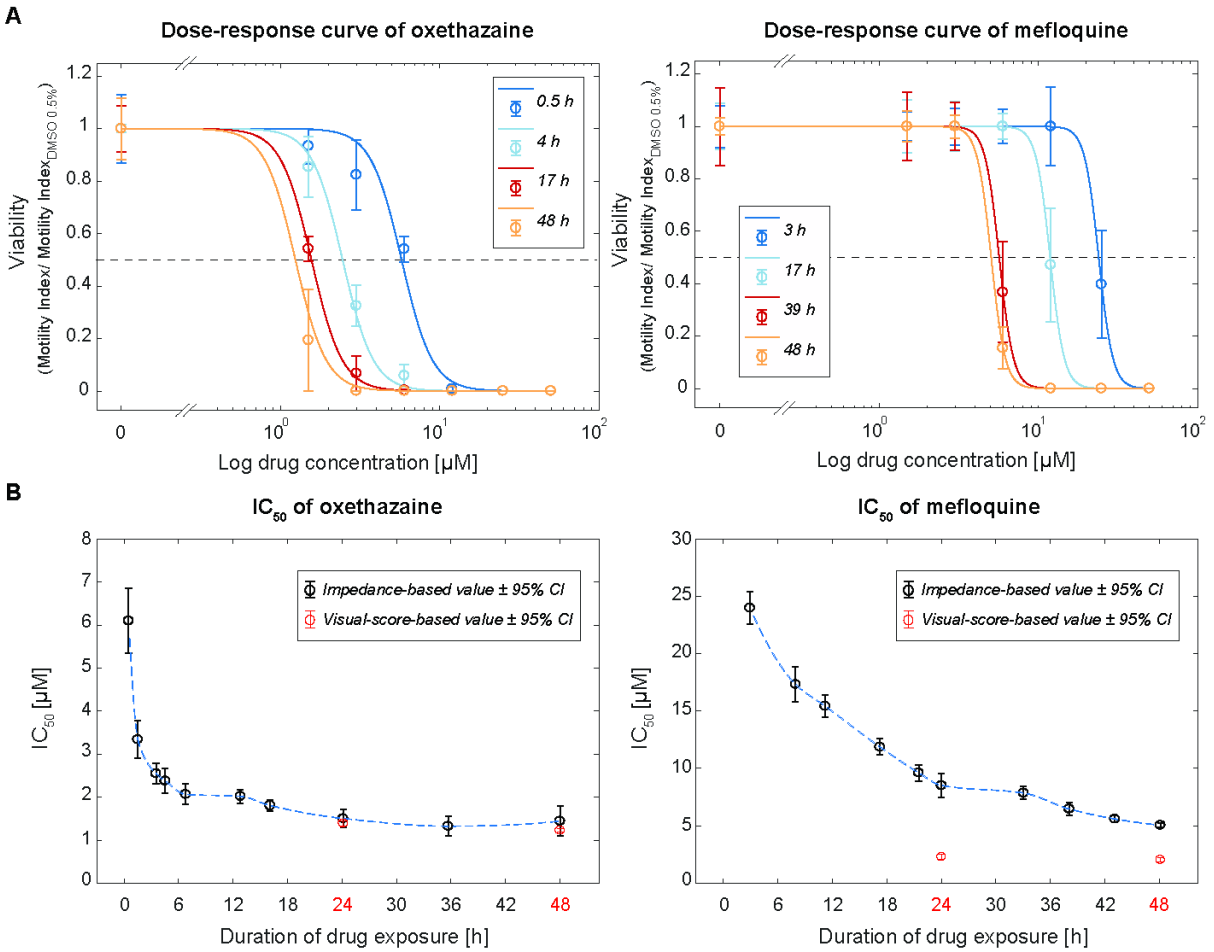

Figure 4. Temporal evolution of the dose-response curves determined through continuous long-term monitoring of NTS viability by impedance-based detection. **A** The graphs show the impedance-based estimations of the NTS viability at four selected time points as a function of drug concentration. The NTS were exposed to six different concentrations (1.5, 3, 6, 12, 25 and 50 µM) of oxethazaine (left) and mefloquine (right) during 48 hours. Each circle represents the mean value of the viabilities of three replicates, and the error bars represent the standard error of the mean. The four sigmoid fits, used to calculate the IC_{50}, values are superimposed to the viability measurements. **B** The temporal evolution of the IC_{50} values for oxethazaine and mefloquine as determined by using impedance-based detection. The IC_{50} values obtained through standard visual scoring at 24 and 48 hours are shown for comparison (marked in red). The circles represent the values obtained through the sigmoidal fits, while the error bars show the 95% confidence intervals.

2.3.5 Characterization of methiothepine drug effect on NTS parasite

As a case study, we challenged our system by investigating the effect of methiothepine on schistosomula. Methiothepine is a tricyclic antipsychotic compound whose behavior on NTS has not been fully characterized *in vitro*.[24] Tricyclic antipsychotic compounds bind to the serotonin transporter (SERT) of helminths and have been studied for their antischistosomal effects.[31] It has been previously shown that SERT antagonists can cause either persistent or transient hyperactivity of helminths and, eventually, can affect parasite viability.[32] To explore the temporal evolution of the dose-response effect, we measured the motility index and the viability of NTS exposed to six different methiothepine concentrations (1.5, 3, 6, 12, 25, 50 μM) for 48 hours. We observed an excitatory effect lasting ~24 hours that was induced by the drug at sub-lethal concentrations (<25 μM at 24 h; **Figure 5A**), which is in line with previous observations of NTS exposed to other members of the tryclic-compound family.[31,32] Live imaging of parasites in the chamber unit confirmed the hyperactivity of NTS that were incubated with sub-lethal methiothepine concentrations (Figure 5B).

After 4 hours of incubation, only the 50 μM-condition caused a drastic decrease in NTS viability (0.2 ± 0.09; Figure 5C). A comparably high level of NTS viability was maintained over 30 hours for lower doses, while, for longer exposure times, methiothepine showed a slow-acting and dose-dependent killing behavior. At the end of the assay, after 48 hours of incubation with the drug, all concentrations higher than 1.5 μM exhibited a viability below 0.5. The extraction of the IC_{50} over time also showed the slow efficacy of methiothepine in killing the NTS (Figure 5D). To inhibit the parasite viability by 50% during the first 24 hours, a concentration of more than 26.81 ± 0.94 μM of methiothepine was required. The IC_{50} calculated after 48 hours using the EIM platform was 2.45 ± 0.9 μM. The IC_{50} values extracted by the standard visual evaluation amounted to 10.88 ± 2.05 μM at 24 hours and 2.22 ± 0.31 μM at 48 hours. Differences in IC_{50} values obtained at 24 hours by the two methods were expected, as the hyperactivity of the NTS introduces additional difficulties to visually score the parasite status for the operator (Movie S4, Supporting Information). Nevertheless, the IC_{50} values obtained at 48 hours with the two different methods are in good accordance.

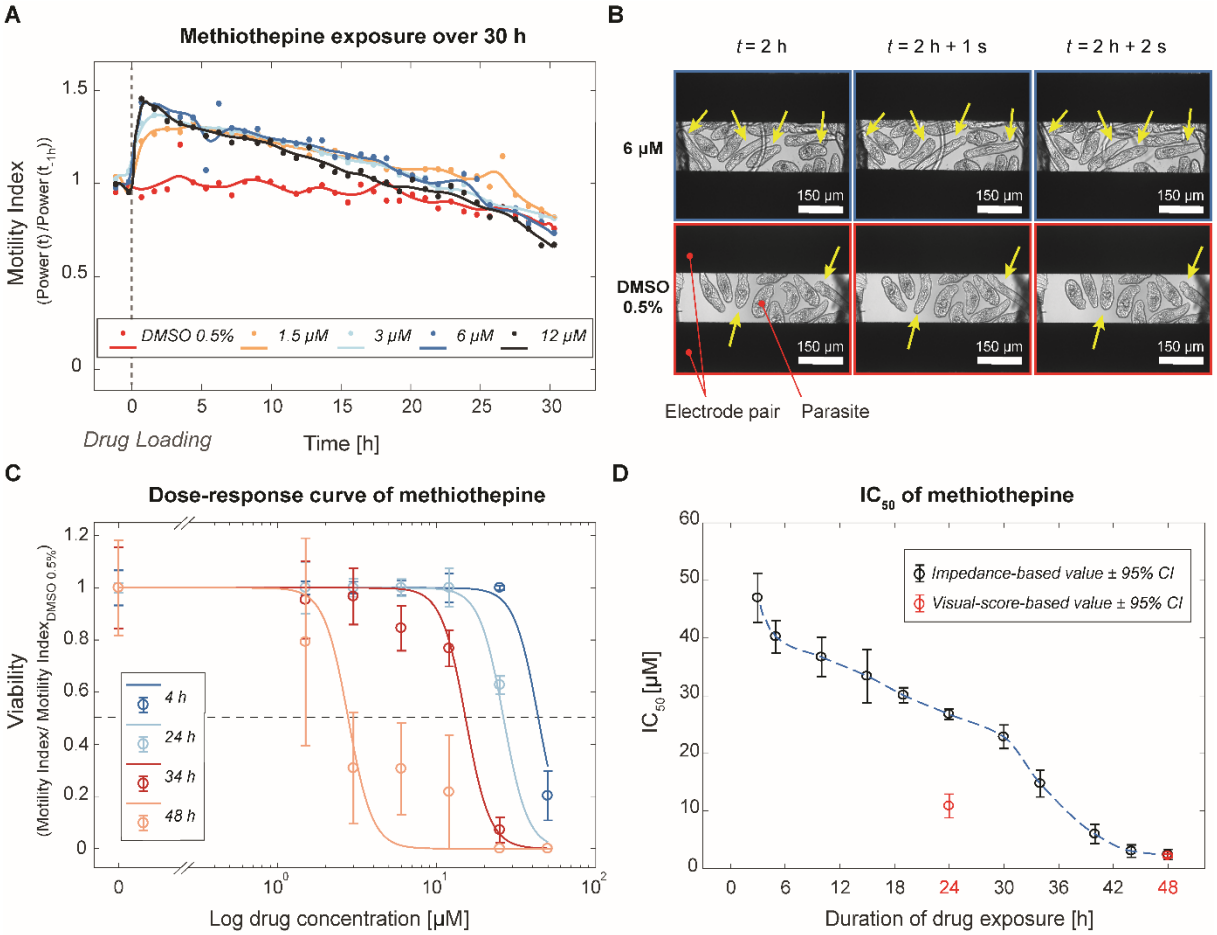

Figure 5. Characterization of NTS parasite motility and viability during long-term exposure to methiothepine. **A** The motility values of the NTS, exposed to four different concentrations of methiothepine, are shown and compared to the motility indices of the vehicle-control sample (NTS exposed to 0.5% v/v DMSO). Each point represents the mean value of the motility indices of three replicates. Trend lines were superimposed to the points to guide the eye for the different tested conditions. **B** Time-lapse images of NTS showed qualitative movement differences between NTS exposed to 6 µM methiothepine and to 0.5% (v/v) DMSO. The yellow arrows indicate parasites that moved between the different frames. **C** The impedance-based viability measurements of NTS at four selected time points are plotted as a function of the drug concentration. The NTS were incubated with six different concentrations of methiothepine (1.5, 3, 6, 12, 25 and 50 µM) during 48 hours. Each circle represents the mean viability value of three replicates, and the error bars represent the standard error of the mean. The sigmoid fit was used to calculate the IC_{50} value at each time point. **D** IC_{50} values, calculated from the impedance-based detection of NTS viability, are compared with IC_{50} values obtained by standard visual scoring at 24 and 48 hours (marked in red). The circles represent the values determined from the sigmoid fits, while the error bars show the 95% confidence intervals.

2.4 Discussion

Advancing the development of automated and medium- or high-throughput approaches for antischistosomal drug screening is of fundamental importance for the identification of new compound candidates. In this work, we introduced a novel platform with integrated electrodes for the automated detection of schistosomula viability by means of an impedance-based method. In particular, we showed how this label-free technique offers an unbiased method to quantitatively score parasite viability, and that the impedance method enables long-term and continuous assessment of drug efficacy.

The EIM platform allows for robust and simple screening of the viability of NTS that have been exposed to different drug concentrations, and it requires minimal operator interference. The use of micron-size electrodes and the small detection volumes reduces the number of NTS that are needed for analysis approximately 10 fold in comparison to the current standard visual evaluation method,[12] and up to 30 fold in comparison to luminescence- and fluorescence-based assays reported in literature.[33,34] The arrangement of the pyramid-shape wells facilitates the loading of the parasite samples with standard multichannel pipettes and ensures the positioning of the parasites on top of the electrodes for over 48 hours. In addition, the 96-well format of the platform enables compatibility with standard lab automation tools, such as automated liquid handlers, which further improves automation and increases the throughput.

The impedance-based readout allows to overcome major limitations associated with the currently used visual evaluation method, which include limited throughput, potential subjectivity and bias in the operator's scoring.[14,35] In a previous proof-of-principle study, we showed the possibility to use impedance measurements of NTS motility as proxy for parasite viability.[21] However, the previous system did not allow for long-term culturing of NTS and could only provide end-point evaluation of the larvae viability. Furthermore, the complex fluidic structure that was used to confine the larvae in the sensing area and to increase the signal-to-noise ratio of the measurements strongly limited the analysis throughput to four recordings in parallel. Here, we were able to preserve the previously demonstrated high sensitivity of the impedance-based characterization by confining the larvae to a small detection volume in an easy-to-operate open fluidic structure. This solution enabled to simplify the platform operation and increase the analysis throughput to up to 32 recordings in parallel. We also determined the Z'-factor, which indicates the quality of an assay based on the difference of mean values of positive and negative controls in reference to the corresponding standard deviations.[36,37] The developed system showed a Z'-factor of 0.63 (calculated from 32 x 4 measurements of pre-

treated motile and dead parasites of the impedance-based assays, $power_{motile}$ = -12.8 ± 1.9 dBμ and $power_{dead}$ = -34.5 ± 0.8 dBμ), which highlights the potential of the platform as a robust and higher throughput antischistosomal screening method according to NIH guidelines.[36] The novel design also enabled the long-term culturing of the parasite larvae to realize a real-time evaluation of drug activity, which is important for providing insights into drug kinetics and for selecting fast-acting compounds.[38] High and fast drug activity along with low toxicity are relevant criteria to select promising antischistosomal lead compounds.[24]

The constant decrease of motility in the control samples during long-term *in vitro* culture, a common behavior of NTS also observed in standard assays, may introduce artifacts in the evaluation of compound efficacy in multi-day drug-exposure experiments using motility-based parasite evaluation. Therefore, medium exchanges may be considered to extend the viability time of the NTS in the platform for long-term assays.

We first validated the EIM platform by recording variations in NTS motility upon dosage of three active drugs triggering antischistosomal effects (Figure S7, Supporting Information). By analyzing the effect of praziquantel on NTS motility, we were able to reproduce the *in vitro* excitatory action of the drug on parasites, which lasted for over 18 hours. This hypermotility is caused by the activity of praziquantel as calcium channel agonist, which increases the calcium concentration in the schistosomula body within minutes of exposure and causes intense and sustained muscular contraction of the parasites.[26,39] In contrast, the exposure of NTS to oxethazaine caused a fast-acting inhibitory effect on their motility.[24] Motility reduction is most likely caused by the high affinity of the drug to the sodium channels of the NTS, which has been shown to have an *in vitro* inhibitory effect on the schistosomula smooth muscles by blocking the action of serotonin.[27] Via our impedance-based detection, we were able to confirm the fast action and the high efficacy of the drug *in vitro*, which showed an IC_{50} value of 3.48 μM already after 1 hour of incubation. To investigate complex antischistosomal drug response, we studied the effect of mefloquine on NTS with the EIM platform. This antimalarial compound is known to induce hyperactivity and to affect NTS viability *in vitro*, which may be attributed to its potential role as an inhibitor of glycolysis and interference with schistosomula metabolic activity.[40] Our impedance-based IC_{50} estimations confirmed the reported lethal effect of mefloquine on NTS showing values below 10 μM after 20 hours of drug exposure.[21] Differences in IC_{50} values, obtained with impedance-based and visual methods were expected for mefloquine at 24 h, as the morphology of the NTS was highly affected at high drug

concentrations, and it was difficult to detect subtle movements of the larvae by eye, which, however, remained detectable using the impedance system.[21,28]

After validating the ability of our method in detecting changes of NTS motility caused by drugs with known *in vitro* effects, we used the EIM platform to analyze the response of the schistosomula to methiothepine. The complex dose- and time-dependent response of the NTS to the compound underlines the importance of continuous monitoring of parasites when investigating the efficacy of new drugs. Methiothepine is an antipsychotic drug of the tricyclic group, which acts as an inhibitor of both the serotonin receptor and the SERT, depending on the dose.[24,29] A transient increase in schistosomula motility was detected for sub-lethal drug concentrations (< 12 μM of methiothepine for the first 24 hours of incubation). This result corroborates the effects observed for two classical SERT inhibitors, fluoxetine and clomipramine, which were shown to induce strongly hyperactive phenotypes.[41] Recently, incubation of NTS with paroxetine, another *S. mansoni* SERT inhibitor, in the 1-10 μM concentration range was reported to have a similar hypermotility effect during the first 24 hours of incubation, while the motility then decreased for longer exposure times.[32] Our measurements demonstrate that methiothepine has a similar effect on NTS for an analogous concentration range, as the schistosomula showed decreased motility after 24 hours. Higher concentrations of methiothepine (> 12 μM) resulted in a rapid loss of motility and a consequent reduction in larvae viability,[42] which confirmed earlier findings[24] and was similar to what has been previously reported for high concentrations of paroxetine.[32]

In summary, we developed a parallelized and automatable drug-screening platform, which continuously provides dose-dependent viability scores of NTS. The drug-dose responses of the parasites to four different antischistosomal compounds that were obtained through impedance detection show good agreement with those obtained from standard visual scoring of NTS motility. This agreement evidences that the impedance-based approach constitutes a reliable alternative method to identify novel drug candidates *in vitro*. The current platform layout enables the operator to use up to 4 chips, which include 32 analysis units in parallel, with a single instrument. The electrical detection method allows for further parallelization to achieve increased throughput with minimal experimental-setup modifications. The chip design, implemented in PDMS, can be easily realized with standard plastic materials to avoid issues related to compound ad/absorption in PDMS, and fabrication processes for mass production, such as injection molding, can be used. Finally, the EIM platform can be readily adapted to other relevant motile schistosome stages, such as cercariae, juvenile and adult parasites, or to

different parasite species by simple modification of the sensing-area design, which will contribute to improve anthelmintic drug-screening applications.

2.5 Experimental section

Culture medium and drugs: M199 medium was obtained from Gibco (cat. no. 22340-020, Thermo Fisher Scientific, Waltham, USA). Penicillin/streptomycin 10′000 U/mL (pen/strep, cat. no. P4333-100ML, Sigma-Aldrich, Buchs, Switzerland) and inactivated fetal calf serum (iFCS, cat. no. 2-01F30-I, Bioconcept AG, Allschwil, Switzerland) were purchased from Bioconcept AG. All media were sterilized by filtration using a 0.22 µm filter bottle (cat. no. 431097-COR, Vitaris AG, Baar, Switzerland). Oxethazaine (cat. no. O5380-5G, Sigma-Aldrich, Buchs, Switzerland), praziquantel (cat. no. P4668-5G, Sigma-Aldrich, Buchs, Switzerland), mefloquine (cat. no. M2319-100MG, Sigma-Aldrich, Buchs, Switzerland) and methiothepine (cat. no. M149-100MG, Sigma-Aldrich, Buchs, Switzerland) were all purchased as racemic powders from Merck (Sigma-Aldrich).

Parasite culture and transformation: *S. mansoni* culturing and NTS transformation were performed according to protocols previously described in literature.[12,43] In brief, *S. mansoni* -infected *Biomphalaria glabrata* snails were placed singularly in 24-well plates and exposed to a neon lamp (36 W, 4000 K, 3350 lumens), for 3-4 hours, to induce the shedding of cercariae. The supernatant was collected and filtered to remove impurities in the solution. The mechanical transformation of the cercariae into NTS was performed by physically removing the tail by constricted passage through a Luer-Lok tip in between two 12 mL syringes. The NTS were resuspended in M199 medium supplemented with 5% (v/v) iFCS, 1% pen/strep and 1% antifungal mix.

In-vitro antischistosomal drug assay: The drug assay in the EIM platform was performed by first dispensing 30 µL of NTS solution with 1 NTS/2 µL. After 1 hour recording of the NTS-induced fluctuations as baseline activity, 30 µL of drug solution (1.5-50 µM in NTS medium) were added, yielding a total volume of 60 µL in each analysis unit. Final drug concentrations ranged between 0.75 µM and 25 µM in a 2x dilution series. In each assay, 0.5% (v/v) DMSO (vehicle control) and blank M199 medium controls were included. All conditions were measured in quadruplicates. NTS viability under each test condition was measured every 15 minutes for 48 hours in the EIM platform. A viability score ranging from 0 to 1 (0 = non motile and dead parasite, 1= motile and alive parasite) was assigned to each test condition and per time point, according to the relative motility of the parasites with respect to the vehicle control motility (see Data Analysis for more information).

In parallel, identical drug concentrations were set up in a 96-well plate (cat. no. 83.3924, Sarstedt, Nümbrecht, Germany) to perform the same experiment by using the standard visual scoring method to compare the results obtained via standard viability detection with the impedance-based characterization. 50 µL of 2 NTS/1 µL suspension were dispensed in each well, and subsequently 50 µL of drug-concentration solutions were added to reach a final drug concentration ranging from 0.75 µM to 25 µM. Each condition was prepared in duplicates or triplicates. A trained operator evaluated the viability of the NTS in the different drug solutions assigning a score from 0 to 3 on a quarter-of-a-point scale. In this scale, 0 represents NTS with complete loss of motility, while 3 represents NTS with good motility, good overall viability and healthy behavior.[12] Visual scoring was carried out after 24 and 48 hours of drug incubation.

Each drug test was performed in a separate experiment.

Chip fabrication: The analysis chip consisted of two parts: a polydimethylsiloxane (PDMS) layer containing the microfluidic structures and a glass slide with a patterned metal layer. The PDMS layer was cast from a 3D-printed master mold (fabricated in Accura SL 5530, Protolabs, Feldkirchen, Germany) by using soft lithography. The silicone and curing agent (Sylgard 184, Dow Corning Corp., Midland, USA) were mixed at a 10:1 (w/w) ratio, degassed and poured onto the master mold. After curing or 2 h at 85 °C, the PDMS layer was peeled off the master mold and cut into individual chips.

The 200-nm-thick platinum electrodes were deposited on a 6-inch, 500-µm-thick borosilicate glass wafer via a lift-off process. Briefly, the wafer was spin-coated with lift-off resist (LOR3B, Microchem Corp., Newton, USA), followed by a positive photoresist (S1813, Rohm-Haas, Schwalbach, Germany) and patterned using photolithography. After Pt deposition, the lift-off of the metal was carried out by using Mr-Rem-400 remover (micro resist technology GmbH, Berlin, Germany). Finally, the glass wafer was diced into individual glass slides (20 mm x 62 mm).

Each PDMS chip and patterned glass slide were aligned using a custom-made alignment tool and irreversibly bonded together after surface treatment using oxygen plasma (Harrick Plasma PDC-002, Harrick Plasma, Ithaca , USA).

Parylene coating of PDMS chip: To prevent drug absorption by PDMS during long-term compound incubation (48 h), we coated the chip surface with parylene-C polymer.[30,44] All microfluidic chips were coated using a parylene coating system (Parylene P6, Diener Electronic GmbH, Ebhausen, Germany). The devices were placed in the center of the rotating trays in the

deposition chamber. 10 g of parylene-C dimer powder (parylene, Diener Electronic GmbH, Ebhausen, Germany) were placed into the evaporator. The system was evacuated to 0.012 mbar before the deposition was initiated. The powder was evaporated in a temperature range of up to 170 °C, cleaved in the pyrolysis tube at 720° C, and deposited onto the samples at 80° C and 0.03 mbar over the course of 4.2 h (Figure S2A, Supporting Information). After the evaporation of the parylene powder, the deposition chamber was cooled down to 41°C and the devices were then removed from the coating system.

The thickness of the deposited parylene-C layer was evaluated by using a 3D optical surface profiler (Zygo Corporation, Middlefield, USA) on a microscope slide (Menzel-Gläser, Thermo Scientific, Dreieich, Germany), placed in the chamber with the devices (Figure S2B, Supporting Information). For this purpose, the parylene layer was cut, one part was pealed from the glass slide and the thickness was measured along the cut.

Rhodamine absorption evaluation: To compare the dye absorption in parylene-coated PDMS and bare PDMS chips, 30 µL of rhodamine B (83689, Sigma-Aldrich, Buchs, Switzerland) solution (0.1 mM in DI water) were loaded into each well chamber. Fluorescence images inside the chambers were captured before the loading of the dye, at 5 min, 1 h, and 2 h after sample loading using an inverted microscope (Nikon Ti-E, Nikon, Egg, Switzerland). During the measurements, the chips were kept in the dark to prevent photobleaching and at 37° C, 5% CO_2 using a stage-top incubator. The microscope was controlled using Youscope software, and offline image analysis was performed using ImageJ (Figure S3, Supporting Information).

EIM platform assembly: The chips were placed between a custom-made printed-circuit board (PCB) and a chip holder (Figure S8, Supporting Information). The PCB was designed in Altium Designer 17.0 and ordered from PCBWay (Hangzhou, China). Electrical connections between the PCB and the analysis chips were obtained by contacting the electrode pads from above using spring-loaded pins (0956-0-15-20-75-14-11-0, Mill-Max Mfg. Corp., Oyster Bay, USA). The PCB featured four window-like openings (15 mm x 58 mm) to allow for visual access to the chips without disassembling the platform.

The chip holder was 3D-printed by means of stereolithography (Protolabs, Feldkirchen, Germany) in ABS-like material (Accura® Xtreme™ White 200, Protolabs, Feldkirchen, Germany). The printing material was selected as to withstand the high-humidity conditions in the incubator and the high force levels required for reliable chip connection. The chip holder also featured four openings to allow for visual examination of the parasites using a standard inverted microscope.

Neodymium block magnets (Q-10-03-02-HN, Supermagnete, Uster, Switzerland) were used to align and keep the chip holder and PCB in position, and to provide the force necessary for pressing the spring-loaded pins onto the electrode pads on the chips for stable electrical connection. The magnets were attached to the chip holder and the PCB with a 2-component white epoxy adhesive (EA 9492, Henkel, Düsseldorf, Germany). Finally, the platform was covered with an omniTray lid (Nunc™ OmniTray™ Single-Well Plate, Thermo Fisher Scientific, Reinach, Switzerland) to prevent medium evaporation from the culture units.

Impedance measurement: Impedance measurements were performed using a HF2-LI impedance spectroscope (Zurich Instruments AG, Zurich, Switzerland). The analysis chips were contacted via a custom-made PCB to route the connections from the impedance spectroscope to the integrated electrodes. An AC voltage with an amplitude of 100 mV and a frequency of 500 kHz was applied between the selected pair of coplanar electrodes. The current flowing through the system was then converted to voltage through a trans-impedance amplifier (HF2TA, Zurich Instruments AG, Zurich, Switzerland) with a 1-kΩ feedback resistor and sampled by the HF2-LI with a sampling frequency of 14 kHz. The acquired signal was filtered with a 2.2-kHz low-pass filter in the impedance spectroscope. The amplitude variation of the sampled current-to-voltage signal was then used for further analysis. A custom-made software, written in Python, was used to control the selection of the electrode pair and to control the signal acquisition.

Microscopy: During the recording of the impedance signals, the platform was placed on the stage of an automated microscope. Microscopic images were obtained using an inverted microscope (Nikon Ti-E, Nikon, Egg, Switzerland), placed in an environmental control box, which maintained a stable temperature of 37 °C, CO_2 of 5 % and a relative humidity ~90 %. Bright-field images were captured on the Nikon microscope using a Nikon Plan Fluor 10X objective (NA 0.3, WD 16 mm). Automated imaging was performed for 20 sec every hour from each analysis unit during the entire experiment. The live micrographs were recorded to compare the results of the gold-standard evaluation (visual scoring) with those obtained by the impedance-based readout. The microscope was controlled using Youscope software, and offline image analysis was performed using ImageJ.

For standard visual assessment, the parasites were incubated in culture medium with the test compounds in a 96-well plate in duplicates/triplicates for 48 hours. Every 24 hours, the drug effects on the parasites were assessed by visual scoring with a light microscope using a magnification of 4-10X.

Computational modeling: A finite-element-method (FEM) model was used to verify the current-density distribution in the microwell (Figure S4A, Supporting Information). The current passing through the electrodes in the measurement chamber was calculated by integrating the current density over the middle orthogonal cross-section area of the microwell in Comsol Multiphysics 5.4 (COMSOL AB, Stockholm, Sweden). To evaluate the current density across the entire depth of the microwell, we derived the current over the microwell height (Figure S4B, Supporting Information).

Data analysis: The voltage-converted current signals were processed and analyzed in MATLAB (The MathWorks Inc., Natick, USA). The recorded signals were filtered using a 0.2-Hz high-pass filter to remove slow signal variation due to solution evaporation. Each analysis unit may exhibit different baseline values due to differences in solution conductivity caused, e.g., by different drug compounds or drug concentrations, or by subtle variations in the alignment of the electrodes with the microwell base. To reduce the influence of such effects, the high-pass-filtered traces were normalized with respect to the mean baseline signal of the respective unit. To quantify the signal fluctuations induced by the parasites, we computed the power of the filtered and normalized signal in a 1-3 Hz bandwidth. This approach minimizes the effect of readout noise, which is present at higher frequencies, while it preserves the signal power that is related to the movement of the NTS between the electrodes. To confirm that the sample was correctly loaded in the microwell, we first measured the signal power during one hour prior to addition of the drug compound. Only analysis units, the signal power of which ranged between [-18.5, -7.1] dBμ (± 3 standard deviations of the average NTS motile value, -12.8 ± 1.9 dBμ), were further analyzed. The runtime calculated power of the measured fluctuations in each unit was normalized to its initial power magnitude (t_{-1hr}) in order to compare measurements with different numbers of NTS in the sensing compartments and to extract motility index parameters. To evaluate NTS viability, we normalized the motility index of every condition to the motility index of the vehicle control. This procedure followed the normalization performed in the standard drug assay using visual scoring and it helped to remove NTS phenotype variations caused by the vehicle.[21] In addition, we assigned a viability value of 1 to all the microwells in which the NTS showed a motility equal or higher than that in the vehicle control microwells.

The viability scores obtained from visual evaluation were averaged across replicates and normalized to the vehicle-control viability score.

The half-maximum inhibitory concentration (IC_{50}) values of the tested drugs were determined for both visual-inspection-based and impedance-based viability scores by applying a nonlinear least-squares analysis. A two-parameter sigmoid function with a constant hill slope was fitted to the viability scoring data. A single average slope was first computed across all experimental time points for each drug and then applied to the fit for the estimation of the IC_{50} during the continuous long-term measurements.

We computed the Z'-factor of our impedance-based assays to determine the suitability of the EIM platform for high-throughput screening applications.[36,37] The Z'-factor is defined as

$$\text{Z'-factor} = 1 - \frac{3\sigma_{+} + 3\sigma_{-}}{|\mu_{+} - \mu_{-}|}$$

where μ_+ and μ_- indicate the mean signal power of alive (motile and pre-treated) and dead (non-motile) schistosomula and σ_+ and σ_- the corresponding standard deviations.

2.6 Acknowledgements

P.S.R. and F.C.L. contributed equally to this work. The work was financially supported by Swiss National Science Foundation under contract CR32I2_166329: “Infected body-on-chip” and the Swiss Commission for Technology and Innovation under contract 25727.1 PFLS-LS: “Broadband high-accuracy impedance analyzer”. The authors acknowledge the clean-room facility at D-BSSE, ETH Zurich, for help and support. Further, the authors would like to thank Carlo Cosimo Campa, Fernando Cardes, Nassim Rousset, and Vijay Viswam, all at D-BSSE of ETH Zurich, for their scientific input and support throughout the project.

2.7 References

[1] L. Conteh, T. Engels, D. H. Molyneux, *Lancet* **2010**, *375*, 239.

[2] H.-B. Weng, H.-X. Chen, M.-W. Wang, *Infect. Dis. Poverty* **2018**, *7*, 67.

[3] D. P. McManus, D. W. Dunne, M. Sacko, J. Utzinger, B. J. Vennervald, X.-N. Zhou, *Nat. Rev. Dis. Prim.* **2018**, *4*, 13.

[4] B. Gryseels, K. Polman, J. Clerinx, L. Kestens, *Lancet* **2006**, *368*, 1106.

[5] D. G. Colley, A. L. Bustinduy, W. E. Secor, C. H. King, *Lancet* **2014**, *383*, 2253.

[6] J. F. Friedman, R. M. Olveda, M. H. Mirochnick, A. L. Bustinduy, A. M. Elliott, *Bull. World Health Organ.* **2018**, *96*, 59.

[7] D. Cioli, L. Pica-Mattoccia, A. Basso, A. Guidi, *Mol. Biochem. Parasitol.* **2014**, *195*, 23.

[8] D. Cioli, L. Pica-Mattoccia, *Parasitol. Res.* **2003**, *90*, 3.

[9] A. C. Mafud, M. P. N. Silva, G. B. L. Nunes, M. A. R. de Oliveira, L. F. Batista, T. I. Rubio, A. C. Mengarda, E. M. Lago, R. P. Xavier, S. J. C. Gutierrez, P. L. S. Pinto, A. A. da Silva Filho, Y. P. Mascarenhas, J. de Moraes, *Toxicol. Vitr.* **2018**, *50*, 1.

[10] R. A. Paveley, Q. D. Bickle, *Parasite Immunol.* **2013**, *35*, 302.

[11] A. M. C. Canavaci, J. M. Bustamante, A. M. Padilla, C. M. Perez Brandan, L. J. Simpson, D. Xu, C. L. Boehlke, R. L. Tarleton, *PLoS Negl. Trop. Dis.* **2010**, *4*, e740.

[12] F. C. Lombardo, V. Pasche, G. Panic, Y. Endriss, J. Keiser, *Nat. Protoc.* **2019**, *14*, 461.

[13] J. Keiser, *Parasitology* **2010**, *137*, 589.

[14] E. Peak, K. F. Hoffmann, *An. Acad. Bras. Cienc.* **2011**, *83*, 649.

[15] D. Das, V. Ramachandra, S. Islam, H. Bhattacharjee, J. Biswas, A. Koul, P. Deka, A. Deka, *Indian J. Ophthalmol.* **2016**, *64*, 794.

[16] T. Manneck, O. Braissant, Y. Haggenmuller, J. Keiser, *J. Clin. Microbiol.* **2011**, *49*, 1217.

[17] L. Tritten, A. Silbereisen, J. Keiser, *Int. J. Parasitol. Drugs Drug Resist.* **2012**, *2*, 98.

[18] R. A. Paveley, N. R. Mansour, I. Hallyburton, L. S. Bleicher, A. E. Benn, I. Mikic, A. Guidi, I. H. Gilbert, A. L. Hopkins, Q. D. Bickle, *PLoS Negl. Trop. Dis.* **2012**, *6*, 1.

[19] N. R. Mansour, Q. D. Bickle, *PLoS Negl. Trop. Dis.* **2010**, *4*, e795.

[20] G. Rinaldi, A. Loukas, P. J. Brindley, J. T. Irelan, M. J. Smout, *Int. J. Parasitol. Drugs Drug Resist.* **2015**, *5*, 141.

[21] K. Chawla, M. M. Modena, P. S. Ravaynia, F. C. Lombardo, M. Leonhardt, G. Panic, S. C. Bürgel, J. Keiser, A. Hierlemann, *ACS Sensors* **2018**, *3*, 2613.

[22] T. Sun, H. Morgan, *Microfluid. Nanofluidics* **2010**, *8*, 423.

[23] S. C. Bürgel, L. Diener, O. Frey, J. Y. Kim, A. Hierlemann, *Anal. Chem.* **2016**, *88*, 10876.

[24] G. Panic, M. Vargas, I. Scandale, J. Keiser, *PLoS Negl. Trop. Dis.* **2015**, *9*, e0003962.

[25] N. Vale, M. J. Gouveia, G. Rinaldi, P. J. Brindley, F. Gärtner, J. M. Correia da Costa, *Antimicrob. Agents Chemother.* **2017**, *61*, 1.

[26] V. Silva-Moraes, F. F. B. Couto, M. M. Vasconcelos, N. Araújo, P. M. Z. Coelho, N. Katz, R. F. Q. Grenfell, *Mem. Inst. Oswaldo Cruz* **2013**, *108*, 600.

[27] R. K. Parakh, N. S. Patil, *Int. J. Res. Med. Sci.* **2018**, *6*, 383.

[28] J. Keiser, T. Manneck, M. Vargas, *J. Antimicrob. Chemother.* **2011**, *66*, 1791.

[29] A. C. K. Fontana, M. S. Sonders, O. S. Pereira-Junior, M. Knight, J. A. Javitch, V. Rodrigues, S. G. Amara, O. V. Mortensen, *Eur. J. Pharmacol.* **2009**, *616*, 48.

[30] H. Sasaki, H. Onoe, T. Osaki, R. Kawano, S. Takeuchi, *Sensors Actuators B Chem.* **2010**, *150*, 478.

[31] M.-H. Abdulla, D. S. Ruelas, B. Wolff, J. Snedecor, K.-C. Lim, F. Xu, A. R. Renslo, J. Williams, J. H. McKerrow, C. R. Caffrey, *PLoS Negl. Trop. Dis.* **2009**, *3*, e478.

[32] B. J. Neves, R. F. Dantas, M. R. Senger, W. C. G. Valente, J. D. M. Rezende-Neto, W. T. Chaves, L. Kamentsky, A. Carpenter, F. P. Silva-Junior, C. H. Andrade, *Medchemcomm* **2016**, *7*, 1176.

[33] E. Peak, I. W. Chalmers, K. F. Hoffmann, *PLoS Negl. Trop. Dis.* **2010**, *4*, e759.

[34] C. Lalli, A. Guidi, N. Gennari, S. Altamura, A. Bresciani, G. Ruberti, *PLoS Negl. Trop. Dis.* **2015**, *9*, e0003484.

[35] B. Ramirez, Q. Bickle, F. Yousif, F. Fakorede, M.-A. Mouries, S. Nwaka, *Expert Opin.*

Drug Discov. **2007**, *2*, S53.

[36] G. S. Sittampalam, N. P. Coussens, M. Arkin, D. Auld, C. Austin, B. Bejcek, M. Glicksman, J. Inglese, P. W. Iversen, J. Mcgee, O. Mcmanus, L. Minor, A. Napper, J. M. Peltier, T. Riss, O. J. Trask, J. Weidner, Eds. , Assay Guidance Manual, Eli Lilly & Company And The National Center For Advancing Translational Sciences, 2004.

[37] J. H. Zhang, T. D. Y. Chung, K. R. Oldenburg, *J. Biomol. Screen.* **1999**, *4*, 67.

[38] M. J. Smout, A. C. Kotze, J. S. McCarthy, A. Loukas, *PLoS Negl. Trop. Dis.* **2010**, *4*, e885.

[39] R. Pax, R. Fetterer, J. L. Bennett, *Comp. Biochem. Physiol. Part C Comp. Pharmacol.* **1979**, *64*, 123.

[40] T. Manneck, J. Keiser, J. Müller, *Parasitology* **2012**, *139*, 497.

[41] N. Patocka, P. Ribeiro, *Mol. Biochem. Parasitol.* **2013**, *187*, 32.

[42] J. P. Boyle, T. P. Yoshino, *J. Parasitol.* **2005**, *91*, 542.

[43] J. N. Milligan, E. R. Jolly, *J. Vis. Exp.* **2011**, 1.

[44] M. W. Toepke, D. J. Beebe, *Lab Chip* **2006**, *6*, 1484.

2.8 Supporting information

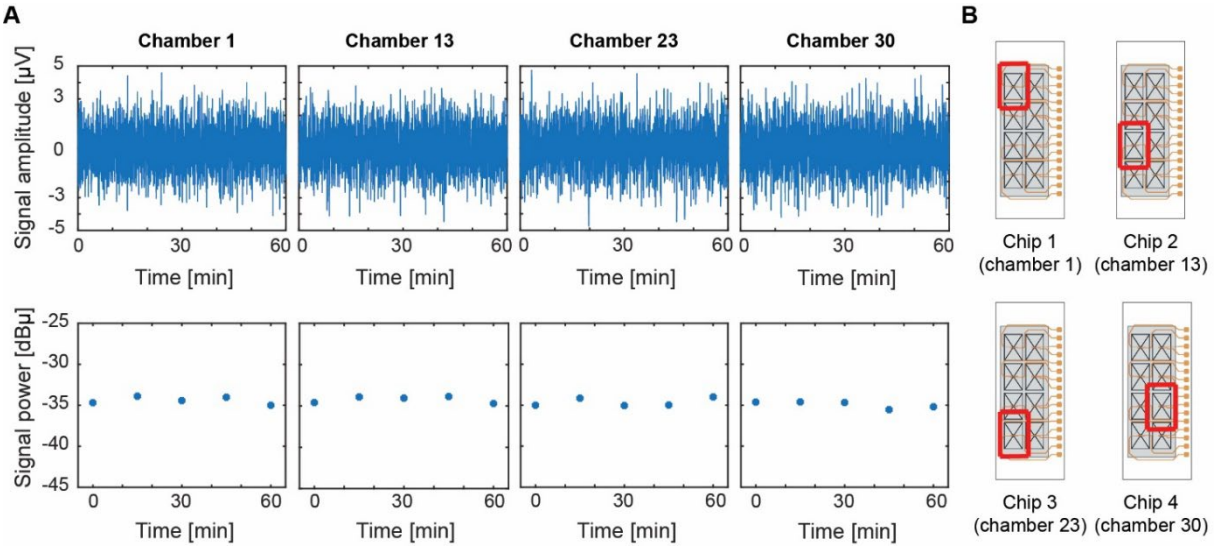

Figure S1. Background noise characterization in the EIM platform. **A** Noise-level characterization was obtained by applying 100 mV AC voltage in four units of four different chips, which were loaded with 30 µL of M199 medium solution. The top graphs show the high-pass-filtered traces of the selected microwells. The bottom graphs represent the signal power of the filtered and normalized signal, which was calculated every 15 min during 1 hour. The power unit refers to 10^{-6} a.u. **B** Positions of the four analysis units from separate chips that have been used for the background noise experiment.

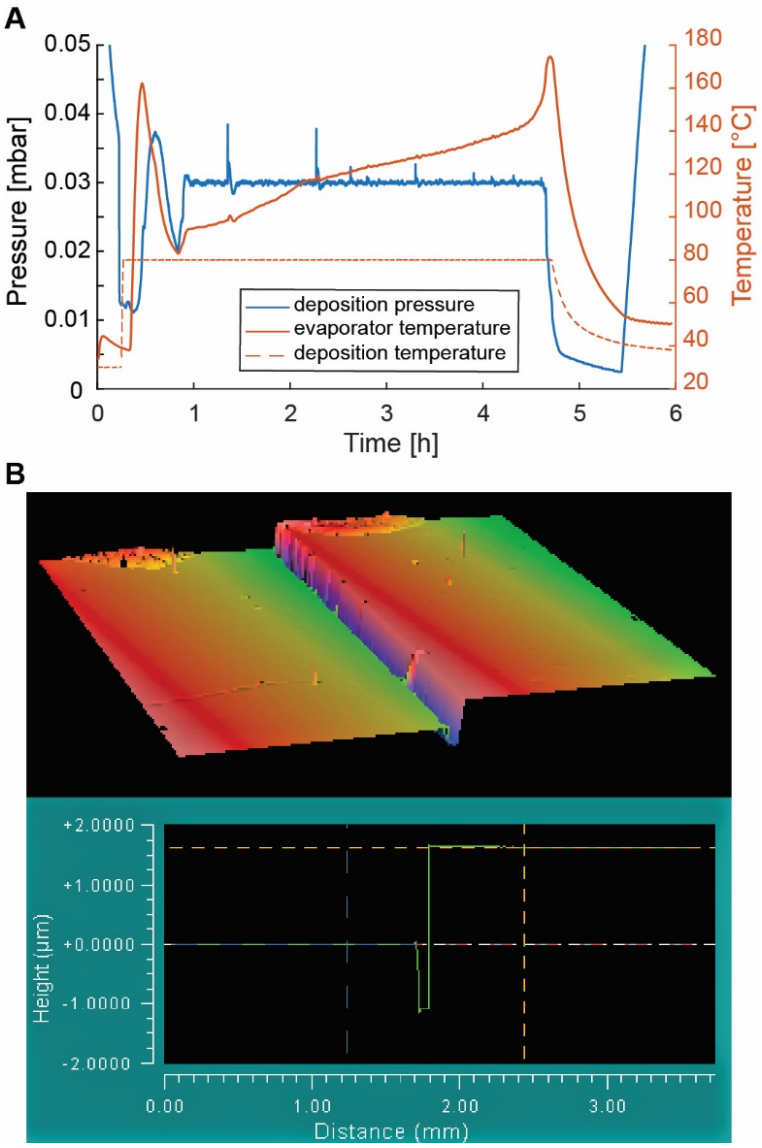

Figure S2. Coating process and deposition evaluation of parylene C layer on PDMS chips. **A** The temperature profile of the evaporator (orange), and the temperature (dashed orange) and pressure inside the deposition chamber (blue) during 6 h of parylene coating are shown in the graph. **B** 3D white-light interferogram of the parylene C layer (top right side) deposited on glass (top left side). A cross section to determine the parylene layer thickness (1.2-1.6 µm) on the substrate is shown in the bottom graph.

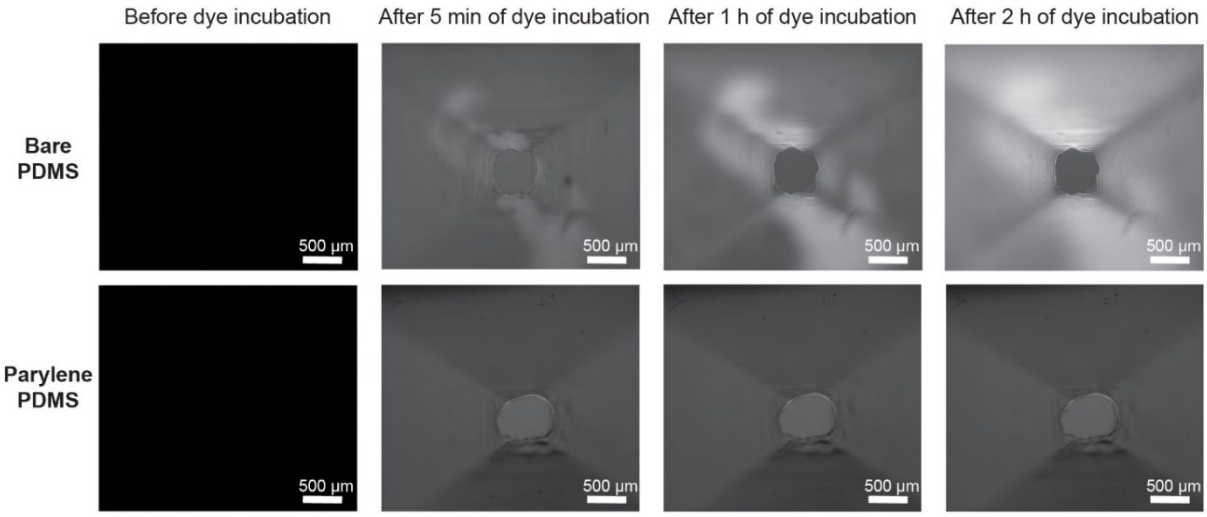

Figure S3. Characterization of PDMS permeability to small hydrophobic molecules. Diffusion of rhodamine B (0.1 mM in DI water) in bare and in parylene-coated PDMS chips was evaluated in parallel. The fluorescence images (top view) after 1 h and 2 h of dye incubation show that large amounts of rhodamine B diffused into the untreated PDMS, while diffusion was significantly less in the parylene-coated chips.

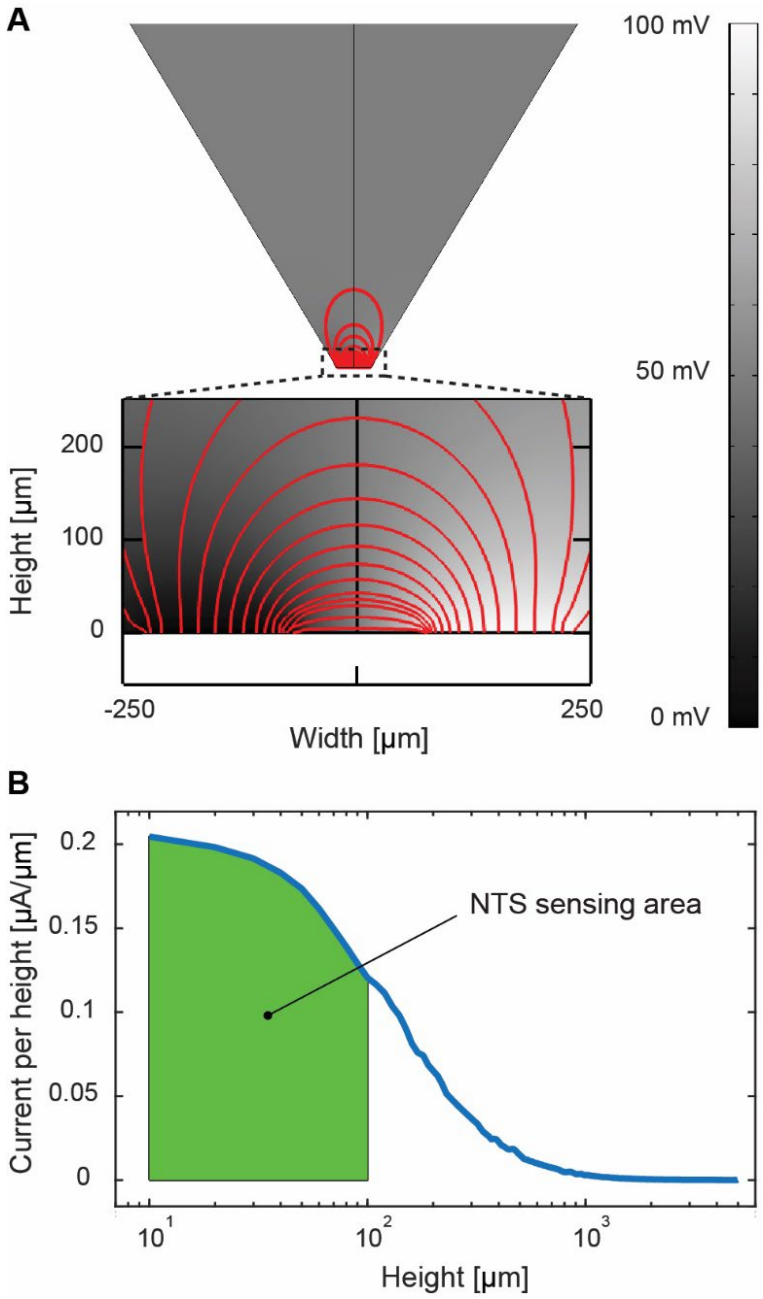

Figure S4. Finite-element-method model of the electrical measurement applied in a single microwell unit of the EIM platform. **A** The current-density distribution, upon applying a 100 mV AC voltage signal from the right electrode, is shown in a lateral cross-section of the microwell. **B** Current-density variation along the height of the microwell. The green-shaded area (corresponding to >40% of the total current) shows that the largest fraction of the current flows within the within a volume defined by 100 µm in height, which coincides with the position of the NTS larvae in the chamber.

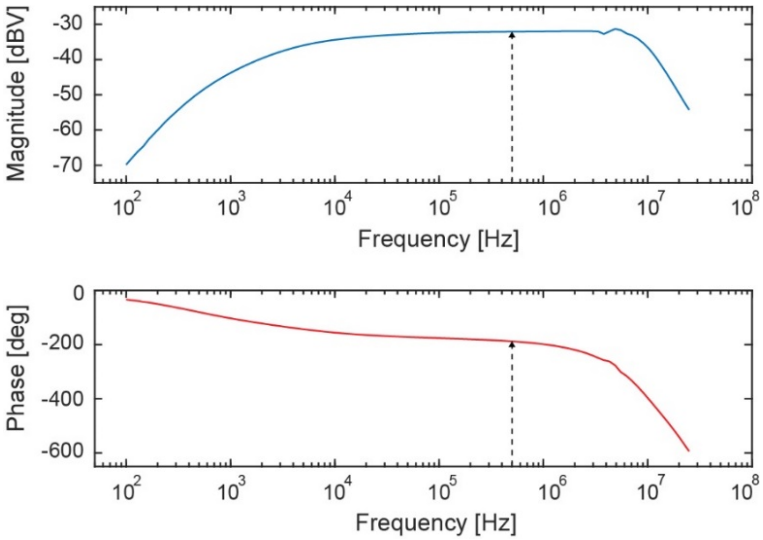

Figure S5. Frequency-response analysis of the EIM platform. The magnitude and phase responses were acquired from the HF2LI spectroscope by applying 100 mV AC voltage (frequency range 100 Hz -25 MHz) in a single unit of the chip, which was loaded with 30 µL of M199 medium solution. The voltage-to-current conversion was made through a trans-impedance amplifier with a 1kΩ feedback resistor. The dashed arrows mark the characteristics of the platform at 500 kHz.

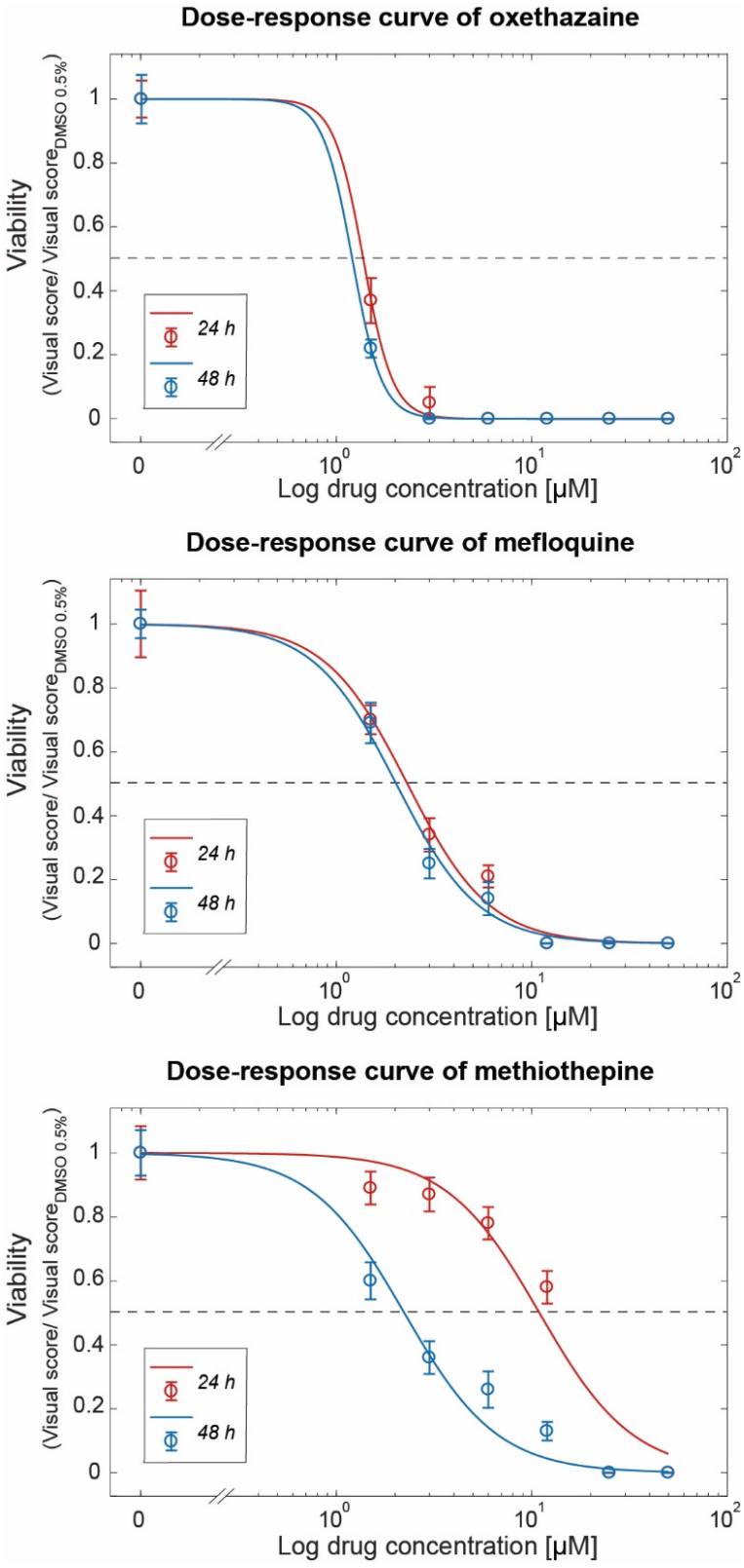

Figure S6. Measurement of the dose-response curves using the standard visual assessment of parasite phenotypes. The graphs show the NTS viability as a function of drug concentration at 24 and 48 hours. The NTS were exposed to six different concentrations (1.5, 3, 6, 12, 25 and 50 µM) of oxethazaine, mefloquine and methiothepine. Each circle represents the mean value of the viabilities of three replicates, and the error bars represent the standard error of the means. The two sigmoid fits used to calculate the IC_{50} values are superimposed to the viability measurement data.

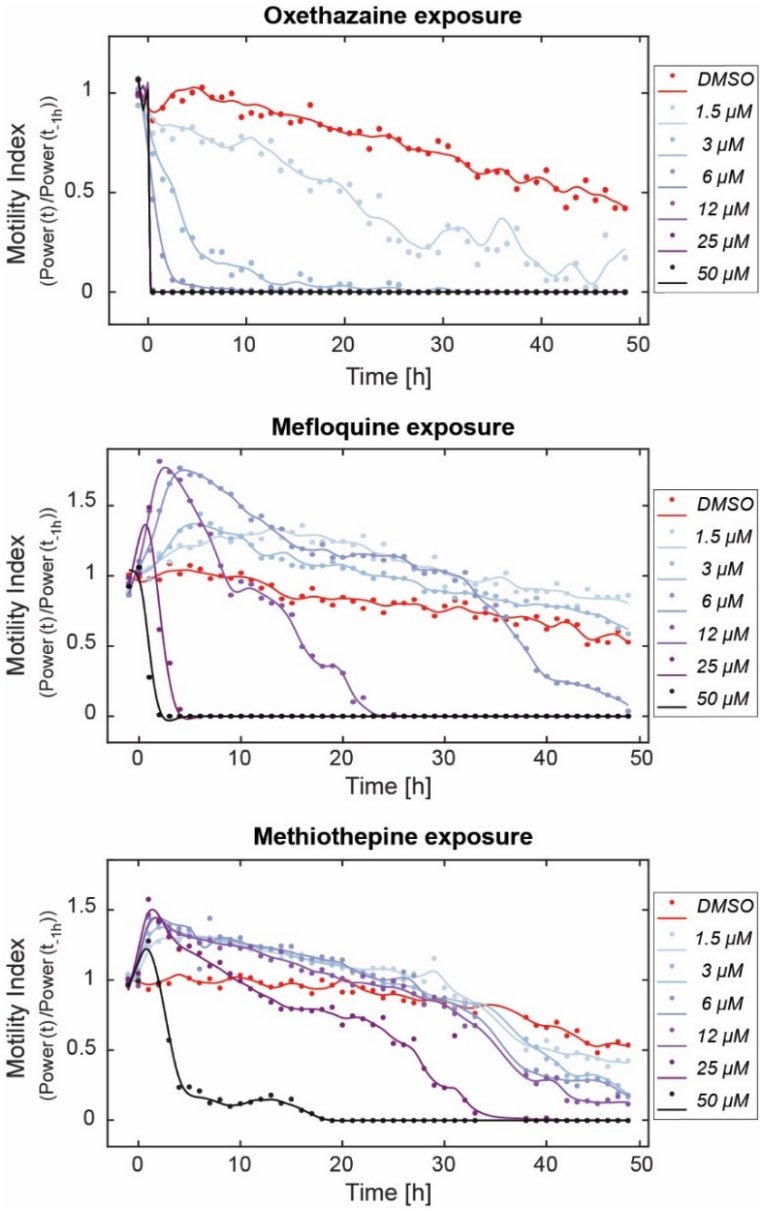

Figure S7. Measurement of drug-induced NTS motility during 48 h using the EIM platform. The motility values of the NTS for six applied concentrations of oxenthazaine, mefloquine and methiothepine drugs are plotted every hour during the entire recording. Each point represents the mean motility index of three analysis units. Seven trend lines are superimposed to the points to guide the eye for the different conditions.

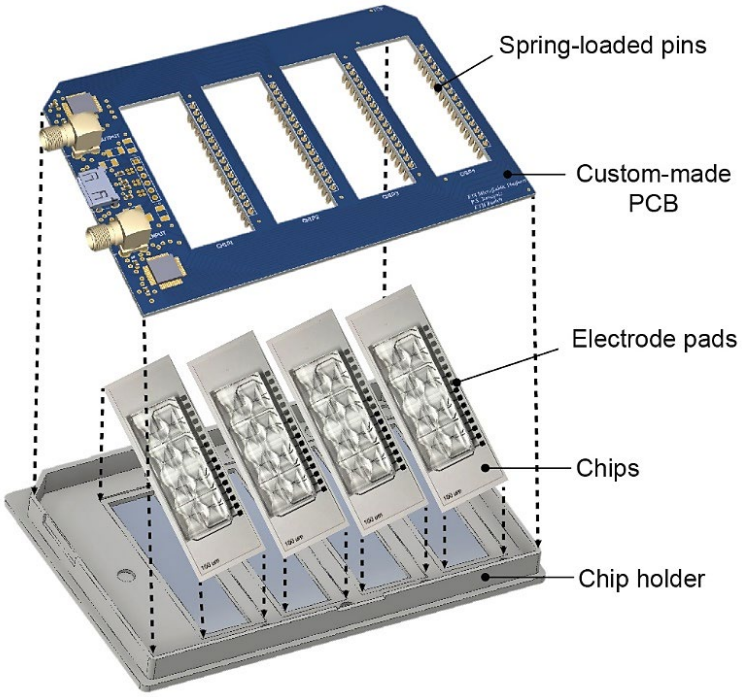

Figure S8. Components and assembly procedure of the EIM platform. The platform is a modular assembly of four chips sandwiched between a custom-made PCB and a 3D-printed chip holder at the bottom. Once the platform has been assembled, the spring-loaded pins are aligned and pushed onto the electrode pads of the chips.

Movie S1: Time-lapse bright-field photographs (acquisition 1 fps) show the motility and morphological changes of the NTS after 0, 24 and 48 hours post drug incubation with 50 and 1.56 µM of oxethazaine in a 96 well-plate.

Movie S2: Time-lapse bright-field photographs (acquisition 1 fps) show the motility and morphological changes of the NTS after 0, 24 and 48 hours post drug incubation with 6.25 and 1.56 µM of praziquantel in a 96 well-plate.

Movie S3: Time-lapse bright-field photographs (acquisition 1 fps) show the motility and morphological changes of the NTS after 24 and 48 hours post drug incubation with 50 and 1.56 µM of mefloquine in a 96 well-plate.

Movie S4: Time-lapse bright-field photographs (acquisition 1 fps) show the motility and morphological changes of the NTS after 0, 24 and 48 hours post drug incubation with 50 and 1.56 µM of methiothepine in a 96 well-plate.

3. REAL-TIME AND AUTOMATED MONITORING OF ANTISCHISTOSOMAL EFFICACY OF A PANDEMIC COMPOUND COLLECTION FOR DRUG DISCOVERY

Paolo S. Ravaynia[1], Stefan Biendl[2,3], Francesco Grassi[4], Jennifer Keiser[2,3], Andreas Hierlemann[1] and Mario M. Modena[1]

[1] ETH Zurich, Dept. of Biosystems Science and Engineering, Bio Engineering Laboratory, Basel, Switzerland and

[2] Swiss Tropical and Public Health Institute, Department of Medical Parasitology and Infection Biology, Basel, Switzerland

[3] University of Basel, Basel, Switzerland

[4] Centre for Microsystems Technology, Ghent University, Gent, Belgium

In preparation for submission

3.1 Abstract

Schistosomiasis is a neglected tropical disease that affects over 200 million people annually. As the standard drug discovery relies on an operator-based visual screening process, and the antischistosomal drug pipeline is currently empty, compound repurposing has become a fundamental source for accelerating drug development. However, the large number of library compounds that can potentially be repurposed requires the use of high-throughput assays and efficient screening strategies. Here, a collection of 57 drug candidates for repurposing is analyzed using a novel impedance-based platform to identify antischistosomal hits *in vitro*. In each assay, the developed system allows for continuous and automated evaluation of 128 conditions in parallel during 72 hours. By initially screening 10-µM compound concentrations against schistosomula, five drugs are identified, which reduce parasite viability by more than 70%. The selected compounds are then more closely investigated in real-time dose-response assays. Upon continuously monitoring larval parasite responses to different drug doses, four compounds reveal high potency and rapid action, which renders them suitable candidates for follow-up *in vivo* tests. The study shows that the presented *in vitro* device is a reliable tool for real-time drug screening analysis of compound libraries at sufficient throughput to identify new promising therapeutics against schistosomiasis.

3.2 Introduction

Schistosomiasis infections afflict annually more than 200 million people worldwide.[1] Among human parasitic diseases, schistosomiasis ranks second behind malaria in terms of effects on socio-economic and public health, especially in tropical areas.[2] The infection occurs through exposure to a parasitic trematode of genus *Schistosoma*, which penetrates human skin during contact with contaminated water and damages urogenital, intestinal and hepatic functions by depositing eggs in the blood vessels surrounding the bladder, intestines, and/or liver.[3] Currently, no vaccine is available to avoid schistosomiasis infections, and treatment relies exclusively on a single drug, praziquantel (PZQ), developed in the 1980s.[4,5] Despite the high efficacy and low cost of PZQ, there is a large risk of developing resistance, as the drug has been widely adopted for morbidity control in endemic areas for more than four decades.[6,7] Cases of significantly reduced susceptibility to PZQ, requiring repeated treatments, have been recently reported.[8,9] Furthermore, the current drug-discovery pipeline for schistosomiasis is alarmingly unproductive due to the low commercial investments for neglected tropical diseases and limited-throughput of standard phenotypic visual screening.[10,11] Thus, reliable and easy-to-use high-throughput screening systems are urgently needed to speed up the antischistosomal drug development and to identify new lead compounds against the human parasite *S. mansoni*.

The microscopic assessment of schistosome viability by a trained operator has been always considered the gold standard of assessing drug efficacy, as it can be easily applied to all parasite stages in *in vitro* and *in vivo* drug studies. However, this laborious and time-consuming procedure has limited throughput and delays the discovery of new compounds.[12,13] The possibility of using larval-stage worms, or newly transformed schistosomula (NTS), which are artificially obtained in large numbers by the successful establishment of the life cycle of *S. mansoni* in the laboratory, has opened new routes for developing high-throughput approaches for antischistosomal drug screening.[14–16] Dye- and colorimetric-based high-throughput assays have been developed for automated detection of larvae viability, however the required number of parasites per well was very large in comparison to the standard visual method for drug testing.[17–19] As an alternative, image-based automated microscopy systems have been implemented to assess and quantify larval motility and morphology during drug screening.[20,21] However, this approach required considerable computational power and extensive storage memory for long-term real-time parasite evaluation. Finally, a simple, label-free, high-throughput impedance-based technique has been successfully applied on cercariae and adults for monitoring and quantifying their motility, nonetheless, this system could not be used to

detect schistosomula movements.[22] Hence, there is a demand for new advanced platforms, capable of large-scale assessment of NTS viability in an automated and continuous way.

Besides the development of novel screening technologies, new antischistosomal therapeutics are direly needed, as the drug development pipeline is dry and not sufficiently supported by pharmaceutical companies.[23,24] For neglected tropical diseases, repurposing (or repositioning) of new or existing drugs, which have been already tested for other indications in humans, is an essential strategy. This solution can help to accelerate the discovery of anthelmintic treatments, to save costs in the drug development process and to shorten transfer from preclinical studies to clinical trials.[25,26] Therefore, libraries of compounds for repurposing of non-profit organizations, such as the *Drugs for Neglected Diseases Initiative* (DNDi) and *Medicines for Malaria Venture* (MVV), offer an important resource for identifying novel lead drugs. To make optimal use of these libraries, simple and automated high-throughput tools are strongly required to implement an efficient and cost-effective screening.

In a previous study, we demonstrated that micro-structured well plates help to reduce compound volumes and the number of parasites needed for testing, and allow for long-term schistosomula culturing. Moreover, the use of micro-structured well plates enables an automated detection of NTS viability by means of electrical impedance spectroscopy (EIS). EIS is a non-invasive and label-free technique for investigating, in real-time, the dielectric-property variations of a target sample over a specific range of frequencies.[27,28] The previously developed small-scale EIS platform included only 32 microwell units and was validated for the continuous long-term assessment of dose-response effects of four established drugs on NTS by comparison with standard visual scoring.[27] However, the adopted rapid-prototyping material, polydimethylsiloxane (PDMS), is known for small-molecule absorption, which often obviates the use of microfluidic analytical platforms, developed in academic labs, for drug-screening applications, and is not amenable to large-scale fabrication. Therefore, the implementation of a higher-throughput impedance-based device with reliable pharmacodynamic analysis should be addressed to boost the antischistosomal screening in both academic and highly standardized industrial settings.

Here, we present the development and use of a new automated impedance-based system, featuring a large number of parasite compartments (128), for highly parallel drug screening of potential antischistosomal compounds with minimal operator intervention. For reliable application in drug discovery, we adopted a standard laboratory plastic material, polystyrene (PS) in order to avoid compound ad/absorption, to reduce fabrication costs and time, and to

increase measurement throughput.[29,30] The developed device offers simultaneous measurements in 128 microwells in parallel, which corresponds to more than 30 drug exposure scenarios with 4 statistical replicates in a single assay. Moreover, we were able to implement a setup to run automated multi-day assays with continuous detection of parasite viability that drastically reduced experimental efforts. The system included four modular platforms in standard microtiter-plate formats, which ensured full compatibility with lab automation tools. In an exemplary drug screening study, we analyzed the activity of 57 compounds, which were selected from the Pandemic Response Box (PRB) of the MVV organization, over 3 days of continuous impedance monitoring. We then identified the five most active antischistosomal drugs and assessed temporal characteristics of dose-dependent responses of the NTS. The obtained results prove that our new highly-parallelized modular plastic platform represents a powerful tool for continuous long-term measurements of the efficacy of libraries of compounds on schistosomula, thereby significantly advancing drug-screening for schistosomiasis.

3.3 Results

3.3.1 Highly parallelized platform for antischistosomal screening

We developed an integrated microwell plastic chip to establish reliable and automated impedance-based monitoring of schistosomula activity with large compound libraries (**Figure 1A**). The chip was fabricated using polystyrene (PS), a standard and well-characterized laboratory plastic material, to avoid absorption and/or adsorption of small hydrophobic drug molecules.[27,29] The PS chips were fabricated using injection molding, which allowed for high-volume and low-cost fabrication (Figure S1, Supporting Information). Each chip included a top PS layer (13 x 38 mm^2) featuring 8 microwell units, which was sealed via double-sided adhesive tape to a polyethylene terephthalate (PET) foil (20 x 61.5 mm^2), equipped with 8 pairs of co-planar platinum electrodes for electrical monitoring of parasite movements. The top-open reservoir microwells were arranged at a 9-mm pitch to allow for loading of the parasite larvae and compound solutions with standard multichannel pipettes, which facilitated system operation. The small microwell volume and dimensions (65 µL, 5 mm in height) resulted in fast and reliable sedimentation of the NTS onto the electrodes (within ~3 min, Figure 1B). To provide enough throughput for drug screening applications, the new platform could accommodate 4 PS chips, and up to 4 platforms could be stacked in an incubator to simultaneously record from 16 chips, so that 128 conditions could be assessed in a single run (Figure 1C). Each platform included a printed circuit board for signal multiplexing and an aluminum holder frame to place the chips. In addition, a PS lid was inserted into each chip-holder frame to cover the open microwell structures and limit evaporation during multi-day assays (Figure S2A, Supporting Information) so as to minimize operator interference.

The developed highly parallelized impedance-based (HPI) system enabled parallel operation of multiple 8-microwell plastic chips and featured a high level of modularity to ensure flexibility and straightforward assembly and sample loading. An electrical-equivalent circuit model of a well with the integrated electrodes, selected among four platforms, is illustrated in Figure 1D. A microwell unit can be modeled as a variable impedance Z_w, which represents the NTS suspension between the electrodes, in series with the resistance of the metal traces on the PET foil and a double-layer capacitance C_{dl}, which is formed at the interface between the platinum electrodes and the medium. To estimate parasite motility, we applied an AC potential to the selected electrode pair and measured the relative fluctuations of Z_w over time, which were caused by the movement of the parasites in between the electrodes, while the average absolute value of the impedance only contained information on solution resistivity and parasite number

(Figure S3, Supporting Information). The multiplexing of the 128 units was performed by an intermediate controller motherboard, which interfaced the lock-in amplifier and the multiplexers and demultiplexers (mux/demux) of each platform for transferring the AC signal to the selected measurement units. Each microwell of the four platforms was sampled at 32 Hz during a 1-min window to detect signal fluctuations, caused by the NTS movements, and was measured every 16 minutes during the experiments to achieve quasi-continuous analysis of drug-induced motility variations.

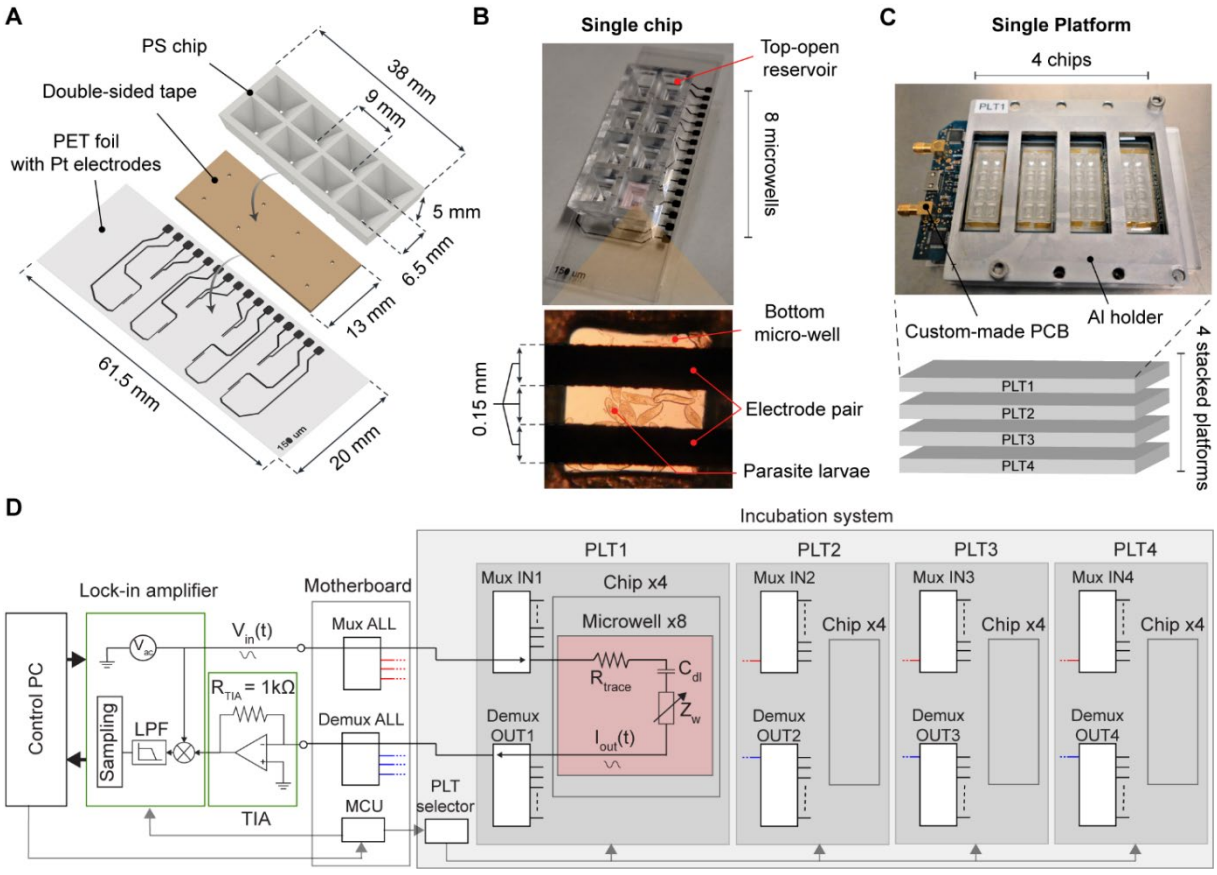

Figure 1. Layout of the modular plastic highly parallelized impedance-based (HPI) system. **A** The chips were fabricated using two transparent plastic components: an injection-molded polystyrene (PS) microwell layer and a polyethylene terephthalate (PET) slide patterned with platinum (Pt) electrodes. The two parts were then sealed together with a double-sided adhesive tape featuring 8 laser-cut holes, which provided access to the electrode pairs for impedance detection. **B** A single plastic chip featured 8 individual testing microwells with top-open reservoir cavities, shaped as an inverted pyramid to promote sedimentation of the parasites to the sensing volume above the coplanar electrodes. **C** Each platform (PLT) could accommodate up to four chips, which were placed in between a custom-made printed circuit board (PCB) and an aluminum (Al) holder. Up to 4 platforms could be measured in parallel for a single experiment. **D** The electrical equivalent circuit of the modular impedance-based system included a lock-in amplifier for generating the AC voltage signal (V_{in}), a motherboard for routing the signal to the selected unit of an 8-microwell chip, and a trans-impedance amplifier (TIA) for current-to-voltage conversion. The voltage signal was finally routed to the input of the lock-in amplifier, where it was multiplied with V_{in}, low-pass filtered (LPF) and sampled, and subsequently stored on a control PC. A microcontroller unit (MCU), soldered on the

motherboard, was used for routing and multiplexing of the four individual platforms and for synchronizing the switching between the 128 microwells and the lock-in amplifier.

The preparation and execution of the impedance-based drug assay with the HPI system was performed on two consecutive days to ensure an easy and robust parasite handling (**Figure 2**). On day -1, the chips were loaded with 30 µL of culture medium for pre-wetting the microwells using a multichannel pipette. The overnight incubation of the chips with plain medium solution, preceded by a 10-min solution degassing, was implemented to remove small air bubbles that could form at the bottom of the microwell compartments and could interfere with the sedimentation and detection of the parasites. On day 0, we first removed 25 µL of pre-wetting medium and then loaded 30-µL larvae solution with ~0.7 NTS μL^{-1} so that 20-25 NTS were loaded into each well. This procedure ensured simple and bubble-free NTS dispensing to all 128 units. We then performed impedance measurements of all the microwells for 1 h to evaluate the initial signal fluctuations of untreated parasites and to confirm correct sample loading. This operation also helped to establish a motility index value for each unit to be able to monitor how the motility of the parasites changed during the assay and to compare measurements of microwells with different numbers of parasites (for normalization details, see also Figure S4, Supporting Information).[31] After the acquisition of larval baseline activity, 30 µL of drug solution were added to the units, each condition in quadruplicates, and the motility of the NTS exposed to the compounds was recorded continuously for 3 days in the four platforms without any intervention by the operator. Controls, for which NTS were cultured in standard medium and medium containing the drug vehicle (0.5 % DMSO), were also included in each assay in quadruplicates. A single assay could therefore accommodate up to 30 different compound exposures and 2 controls in quadruplicates. At the end of each drug assay, we confirmed that the long-term impedance-based measurements showed Z'-factor scores above 0.5 and signal-windows higher than 2, as recommended by the NIH guidelines for drug screening (Table S1, Supporting Information).[32,33]

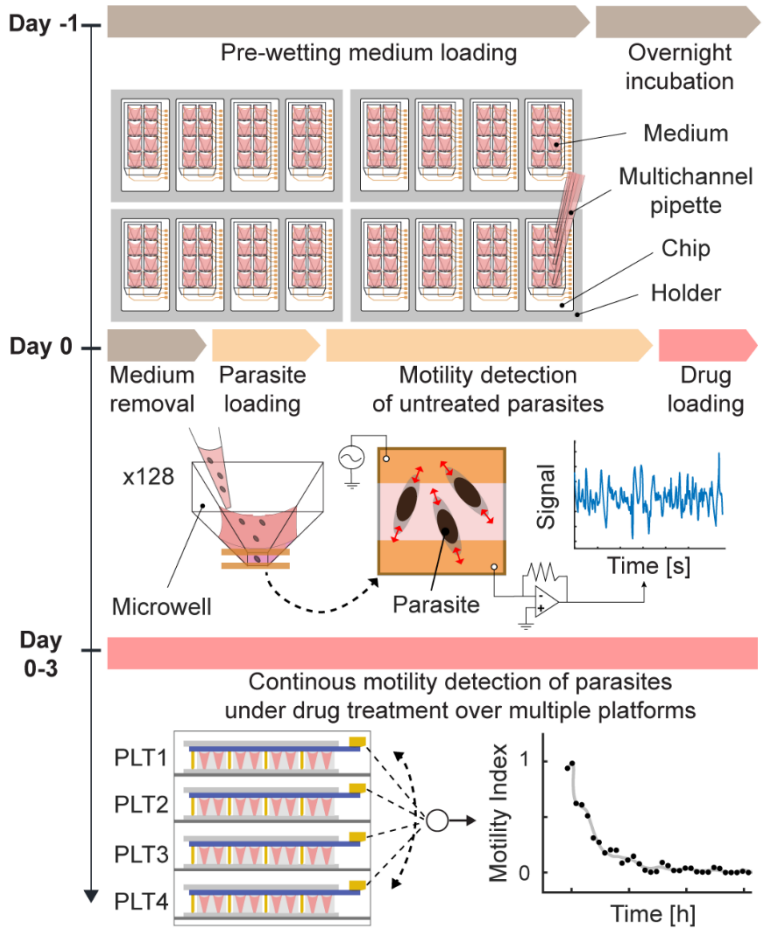

Figure 2. Operation of the automated highly parallelized impedance-based (HPI) device. The experimental timeline is shown at the left side, while the corresponding steps for performing the impedance-based assay are displayed at the right. On day -1, all 16 chips were first loaded with 30 µL of standard medium using a multichannel pipette. On day 0, after an overnight degassing of the plain medium in the chips, 25 µL of culture medium in each microwell were replaced by 30 µL of NTS solution. Impedance-based motility detection of untreated parasites was then performed for 1 hour before adding 30 µL of drug solution into each PS microwell. During the 3 days of drug exposure, the impedance detection of schistosomula status was continuously running without operator interference and by switching every 4 min between the four stacked platforms (PLT). The drug-induced NTS motility variations from all 128 wells were continuously recorded until the end of the assay.

3.3.2 Drug screening study for antischistosomal discovery

The overall screening cascade executed through standard visual inspection and automated impedance-based detection is presented in **Figure 3A**. For a first assessment of the antischistosomal activity of the PRB drugs with a standard end-point assay, the entire library (400 compounds) was initially screened against *S. mansoni* larvae using operator-based visual phenotypic evaluation. For this preliminary screening, 100 µL of NTS suspension (50-100 larvae per 100 µL) were loaded into each well of a clear flat-bottom 96-well plate, and 100 µL of drug solution were subsequently added to reach a final concentration of 10 µM (Figure 3B). After 72 hours of compound incubation, the phenotypic parasite behavior was visually

evaluated for each condition according to the standard scoring method.[12] Briefly, a trained operator optically assessed each well under the microscope and assigned a score using a descending quarter-of-a-point scale from 3 (normal larval movement and no morphological changes) to 0 (no larval movement and a complete loss of integrity). After the first visual screening, we selected a sub-library of 57 compounds from the PRB, which showed a wide-spectrum range of *in vitro* activity inhibition, from 0 to 100% (completely inactive to very active molecules against NTS). The selection also matched the composition of the entire MVV drug collection in that it included similar fractions of antibacterial, antiviral or antifungal compounds (see Figure S5, Supporting Information).

The 57 identified drugs were subsequently analyzed with our novel HPI platform to characterize in a continuous and automated manner their activity profiles on NTS (Figure 3A). The impedance screening was implemented by dispensing ~25 NTS in 65 µL of medium containing a 10-µM concentration of the PRB compounds into each unit of the 8-microwell chip (Figure 3C). By continuously recording the drug-induced NTS signal variations in all 128 microwells in parallel, we assessed the *in vitro* pharmacodynamic profile of each compound to identify the best-performing antischistosomal drugs, which showed an activity inhibition of more than 70% after 3 days of exposure. To further investigate the temporal evolution and dose-dependent characteristics of the most active drugs, we finally analyzed the potency of the hits compounds in a dose-response assay with six different concentrations (1.5, 3, 6, 12, 25, 50 µM) during 72 hours of continuous measurement using, again, our automated device.

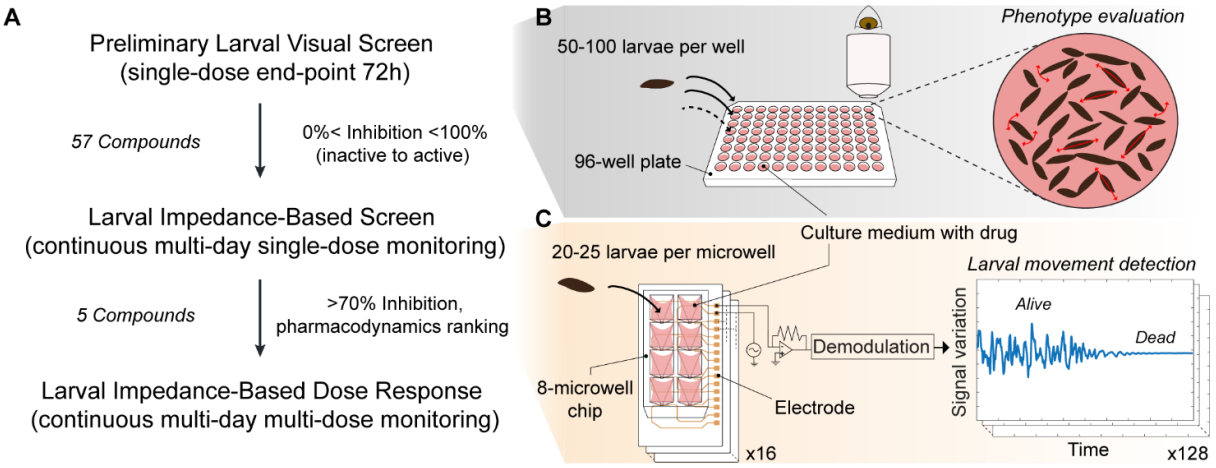

Figure 3. Visual and impedance-based evaluation for *in vitro* screening of the Pandemic Response Box (PRB) library against *S. mansoni* larvae. **A** The screening sequence started by scoring the activity of the entire PRB on NTS using standard visual inspection after 72 h of drug incubation. Then, 57 compounds were selected, which represented the entire range of visually observed activity effects, and analyzed by using the automated impedance-based system. After 3 days of continuous impedance-based monitoring of drug efficacy, the five most active antischistosomal compounds were identified and ranked. The key criterion included a

reduction of NTS viability index by more than 70%. Finally, the selected hits were further characterized by continuous dose-response analysis on chip. **B** The visual phenotypic screen was carried out by loading 50-100 larvae in each well of a 96-well plate, which contained culture medium and test compounds at 10 µM (single dose). After 3 days of drug exposure, the operator scored the morphology and the motility of the NTS in each well under the microscope. **C** For the automated impedance-based screening, each well of an 8-microwell chip was loaded with 20-25 parasites in culture medium with 10 µM (single dose) of the test compound. Every microwell was equipped with a pair of coplanar electrodes for detecting NTS motility by measuring AC impedance variations between the electrodes. By recording the signal fluctuations caused by larvae movements in each well of the 16 chips, which were used in parallel (total of 128 wells), the real-time pharmacodynamic activity of each drug was acquired during 72 hours.

3.3.3 Multi-day monitoring of the Pandemic Response Box subset efficacy

The impedance-based results of the continuous 3-day motility monitoring of NTS, incubated with the 57 selected drugs at 10 µM, are shown in **Figure 4A**. The HPI system allowed for differentiating inhibitory ($motility_{drug} < motility_{control}$) and excitatory ($motility_{drug} > motility_{control}$) compound effects - both transient and permanent - on the parasite larvae behaviors. Upon addition of the 57 PRB solutions to the microwells (t = 0 h), 7 drugs (A-G6, A-H2, C-C5, E-A6, E-B8, E-D5, and E-G4) caused a substantial fast transient or permanent decrease in motility (> 40%) during the first 10 h of continuous measurements in comparison to vehicle control conditions. In contrast, 4 compounds (C-F5, D-A3, D-A4, and E-B3) caused a significant transient or sustained increase (> 30%) in NTS motility during the first 20 h of evaluation. Moreover, we compared the rapid transient maximum inhibition of the two most effective compounds, C-C5 and A-H2, to the minimum motility value of the vehicle control condition within the same time window (first 5 h) using the Kruskal-Wallis test, followed by Dunn-Sidák test (Figure S6A, Supporting Information). In this comparison, the motility indices of the replicates treated with 10-µM A-H2 were significantly smaller (0.27 ± 0.09, $p < 0.01$) than of the controls in DMSO (0.81 ± 0.06). The same analysis was performed for the fast-acting compounds causing strong excitation, D-A3 and E-B3. We found a significant difference ($p < 0.01$) between the motility indices of parasites, treated with 10 µM of E-B3 (1.63 ± 0.17), and those of the vehicle control (1.09 ± 0.05) during the first 10 h (Figure S6B, Supporting Information).

By applying a threshold of 70% relative inhibition of parasite viability (motility index upon drug exposure normalized to that of vehicle controls)[27] after 72 h of constant drug exposure, five hit compounds (E-D5/MMV688991, C-C5/MMV1578555, A-H2/MMV1634491, A-D8/MMV1582497, and D-A4/MMV394033) were selected and ranked according to their dynamics using the impedance-based screen (Figure 4B; for viability and phenotypic details

see also Table S2 and Figure S7, Supporting Information). After 3 h of drug dosage, E-D5 exhibited the fastest *in vitro* lethal effect on schistosomula. The second fast-killing compound was C-C5, which led to complete inhibition of parasite motility at 25-30 h. We selected two more drugs (A-H2 and A-D8), which displayed a similar response and a high killing efficacy after around 40 h of incubation. Finally, a last compound was selected (D-A4), which showed a peculiar biphasic NTS response profile over 3 days of measurements, with a transient excitation in the first 10 h, followed by a delayed monotonic motility decrease during the last 30 h of continuous monitoring, reaching a final motility index value of ≈0.2.

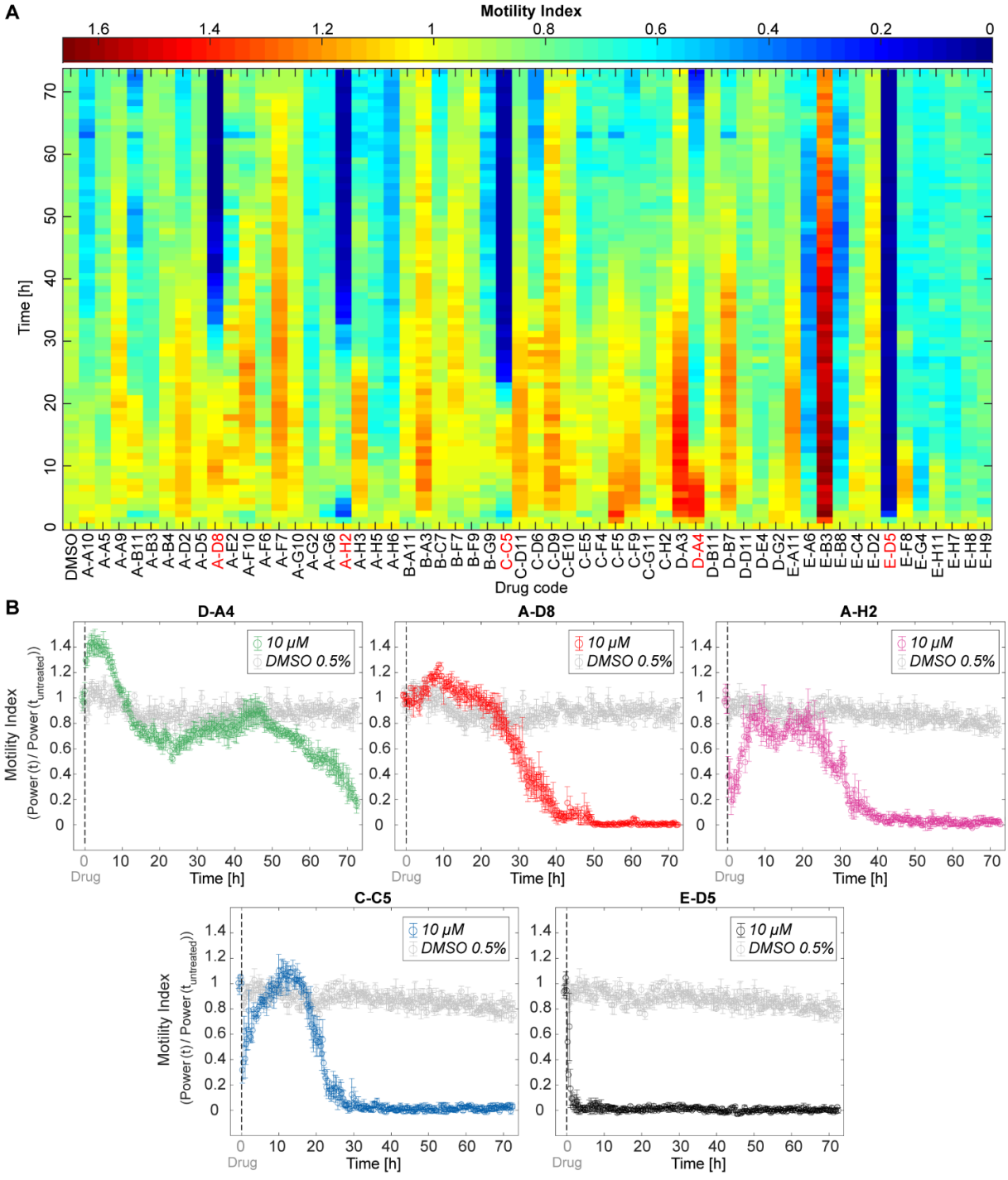

Figure 4. Monitoring of larval motility during *in vitro* testing of the selected Pandemic Response Box (PRB) drugs through impedance-based continuous measurements. **A** The heat-map shows the variations in the motility index of schistosomula upon exposure to the 57 test compounds during 72 hours of real-time acquisition with the HPI platform. Colors of the top scale bar indicate the NTS motility levels upon exposure to the drugs, which were normalized to the 1-h pre-treatment phase. All PRB drugs were applied at 10 μM in quadruplicates, and each color box represents the average parasite motility response (average of four wells) to each compound every hour. The codes of the five best-performing drugs are highlighted in red. **B** The motility graphs show the NTS responses to the five hit compounds, identified during the screening, which were compared to the vehicle-control sample (parasites in 0.5% v/v DMSO, in gray color). The vertical dashed lines indicate the times at which the drugs were dosed. Each circle represents the mean value of the motility index, measured in parallel and averaged over four microwells every 16 min. Error bars indicate the standard error of the mean.

3.3.4 Continuous dose-response characterization of the five hit compounds

We then dosed six serially-diluted concentrations (1.5, 3, 6, 12, 25, 50 μM) of A-D8, D-A4, C-C5, A-H2, and E-D5 in the HPI system to the parasite larvae to characterize, in real time, the dose-dependent responses during 72 hours. The long-term dose-response curves of the five hit compounds are shown in **Figure 5A** (the real-time motility indexes are reported in Figure S8, Supporting information). The viability of the larvae, exposed to the highest drug concentrations (50 and 25 μM) of A-D8, dropped to zero within the first 20 h, indicating that the NTS were efficiently killed by the compound at these doses. In the case of NTS exposure to 12 and 6 μM of A-D8, parasite viability ceased after 36 and 60 h, respectively. For the two lower concentrations (3 and 1.5 μM), the larvae remained viable and displayed good motility levels during the entire assay. 50 and 25 μM dosages of D-A4 showed high efficacy after 9 and 30 h, whereas 12 μM caused full inhibition at 72 h, displaying again the biphasic NTS response that had been observed for 10 μM in the screening phase (Figure 4B and Figure S8, Supporting information). For lower concentrations (6 and 3 μM) of D-A4, we noticed a considerable reduction in viability (0.58 ± 0.09 and 0.38 ± 0.06) after 3 days. The third hit compound (C-C5) exhibited a slight time delay (10-20 h) for killing the parasite at the highest doses due to an initial inhibition-and-recovery pattern that had been observed in the preceding 10-μM test (Figure 4B and Figure S8, Supporting information). Nonetheless, all concentrations larger than 3 μM were efficiently killing the larvae within the 72-h exposure. The lethal effect of A-H2 against schistosomula for the two highest concentrations appeared already after 10 h; however, longer exposure times were required for 12 and 6 μM, which showed complete inhibition of parasite viability after 48 and 72 h, respectively. With E-D5 we obtained dose-response curves indicating higher lethality in comparison to the other tested compounds. The larvae exposed to 50, 25, and 12 μM were dead already after 6 h, whereas those exposed to 6 and 3 μM reached viability indices of 0.03 ± 0.01 and 0.19 ± 0.02 at 72 h.

The antischistosomal potencies of all hit compounds were further examined and ranked by computing the IC_{50} over time, which corresponds to the concentration at which a 50% inhibition of parasite viability occurs, and by assessing the total effective drug exposure (area under the curve or AUC, Figure 5B). The temporal evolution of the IC_{50} of the less potent compound A-D8 (AUC: 895 μM h) featured a 24-h monotonic decrease to 8.0 ± 1.6 μM with values of 5.2 ± 0.4 μM at 48 h and 3.9 ± 0.4 μM at 72 h. For D-A4 (AUC: 863 μM h), the IC_{50} rapidly dropped to 8.3 ± 1.5 μM after 20 h, however, the values then slightly increased between 24 and 48 h due to the biphasic NTS response behavior at lower doses (< 12 μM). After 72 h, the potency value of D-A4 was 3.8 ± 0.7 μM. The IC_{50} progression of C-C5 (AUC: 826 μM h) displayed a significant decrease over the first two days, reaching 7.4 ± 1.0 μM and 3.3 ± 0.3 μM at 24 and 48 h. The IC_{50} value did not change considerably over the last 24 h of the evaluation and settled at 2.1 ± 0.2 μM. In the case of the second-potent compound A-H2 (AUC: 578 μM h), the IC_{50} decreased during the first day of drug exposure to 9.7 ± 1.3 μM, reaching a final value of 2.3 ± 0.3 μM after two more days of continuous measurements. Finally, E-D5 (AUC: 314 μM h) was the most-potent and fastest-acting drug in the dose-response assay, featuring an IC_{50} of 7.3 ± 1.6 μM already after 3 h and reaching a final value of 1.9 ± 0.2 μM after 72 h.

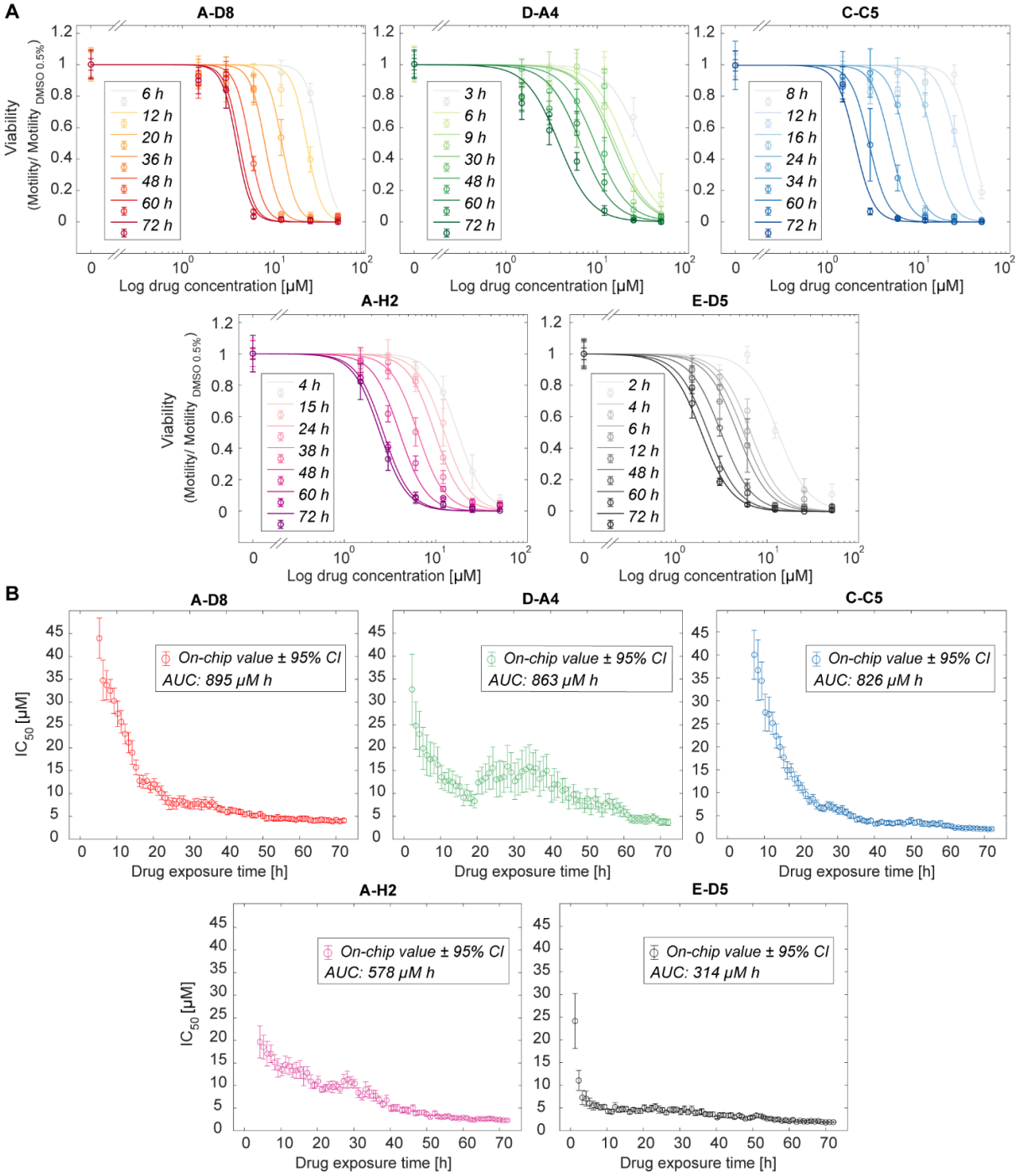

Figure 5. Continuous dose-response characterization of the five hit compounds by long-term impedance-based assessment of NTS viability. **A** The graphs show the impedance-based estimations of schistosomula viability at seven selected time points as a function of the drug concentration for all hits. The NTS were incubated with six different concentrations (1.5, 3, 6, 12, 25, and 50 µM) of each compound and monitored during 72 hours. Each circle represents the mean viability value of four replicates, normalized to the vehicle control condition (NTS in 0.5% v/v DMSO). Error bars indicate the standard error of the mean. The sigmoidal fits were used to calculate the IC_{50} value at each time point for the five drugs. **B** The plots display the temporal evolution of the IC_{50} values for the five selected compounds. The IC_{50} estimations were calculated from the impedance-based measurement data of NTS viability. Error bars show the 95% confidence intervals. In the figure legends, the area-under-the-curve (AUC) values are also reported.

3.4 Discussion

In this study, we screened 57 repurposable drugs with the aim of finding novel promising compounds with high potency, fast action and low potential developing costs against the larval stage of *S. mansoni* using an impedance-based method.[25] We selected compounds from the MMV's Pandemic Response Box library, which contains a collection of structurally diverse molecules that are active against bacteria, viruses, or fungi. For the *in vitro* screening, we implemented a highly parallelized, impedance-based (HPI) system to measure, continuously and in an automated manner, the viability of *S. mansoni* larvae during multi-day drug-exposure tests with minimal efforts. The HPI system enabled to recognize both, excitatory and inhibitory effects, of tested PRB compounds on NTS during 72 h of drug exposure (Figure 4A). Interestingly, most of the drugs that rapidly induced hypermotility at 10 µM did not show high antischistosomal activity after the complete assay duration. In contrast, transiently or permanently inhibitory compounds were more successful in killing the NTS within the course of the 10-µM exposure. In addition, few drugs displayed a peculiar biphasic response that would have been completely missed with non-continuous monitoring.

In our single-dose impedance-based screening, we found five antischistosomal hit compounds, which included two antibacterials (A-D8/MMV1582497 and C-C5/MMV1578555), two antivirals (D-A4/MMV394033 and E-D5/MMV688991), and one antifungal (A-H2/MMV1634491). Among these compounds, E-D5, commercially known as nitazoxanide, had been previously identified as antischistosomal, which confirms the suitability of our system for drug screening.[14,34]

For further characterization, we examined the selected five drugs with a continuous dose-response screening using our chips. All compounds showed inhibition concentration (IC_{50}) values below 4 µM after 72 h of exposure, which renders them suitable for *in vitro* follow-up tests on adult-stage parasites. Moreover, the differences in the characteristics of dose- and time-dependent responses of the NTS to each drug highlight the importance of continuous monitoring of parasite activity for testing of new promising compounds (Figure S8, Supporting information). Using our impedance-based real-time detection, we revealed the fast action and high efficacy of E-D5, which displayed an IC_{50} of less than 5 µM already after 8 h of incubation, compared to the slower activity decrease upon dosage of A-H2, C-C5, D-A4, and A-D8. By assessing the drug efficacy every 16 min, we could rank the potency of the selected compounds based on the area under the curve (AUC) of the complete IC_{50} temporal transition (Figure 5B). With such an analysis, scientists will have the possibility to prioritize drugs to be promoted to

additional pre-clinical studies not only based on final IC_{50} values, but also considering fast action and low effective dose. For example, both compounds, A-H2 and C-C5, featured similar IC_{50} values as E-D5 at 72 h, however their slower kinetics resulted in a much higher AUC during the whole assay.

Recording the temporal evolution of dose-response relationships is also beneficial for comparing drug potency results to other *in vitro* tests that are used for preclinical selection of active compounds. Four of the selected hits (E-D5, A-H2, C-C5, and A-D8) were reported to feature cytotoxicity (CC_{50}) values above 20 µM at 48 h (cytotoxicity is commonly measured with Chinese hamster ovarian (CHO) cells), which yields an average CC_{50}/IC_{50} ratio of more than 4 for these compounds (Table S3, Supporting information).[35] Conversely, the CC_{50} value of D-A4 was reported to be 1.4 µM [35], so that D-A4 features a comparably low CC_{50}/IC_{50} ratio and would probably be excluded from further testing. The other four drugs would therefore be more indicated for *in vivo* follow-up studies against adult schistosomes owing to their sufficiently high *in vitro* efficacy/cytotoxicity ratio. Furthermore, all these four compounds comply with the Lipinski rules-of-five, a rule of thumb to determine if a chemical compound with a certain pharmacological or biological activity has chemical and physical properties that would make it a likely orally active drug in humans.[36] Oral administration would render these drugs highly attractive for antischistosomal clinical studies and would be the preferred mode for schistosomiasis treatment (Table S4, Supporting information).[36,37] Only A-H2 fails the lipophilicity criteria (AlogP > 5) by a small margin, however this failure should be unlikely to significantly impair absorption as predicted by the Lipinski rules.[38]

Novel *in vitro* high-throughput strategies to assess schistosomula viability using automated and affordable assays for drug-screening are extremely needed for finding new therapeutics against human schistosomiasis that causes more than 200 000 deaths per year.[16,39] Currently, standard drug-screening entails the viability evaluation of NTS that have been exposed to test compounds by visual scoring of a trained operator. This screening approach is not scalable and labor-intensive, it requires comparably large numbers of parasites (50-100) per well for observation and highly-trained staff for the evaluation of parasite viability, which limits the number of analyses per assay. Moreover, the visual viability evaluation of the NTS is prone to operator-based biases and errors.[12,13] These limitations become more evident when large libraries of compounds need to be screened. To overcome some of these shortcomings, we developed an automated impedance-based system that can continuously measure NTS viability during multi-day drug-exposure tests with minimal operator intervention. The HPI system was

demonstrated to enable the parallel screening of a drug sub-library at a single concentration and the evaluation of dose-dependent pharmacodynamic profiles of multiple compounds.

By making use of miniaturized culturing compartments, our HPI device provides a 5-fold reduction of the number of NTS per condition and a 3-fold reduction of compound-solution volumes in comparison to standard visual-evaluation methods. In an advance over our previously developed platform,[27] we avoided materials like PDMS that feature unspecific absorption of small molecules and are not suitable for drug screening applications (Figure S9, Supporting information).[29,40] Furthermore, we developed a parallelized, user-friendly and pump-free system, which was produced using injection molding of polystyrene to reduce fabrication costs (~2 CHF per chip) and to increase measurement throughput for large screening applications. By using only standard laboratory plastic materials (PS-PET substrates) for the chips, we could increase the drug assay duration to more than 3 days (Figure S4D, Supporting information), with 72 hours being the standard assay time for visual screening.

Our work demonstrates that impedance-based detection of NTS viability can be applied in medium-to-high throughput assays in accordance with NIH assay guidelines for high-throughput screening applications (Table S1, Supporting information).[32] In comparison, a parallelized impedance-based instrument for *in vitro* antischistosomal testing (xWORM), developed by another group, requires a comparably large number of parasites (≈500 per well) to assess motility and could not be used to efficiently monitor schistosomula movements, while larval parasites are the most convenient sample to use for large *in vitro* drug studies.[22,41] Alternative detection techniques for parallelized *in-vitro* assessment of antischistosomal compounds were also presented in literature. Fluorescence-based and colorimetric-based detection using plate-reader instruments provide a high level of automation. However, to achieve detectable and reliable signals, these methods require 200-400 NTS per well and are limited to end-point analysis that does not provide any information on pharmacodynamics, which can be captured in our impedance-based measurements.[17–19] Finally, a parallelized microscopy system (WormAssay) showed that automated video analysis could be used to evaluate parasite motility during different discrete time-points in a 96-well-plate format.[21] However, WormAssay was only applied to adult-stage parasite screening, required significant computational resources and, hence, featured limited scalability in comparison to our impedance-based readout (≈1 MB per unit per time point).

3.5 Conclusion

In conclusion, we developed an automated highly parallel, impedance-based system, which can be used to continuously assess the efficacy of drugs on NTS during more than 72 h *in vitro* testing. The current layout enables to operate up to 16 chips and 128 analysis units in parallel using a single instrument, while the modularity of the design allows for further upscaling. The device performance was demonstrated in single-dose screenings and dose-response analyses and requires minimal operator interference. The system modularity and throughput, the use of standard plastic materials for component fabrication, and, in particular, the large amount of information that is available through continuous monitoring of NTS responses to compounds will help to significantly advance preclinical antischistosomal studies. Finally, the identification of hit compounds during the screening reported here demonstrates the potential of our device for discovering new drugs to treat schistosomiasis.

3.6 Experimental section

Compounds and culture media: The 400 compounds contained in the drug library, termed "Pandemic Response Box" (PRB), were provided by Medicines for Malaria Venture (MMV, Geneva, Switzerland) in five 96-well plates, dissolved in 10 µL of pure dimethyl sulfoxide (DMSO) at a concentration of 10 mM. These stock solutions were further diluted (1:10) in DMSO (cat. no. D2650-5X5ML, Sigma-Aldrich, Buchs, Switzerland), aliquoted and stored at -20°C until further use.

M199 culture medium, which was used for incubation and *in vitro* drug assays of *S. mansoni* newly transformed schistosomula (NTS), was prepared by supplementing Medium 199 (cat. no. 22340-020, Gibco, Waltham, USA) with 1% penicillin (10000 U/ml) and streptomycin (10 mg/ml) solution (pen/strep, cat. no. P4333-100ML, Bioconcept AG, Allschwil, Switzerland) and 5% v/v inactivated fetal calf serum (iFCS, cat. no. 2-01F30-I, Bioconcept AG, Allschwil, Switzerland).

All media were sterilized by filtration using a 0.22-µm-filter bottle (cat. no. 431097-COR, Vitaris AG, Baar, Switzerland).

Parasite preparation: Cercariae of *S. mansoni* were obtained from infected intermediate host snails (Biomphalaria glabrata) and mechanically transformed to newly transformed schistosomula (NTS) as described previously.[12,42] In brief, *S. mansoni*-infected Biomphalaria glabrata snails were placed singularly in 24-well plates and exposed to a neon lamp (36 W, 4000 K, 3350 lumens) for 3-4 h to induce the shedding of cercariae. The supernatant was collected and filtered to remove impurities in the suspension. The mechanical transformation of the cercariae into NTS was performed by physically removing the tail by constricted passage through a Luer-Lok tip in between two 12 mL syringes. After washing in Hanks' balanced salt solution (HBSS, cat. no. 14175, Gibco, Waltham, USA), supplemented with 1% penicillin (10000 U/ml) and streptomycin (10 mg/ml) solution, NTS were re-suspended in M199 culture medium and kept overnight at 37 °C and 5% CO_2.

In vitro visual drug-sensitivity assay: The 400 compounds contained in the PRB compound library were initially screened for their activity against NTS following the standard screening procedure based on visual scoring.[12] In brief, 50-100 NTS were incubated in culture medium with the test compounds at 10 µM at 37 °C, 5% CO_2 for 3 days in 96-well plates (cat. no. 83.3924, Sarstedt, Nümbrecht, Germany). After 72 h of incubation, a trained operator evaluated the NTS phenotype by microscopic readout (magnification 10-40×, Carl Zeiss, Jena, Germany)

using a viability scale from 0 (dead) to 3 (healthy and motile parasites) estimating death, changes in motility, and morphological alterations.

For all experiments, the highest concentration of DMSO (0.5% v/v) in culture medium served as control. For *in vitro* phenotypic drug sensitivity assays, each experimental condition was tested in triplicates and repeated at least once.

Larval impedance-based drug assay: The drug assay in the plastic chips was carried out in three main steps: (i) medium pre-wetting procedure at day -1, (ii) parasite loading at day 0 and (iii) drug addition after 1 h of NTS culturing in the microwells. On the day before the assay, the pre-wetting procedure was performed by dispensing 30 µL of plain M199 medium in all 128 microwells. The assembled platforms were subsequently inserted in a vacuum desiccator (Nalgene 5310-0250, Sigma-Aldrich, Buchs, Switzerland) for 10 min to degas the medium. After the degassing step, the chips were kept in the incubator at 37 °C and 5% CO_2 overnight. On the day of the assay, the plain pre-wetting medium was used to record 30-min signal traces to establish the baseline noise background in each microwell before the insertion of the larvae. After that, 25 µL of pre-wetting medium were removed from each microwell, and 30 µL of larvae solution with 0.7 NTS μL^{-1} were dispensed. The signal fluctuations caused by untreated NTSs were acquired for 1 h to establish baseline parasite activity and for calculating the respective motility index of each microwell. Finally, 30 µL of drug solution were loaded in each microwell, resulting a final volume of 65 µL per analysis unit.

In the drug-screening phase, all compounds were tested at a fixed concentration of 10 µM, whereas in the dose-response assay the overall drug concentrations ranged between 1.5 and 50 µM (1.5, 3, 6, 12, 25 and 50 µM). In each drug experiment, 0.5% v/v DMSO (vehicle control) and plain M199 medium controls were also included, and all conditions were evaluated in quadruplicates. Impedance-based larval motility and viability indices for each test condition were measured every 16 min during 72 h in each platform. The viability index ranged from 0 to 1 (0 = no fluctuations, dead parasites; 1= motile and alive parasites) and was computed by normalizing the NTS motility under each drug exposure with respect to motility in the vehicle control (see Data analysis and statistics section for more information).

Plastic chip fabrication: The 8-microwell chip design was developed based on a previously used poly(dimethylsiloxane) (PDMS) device.[27] The chip was realized entirely in standard laboratory plastic materials to avoid drug ad/absorption by PDMS during long-term compound testing.[29,30] The plastic device consisted of two main parts: a top polystyrene (PS) layer containing 8 microwells and a bottom poly(ethylene terephthalate) (PET) foil, patterned with 8

pairs of co-planar platinum electrodes. The PS layer was fabricated using injection molding, the optimized mold scheme is shown in Figure S1A (Supporting Information), all chips were provided by Protolabs (Protolabs, Feldkirchen, Germany) at costs of ~2 CHF per unit. The injection and ejection mark points of the PS parts were chosen so as to not interfere with the bonding of the bottom to the PET slide (Figure S1B, Supporting Information). The 200-nm-thick platinum electrodes were deposited on a 6-inch laser-cut PET wafer (ES301400 PET Film, Goodfellow Cambridge Ltd, Huntingdon, England) via a shadow-mask process. Briefly, a metal mask (1.4310 +C1300 20mm, Lasercut AG, Bäretswil, Switzerland) was mounted on the PET wafer with a magnetic holder located underneath. After 40 min of platinum sputtering, the PET wafer was diced into 10 individual slides by laser-cutting (Figure S1C-D, Supporting Information). Finally, each PS chip and patterned PET slide were aligned using a custom-made alignment tool and bonded with double-sided adhesive tape (468MP, 3M Company, Saint Paul, USA).

Chip preparation: Before the sealing procedure, both PS and PET substrates were cleaned two times by immersion and ultra-sonication in isopropanol and dried using an air gun. The PS chips and PET slides were then rendered hydrophilic to facilitate liquid loading during the drug assay by oxygen plasma surface treatment for 40 sec (Harrick Plasma PDC-002, Harrick Plasma, Ithaca, USA).[30] After PS-PET bonding, each microwell was coated with 10 µL of Biolipidure (NOF America Corporation, WhitePlains, NY, USA) and incubated at room temperature for 5 min. Biolipidure solution was withdrawn completely from the microwells using a vacuum pump, and the devices underwent a second coating step to increase long-term surface hydrophilicity. After incubating for another 5 min with Biolipidure, the coating solution was removed again, and all chips were dried overnight and UV-sterilized in a laminar-flow hood.

Platform assembly: Up to four PS chips were assembled into a platform. Every chip was covered with a laser-cut PS lid to avoid medium evaporation and was placed between a custom-made printed circuit board (PCB) and an aluminum (Al) holder plate (Figure S2A, Supporting Information). The PCB design was described in detail elsewhere.[27] Briefly, the board featured 2 analog SMA connectors as input/output ports for the impedance spectroscope and 64 spring-contact connectors for interfacing with the electrode pads of the four chips. The Al holder was realized by water-jet cutting (EN AW-5083/ 3.3547/ Al-Mg4.5Mn, Xometry Europe GmbH, Ottobrunn, Germany). The holder frame featured four openings to enable microscopy inspection of the parasites in each chip and eight screw holes for adjusting the contact force.

Up to four assembled platforms were then stacked and operated in a single incubator compartment (Figure S2B, Supporting Information), allowing for operating 128 microwell units in parallel under identical testing conditions. During the 3-day drug assay, the platforms were kept in the incubator at 37 °C and 5% CO_2.

Impedance-based measurement and setup: The impedance measurements were performed using a HF2-LI impedance spectroscope (Zurich Instruments AG, Zurich, Switzerland). A 500-kHz voltage signal with an amplitude of 100 mV was applied to the electrode pairs of each microwell unit. The frequency of the sinusoidal carrier signal (500 kHz) was chosen to enable fast multiplexing (1.5 µs) between all the units and to minimize the signal attenuation in the platforms (≈−29 dBV in magnitude, Figure S3, Supporting Information). The AC current was then converted to a voltage signal through a trans-impedance amplifier (HF2TA, Zurich Instruments AG, Zurich, Switzerland) with a 1-kΩ feedback resistor, digitalized at a sampling frequency of 14 kHz and filtered with a 2.2-kHz low pass. A custom-made Python software, installed on a control PC station, was implemented to define the selection scheme of the microwells over the four parallel platforms and the switching-time protocol of the signal recordings. The voltage signal magnitude was then used for further analysis (see section Data analysis and statistics for more information).

Absorption evaluation on chip: PS is a validated material for cell-culture applications and offers substantial advantages over PDMS for use with microfluidic systems for *in vitro* drug testing.[27,30,43–45] To confirm that PS did not feature substantial molecule absorption, 50 µL of 100 µM rhodamine-B (83689, Sigma-Aldrich, Buchs, Switzerland) solution were loaded into the microwells and incubated for 24 hours.[43] Fluorescence images of the microwells were captured before the loading of the dye, at 1 and 24 h after sample loading, and after wash-out of the dye by means of an inverted microscope (Nikon Ti-E, Nikon, Egg, Switzerland), as shown in Figure S9A (Supporting Information). The chip was incubated at 37 °C and 5% CO_2. After 1 day of dye incubation, 50 µL of supernatant solution of each microwell unit were collected and compared to 50 µL of rhodamine B reference solutions (1.5, 3.3, 6.2, 12.5, 25, 50, and 100 µM), which were incubated in a 96-well microplate (675090, Greiner Bio-One GmbH, St. Gallen, Switzerland). The relative fluorescence intensity of all samples was measured using a microplate reader (Infinite M200 Pro, TECAN, Männedorf, Switzerland) at 550 nm excitation - 580 nm emission (Figure S9B, Supporting Information). All conditions were analyzed in quadruplicates.

Imaging: For additional NTS phenotypic evaluation, bright-field images of the parasites, incubated with the PRB compounds in the microwells, were acquired after 72 h using an inverted microscope (Nikon Ti-E, Nikon, Egg, Switzerland) with a Nikon Plan Fluor 10X objective (NA 0.3, WD 16 mm).

Data analysis and statistics: The data analysis was performed using custom scripts in MATLAB R2018b (The MathWorks Inc., Natick, USA). The recorded signal magnitude was filtered using a high-pass filter at 0.2 Hz to remove slow baseline drift due to medium evaporation during multi-day assays. To reduce baseline differences between microwell measurements, related to diverse drug solution compositions or drug concentrations, the high-pass-filtered signals were normalized with respect to the mean baseline signal of the respective microwell compartment. To quantify the signal fluctuations induced by NTS movements, the power of the filtered and normalized signal was computed in a 1-3 Hz bandwidth. Only the signals exhibiting an average power above -20 dBμ, which corresponded to a signal-to-noise ratio of > 10, in the first hour of measurements before drug loading were considered for analysis. To compare measurements with different numbers of larvae across the 128 microwells and to extract the motility index parameter, the power of NTS-treated fluctuations in each unit was normalized to a signal range between the initial noise power value, obtained without the parasites ($t_{-1.5hr}$), and the power amplitude after loading of untreated NTS (t_{-1hr}). To compute the NTS viability ratio, the motility index of every condition was normalized to the motility index of the vehicle control (DMSO). Every condition was analyzed in quadruplicates.

The half-maximum inhibitory concentration (IC_{50}) values of the selected drugs were calculated from the impedance-based viability estimations by applying a nonlinear least-squares analysis. A two-parameter sigmoid function with a constant hill slope was fitted to the viability data of each hit. An average hill slope, computed across 72 h of continuous impedance-based characterization of each compound, was applied to the fit for assessment of the IC_{50} values over time. In the dose-response analysis, a maximum viability value of 1 was assigned to all units in which the NTS exhibited a motility equal to or higher than that of the vehicle control (DMSO).

The visual viability scores of the compounds of the PRB library were obtained by averaging across triplicates and normalizing to the vehicle-control (DMSO) viability.

Z'-factor and signal window scores, which provide information on the suitability of a system for high-throughput screening applications, were computed following the NIH assay guidance manual.[32] Two types of motility indices and their respective variations were analyzed to assess system suitability to detect active compounds during a screen: (i) positive-control motility

representing the maximum output obtained with parasites exposed to only the drug vehicle (DMSO) and (ii) negative-control motility originating from the noise background upon M199 medium incubation of the chip.

Physicochemical properties of the hit compounds were calculated using the RDKit (version 2020.09.2) from Open-Source Cheminformatics (available online, https://www.rdkit.org/). The *in silico* analysis was performed to assess conformity with Lipinski's rules considering the molecular weight, the lipophilicity (AlogP, atom-based method by Ghose and Crippen), the number of H-bond acceptors and the number of H-bond donors.[36,46]

All results are displayed as mean values with error bars representing the standard error of the mean (SEM), unless specified otherwise. To compare samples from more than two populations, the Kruskal-Wallis H test was adopted. In case the null hypothesis of the test that the distribution of the dependent variables is the same in the studied populations was rejected, a post-hoc Dunn test with Sidák correction was performed for multiple comparisons (Dunn-Sidák multiple-comparison test). Sample sizes and data presentation are specified in each figure caption.

3.7 Acknowledgements

The work was financially supported by Swiss National Science Foundation under contract CR32I2_166329: “Infected body-on-chip” and the Swiss Commission for Technology and Innovation under contract 25727.1 PFLS-LS: “Broadband high-accuracy impedance analyzer”. The authors acknowledge the Medicines for Malaria Venture (MMV) for designing and supplying the Pandemic Response Box. Further, the authors acknowledge the clean-room facility at D-BSSE, ETH Zurich, for help and support with device fabrication. Finally, the authors would like to thank their colleagues at D-BSSE of ETH Zurich, in particular Dr. Fernando Cardes and Silvia Ronchi, for scientific input.

3.8 References

[1] D. P. McManus, D. W. Dunne, M. Sacko, J. Utzinger, B. J. Vennervald, X. N. Zhou, *Nat. Rev. Dis. Prim.* **2018**, *4*, 1.

[2] A. F. Adenowo, B. E. Oyinloye, B. I. Ogunyinka, A. P. Kappo, *Brazilian J. Infect. Dis.* **2015**, *19*, 196.

[3] B. Gryseels, *Infect. Dis. Clin. North Am.* **2012**, *26*, 383.

[4] A. J. Molehin, *J. Biomed. Sci.* **2020**, *27*, 1.

[5] N. Vale, M. J. Gouveia, G. Rinaldi, P. J. Brindley, F. Gärtner, J. M. Correia da Costa, *Antimicrob. Agents Chemother.* **2017**, *61*, 1.

[6] W. Wang, L. Wang, Y. S. Liang, *Parasitol. Res.* **2012**, *111*, 1871.

[7] R. Bergquist, J. Utzinger, J. Keiser, *Infect. Dis. Poverty* **2017**, *6*, 1.

[8] T. Crellen, M. Walker, P. H. L. Lamberton, N. B. Kabatereine, E. M. Tukahebwa, J. A. Cotton, J. P. Webster, *Clin. Infect. Dis.* **2016**, *63*, 1151.

[9] D. Cioli, L. Pica-Mattoccia, A. Basso, A. Guidi, *Mol. Biochem. Parasitol.* **2014**, *195*, 23.

[10] L. Conteh, T. Engels, D. H. Molyneux, *Lancet* **2010**, *375*, 239.

[11] H.-B. Weng, H.-X. Chen, M.-W. Wang, *Infect. Dis. Poverty* **2018**, *7*, 67.

[12] F. C. Lombardo, V. Pasche, G. Panic, Y. Endriss, J. Keiser, *Nat. Protoc.* **2019**, *14*, 461.

[13] B. Ramirez, Q. Bickle, F. Yousif, F. Fakorede, M.-A. Mouries, S. Nwaka, *Expert Opin. Drug Discov.* **2007**, *2*, S53.

[14] M.-H. Abdulla, D. S. Ruelas, B. Wolff, J. Snedecor, K.-C. Lim, F. Xu, A. R. Renslo, J. Williams, J. H. McKerrow, C. R. Caffrey, *PLoS Negl. Trop. Dis.* **2009**, *3*, e478.

[15] J. Keiser, *Parasitology* **2010**, *137*, 589.

[16] E. Peak, K. F. Hoffmann, *An. Acad. Bras. Cienc.* **2011**, *83*, 649.

[17] G. Panic, D. Flores, K. Ingram-Sieber, J. Keiser, *Parasites and Vectors* **2015**, *8*, 1.

[18] P. H. N. Aguiar, N. M. G. S. Fernandes, C. L. Zani, M. M. Mourão, *Parasites and Vectors* **2017**, *10*, 1.

[19] E. Peak, I. W. Chalmers, K. F. Hoffmann, *PLoS Negl. Trop. Dis.* **2010**, *4*, e759.

[20] R. A. Paveley, N. R. Mansour, I. Hallyburton, L. S. Bleicher, A. E. Benn, I. Mikic, A. Guidi, I. H. Gilbert, A. L. Hopkins, Q. D. Bickle, *PLoS Negl. Trop. Dis.* **2012**, *6*, 1.

[21] C. Marcellino, J. Gut, K. C. Lim, R. Singh, J. McKerrow, J. Sakanari, *PLoS Negl. Trop. Dis.* **2012**, *6*, DOI 10.1371/journal.pntd.0001494.

[22] G. Rinaldi, A. Loukas, P. J. Brindley, J. T. Irelan, M. J. Smout, *Int. J. Parasitol. Drugs Drug Resist.* **2015**, *5*, 141.

[23] B. Pedrique, N. Strub-Wourgaft, C. Some, P. Olliaro, P. Trouiller, N. Ford, B. Pécoul, J. H. Bradol, *Lancet Glob. Heal.* **2013**, *1*, 371.

[24] P. Trouiller, P. Olliaro, E. Torreele, J. Orbinski, R. Laing, N. Ford, *Lancet* **2002**, *359*, 2188.

[25] G. Panic, U. Duthaler, B. Speich, J. Keiser, *Int. J. Parasitol. Drugs Drug Resist.* **2014**, *4*, 185.

[26] G. Panic, M. Vargas, I. Scandale, J. Keiser, *PLoS Negl. Trop. Dis.* **2015**, *9*, e0003962.

[27] P. S. Ravaynia, F. C. Lombardo, S. Biendl, M. A. Dupuch, J. Keiser, A. Hierlemann, M. M. Modena, *Adv. Biosyst.* **2020**, *4*, 1.

[28] T. Sun, H. Morgan, *Microfluid. Nanofluidics* **2010**, *8*, 423.

[29] B. J. van Meer, H. de Vries, K. S. A. Firth, J. van Weerd, L. G. J. Tertoolen, H. B. J. Karperien, P. Jonkheijm, C. Denning, A. P. IJzerman, C. L. Mummery, *Biochem. Biophys. Res. Commun.* **2017**, *482*, 323.

[30] P. M. Van Midwoud, A. Janse, M. T. Merema, G. M. M. Groothuis, E. Verpoorte, *Anal. Chem.* **2012**, *84*, 3938.

[31] K. Chawla, M. M. Modena, P. S. Ravaynia, F. C. Lombardo, M. Leonhardt, G. Panic, S. C. Bürgel, J. Keiser, A. Hierlemann, *ACS Sensors* **2018**, *3*, 2613.

[32] J. Strovel, S. Sittampalam, N. P. Coussens, M. Hughes, J. Inglese, A. Kurtz, A. Andalibi, L. Patton, C. Austin, M. Baltezor, M. Beckloff, M. Weingarten, S. Weir, *Assay Guidance Manual*, National Institutes Of Health, **2004**.

[33] R. Macarró, R. P. Hertzberg, *Mol. Biotechnol.* **2011**, *47*, 270.

[34] M. Maccesi, P. H. N. Aguiar, V. Pasche, M. Padilla, B. M. Suzuki, S. Montefusco, R. Abagyan, J. Keiser, M. M. Mourão, C. R. Caffrey, *Parasites and Vectors* **2019**, *12*, 1.

[35] J. Reader, M. E. van der Watt, D. Taylor, C. Le Manach, N. Mittal, S. Ottilie, A. Theron, P. Moyo, E. Erlank, L. Nardini, N. Venter, S. Lauterbach, B. Bezuidenhout, A. Horatscheck, A. van Heerden, N. J. Spillman, A. N. Cowell, J. Connacher, D. Opperman, L. M. Orchard, M. Llinás, E. S. Istvan, D. E. Goldberg, G. A. Boyle, D. Calvo, D. Mancama, T. L. Coetzer, E. A. Winzeler, J. Duffy, L. L. Koekemoer, G. Basarab, K. Chibale, L. M. Birkholtz, *Nat. Commun.* **2021**, *12*, DOI 10.1038/s41467-020-20629-8.

[36] C. A. Lipinski, F. Lombardo, B. W. Dominy, P. J. Feeney, *Adv. Drug Deliv. Rev.* **2012**, *64*, 4.

[37] M. L. A. Ferrari, P. M. Z. Coelho, C. M. F. Antunes, C. A. P. Tavares, A. S. Da Cunha, *Bull. World Health Organ.* **2003**, *81*, 190.

[38] J. H. McKerrow, C. A. Lipinski, *Int. J. Parasitol. Drugs Drug Resist.* **2017**, *7*, 248.

[39] M. A. Verjee, **2019**, 153.

[40] S. Torino, B. Corrado, M. Iodice, G. Coppola, *Inventions* **2018**, *3*, 1.

[41] E. M. Tekwu, W. K. Anyan, D. Boamah, K. O. Baffour-Awuah, S. Keyetat Tekwu, V. Penlap Beng, A. K. Nyarko, K. M. Bosompem, *Biomark. Res.* **2016**, *4*, 21.

[42] J. N. Milligan, E. R. Jolly, *J. Vis. Exp.* **2011**, 1.

[43] C. Lohasz, N. Rousset, K. Renggli, A. Hierlemann, O. Frey, *SLAS Technol.* **2019**, *24*, 79.

[44] M. W. Toepke, D. J. Beebe, *Lab Chip* **2006**, *6*, 1484.

[45] H. Sasaki, H. Onoe, T. Osaki, R. Kawano, S. Takeuchi, *Sensors Actuators B Chem.* **2010**, *150*, 478.

[46] A. K. Ghose, G. M. Crippen, *J. Chem. Inf. Comput. Sci.* **1987**, *27*, 21.

3.9 Supporting information

3.9.1 Supplementary figures

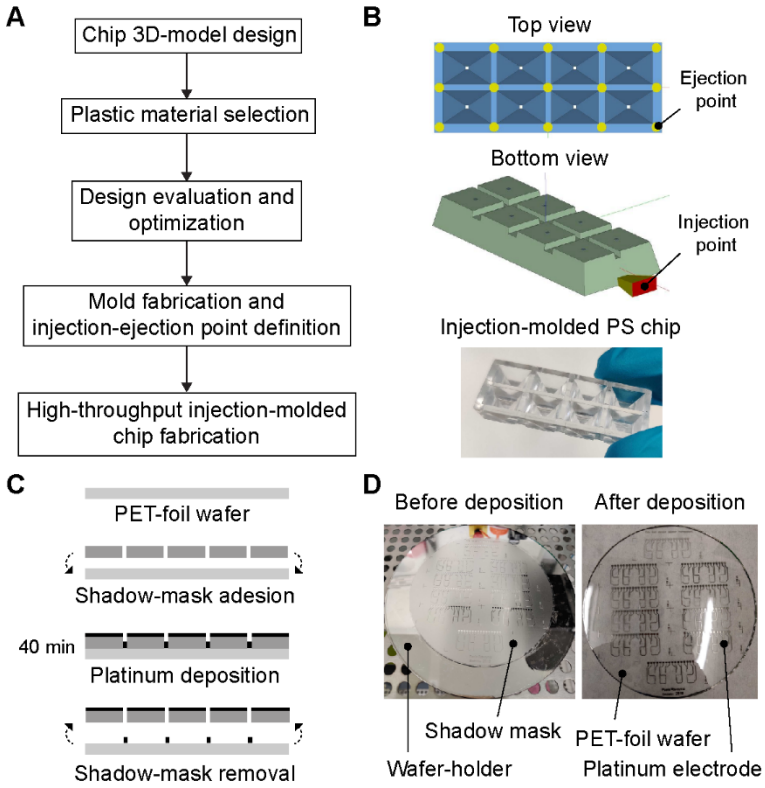

Figure S1. Fabrication procedure of the plastic chip. **A** The flow diagram lists the main steps of the high-throughput plastic chip production. The process started from the design of the 3D-micro-well model using CAD software (Autodesk Inventor) and optimization of the final layout according to the requirements of injection molding of polystyrene (PS) to obtain high-quality and defect-free pieces. The PS design requirements included uniform wall thickness, oblique lateral surfaces, round corners, and inclusion of cavity channels to ensure flat and planar blocks in the bottom sealing area. After defining the injection and ejection mark points on the fabricated mold, the high-throughput production of PS chips was achieved. **B** The position of the ejection and injection points on PS chip (top and bottom view), the positions of which were selected to not obstruct the bonding with polyethylene terephthalate (PET) substrate. **C** Fabrication procedure of PET slides patterned with platinum electrodes using a shadow-mask process. In the first step, the metal mask was attached to the PET foil by magnetic force, and the entire wafer was placed in an ion-sputtering chamber. After 40 minutes of platinum deposition, the pattern of the metal layer was transferred to PET substrate, and the shadow mask was removed. **D** The photographs show the 6-inch PET wafer covered with the metal mask before deposition (left) and the final platinum electrodes successfully patterned on the plastic foil (right). On a single wafer, 10 identical electrode units could be realized.

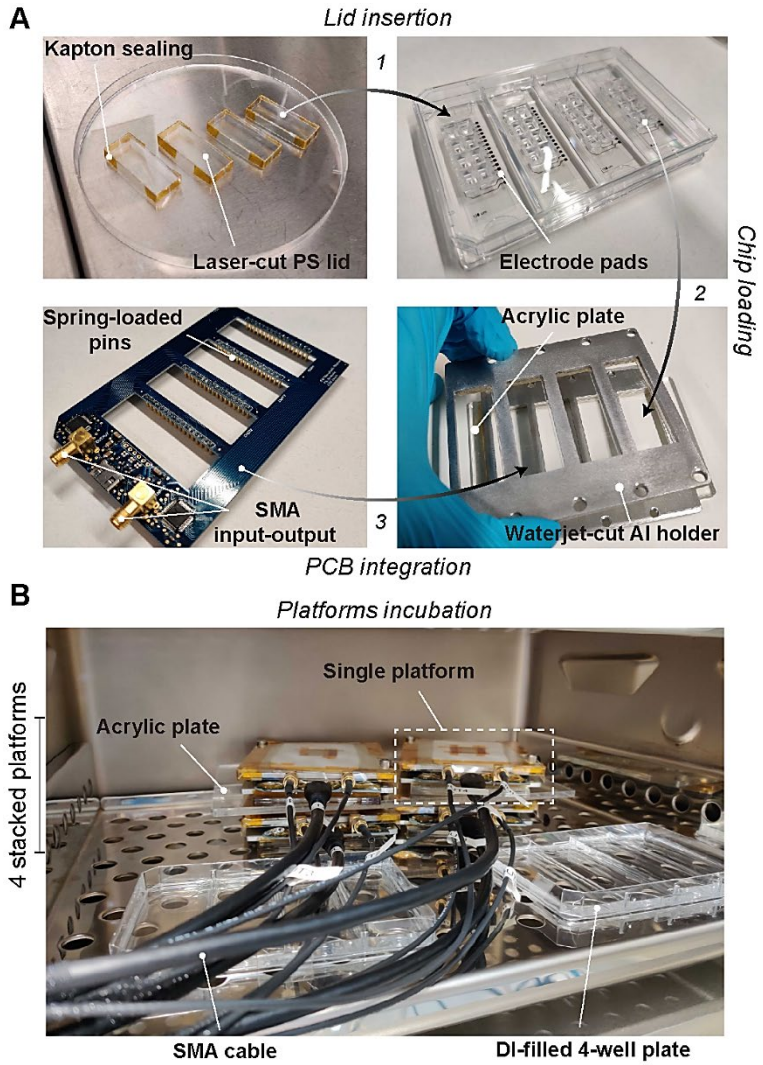

Figure S2. Components and assembly procedure of the highly parallelized impedance-based (HPI) system. **A** Each platform includes four PS chips sandwiched between a custom-made PCB and an aluminum (Al) holder. The chips are covered with laser-cut PS lids (sealed with Kapton tape at the corners) to prevent medium evaporation from the top-open microwells. Once the entire platform has been assembled, the spring-loaded pins are aligned and pushed onto the electrode pads of the chips by easily screwing the Al holder. **B** The picture shows the overall system including four stacked platforms in a single incubator compartment during the impedance-based drug assay. At the beginning of every experiment, two DI-filled 4-well plates were inserted to reduce medium evaporation from the platforms.

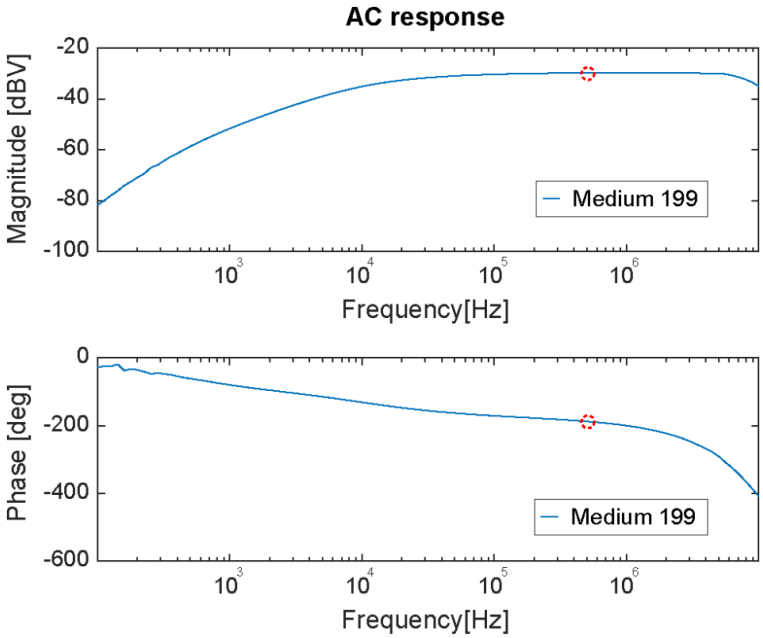

Figure S3. Frequency-response analysis of the impedance-based platform. The magnitude and phase responses were acquired with an HF2LI spectroscope (Zurich Instruments AG, Zurich, Switzerland) by applying 100 mV AC voltage within a frequency range of 100 Hz -10 MHz to a single micro-well unit of the PS chip, which was loaded with 60 µL of plain M199 medium solution. The current-to-voltage conversion was made through a trans-impedance amplifier with a 1-kΩ feedback resistor, and the demodulated signal is plotted as 100 consecutive points in a logarithmic frequency scale. The red circles mark the characteristics of the platform at 500 kHz, which was the frequency of choice for impedance-based parasite detection.

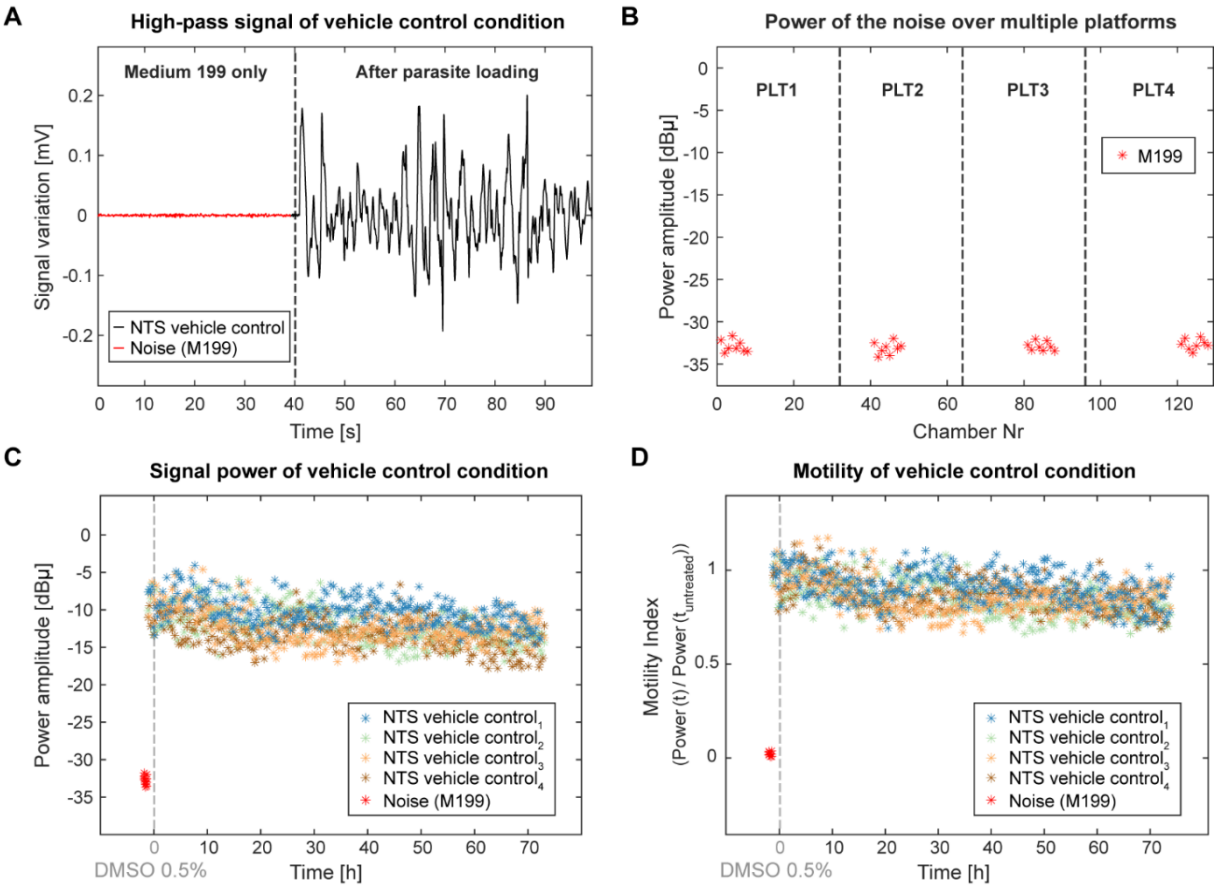

Figure S4. Detection of impedance-based parasite motility and background noise in the plastic platforms. **A** The graph shows an example of 100 s of signal recording before and after parasite loading in a single microwell unit. The high-pass signal (0.2 Hz) in the first 40 s displays the readout background noise in a well containing only medium (in the µV range). In the next 60 s, the signal output of motile NTS, exposed to the drug vehicle (DMSO), produced clear fluctuations around zero due to parasite movements between the electrodes. The trace was acquired using a 500 kHz sinusoidal excitation. **B** Power of the high-pass-filtered noise signals recorded for 60 sec from 32 separate chamber/microwell units in four parallel platforms (PLT). The signal power was calculated in the 1-3 Hz frequency range. The power measured in microwells containing only culture medium (M199) ranged between -31.6 and -34.4 dBµ. **C** The signal power of four replicates containing motile schistosomula under 0.5% DMSO condition was calculated in a 1-3 Hz bandwidth during a time window of 60 s and measured every 16 min for 72 hours. First, 30 µL of culture medium solution were loaded into all analysis-unit chambers. After 30 min of noise recording, the measurement was stopped, and 25 µL of medium in each microwell were replaced with an equal volume of NTS suspension. Afterward, the impedance detection of movements of NTS, incubated with plain medium was performed for 1 hour before loading the vehicle-control solution. After dispensing an additional 30 µL of DMSO vehicle per microwell, the impedance data acquisition was restarted and the recordings of vehicle-exposed NTS signals continued until the end of the assay. **D** The graph shows the motility index variations of the four vehicle-control samples during 72 hours of continuous recording. The motility index was calculated by normalizing the runtime NTS-treated power variations to the power of the first 1.5-h window for each condition.

A

Drug code	MVV ID	Drug type
A-A9	MMV1579783	ANTIBACTERIALS
A-A10	MMV1633967	ANTIBACTERIALS
A-B11	MMV1580853	ANTIBACTERIALS
A-D8	MMV1582497	ANTIBACTERIALS
A-F7	MMV030787	ANTIBACTERIALS
A-F10	MMV000043	ANTIBACTERIALS
A-G10	MMV003137	ANTIBACTERIALS
B-A3	MMV1613560	ANTIBACTERIALS
B-A11	MMV1549626	ANTIBACTERIALS
B-C7	MMV1580851	ANTIBACTERIALS
B-F7	MMV141011	ANTIBACTERIALS
B-F9	MMV1582382	ANTIBACTERIALS
B-G9	MMV002354	ANTIBACTERIALS
C-C5	MMV1578555	ANTIBACTERIALS
C-D6	MMV1581558	ANTIBACTERIALS
C-D9	MMV002665	ANTIBACTERIALS
C-D11	MMV1578570	ANTIBACTERIALS
C-E5	MMV1634402	ANTIBACTERIALS
C-E10	MMV099714	ANTIBACTERIALS
C-F4	MMV687696	ANTIBACTERIALS
C-F5	MMV1634399	ANTIBACTERIALS
C-F9	MMV1581545	ANTIBACTERIALS
C-G11	MMV1782403	ANTIBACTERIALS
C-H2	MMV689758	ANTIBACTERIALS
E-A11	MMV1580843	ANTIBACTERIALS
E-H11	MMV003069	ANTIBACTERIALS
D-A3	MMV1593515	ANTIVIRALS
D-A4	MMV394033	ANTIVIRALS
D-B7	MMV1580492	ANTIVIRALS

Drug code	MVV ID	Drug type
D-B11	MMV1593511	ANTIVIRALS
D-D11	MMV1581377	ANTIVIRALS
D-E4	MMV642550	ANTIVIRALS
D-G2	MMV690480	ANTIVIRALS
E-A6	MMV1580482	ANTIVIRALS
E-B3	MMV002505	ANTIVIRALS
E-B8	MMV637413	ANTIVIRALS
E-C4	MMV1580485	ANTIVIRALS
E-D2	MMV1782103	ANTIVIRALS
E-D5	MMV688991	ANTIVIRALS
E-F8	MMV1580488	ANTIVIRALS
E-G4	MMV1782097	ANTIVIRALS
E-H7	MMV019724	ANTIVIRALS
E-H8	MMV1782222	ANTIVIRALS
E-H9	MMV1006203	ANTIVIRALS
A-A5	MMV1578560	ANTIFUNGALS
A-B3	MMV000059	ANTIFUNGALS
A-B4	MMV002337	ANTIFUNGALS
A-D2	MMV1634386	ANTIFUNGALS
A-D5	MMV1782212	ANTIFUNGALS
A-E2	MMV637528	ANTIFUNGALS
A-F6	MMV1782225	ANTIFUNGALS
A-G2	MMV1645051	ANTIFUNGALS
A-G6	MMV1782354	ANTIFUNGALS
A-H2	MMV1634491	ANTIFUNGALS
A-H3	MMV396785	ANTIFUNGALS
A-H5	MMV1782224	ANTIFUNGALS
A-H6	MMV689401	ANTIFUNGALS

B

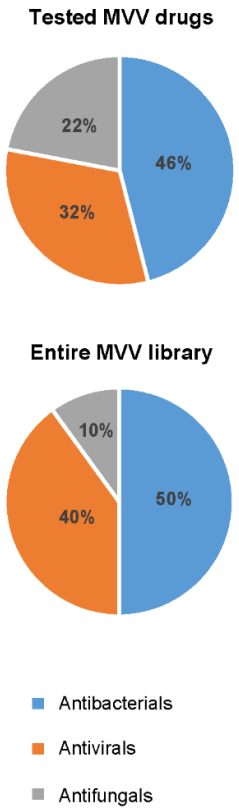

C

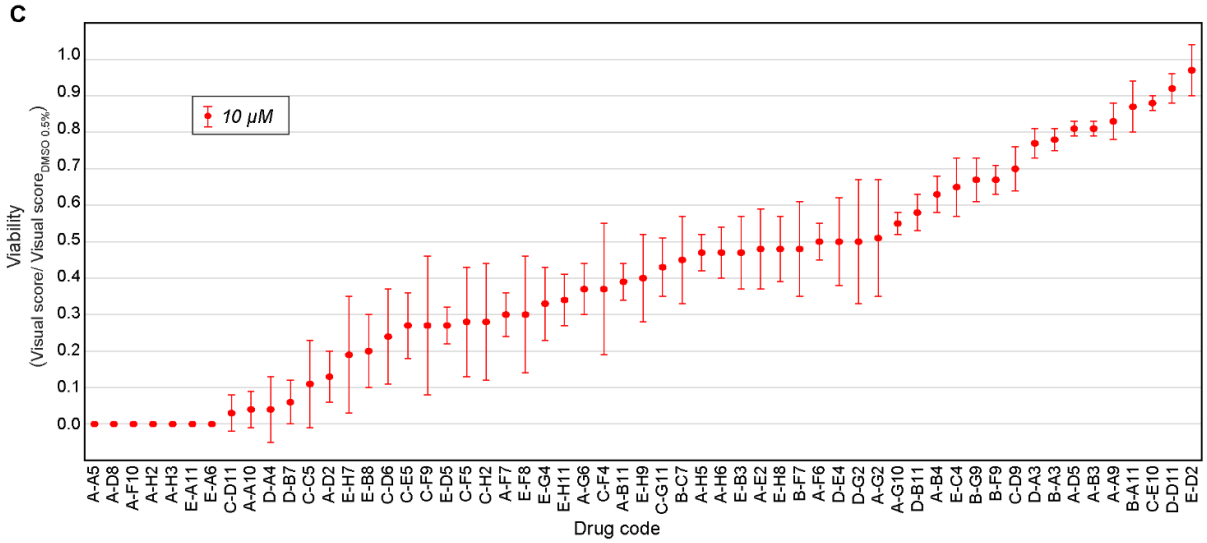

Figure S5. Set of 57 MVV compounds against *S. mansoni* larvae selected by standard visual phenotypic evaluation in 96-well plates. **A** The table lists the MMV ID number for each compound and the corresponding original target application (antibacterials, antivirals, and antifungals). **B** Composition of the entire Pandemic Response Box library (400 drugs) and the selected 57 compounds. The distribution of the tested compound set was similar to that of the

main box. **C** The graph shows the visual-based viability score of NTS after 72 hours of constant exposure to the 57 selected drugs at a concentration of 10 μM. Each point represents the mean viability value of three replicates for each compound, normalized to the vehicle control condition (0.5% v/v DMSO). The error bars represent the standard error of the mean. All viability scores ranged from a maximum value of 1, which describes a good and healthy parasite, to a minimum value of 0, which denotes complete loss of NTS integrity.

Table S1. Statistical evaluation of the results obtained with the HPI device for high-throughput screening applications. The Z'-factor and Signal-window parameters were calculated using the motility index at 72 hours from 8 positive and 8 negative control replicates in each experiment, following the NIH assay guidance manual (https://www.ncbi.nlm.nih.gov/books/NBK53196/).[1] For a good and reliable screening assay, Z'-factor should be above 0.5 and the signal window values larger than 2.

On-chip trial	*Assay 1*	*Assay 2*	*Assay 3*
Z'-factor (Motility Index at 72h)	0.67	0.58	0.59
Signal-window (Motility Index at 72h)	7.26	4.39	4.86
Positive control samples (0.5% DMSO)	8	8	8
Negative control samples (Noise-M199)	8	8	8

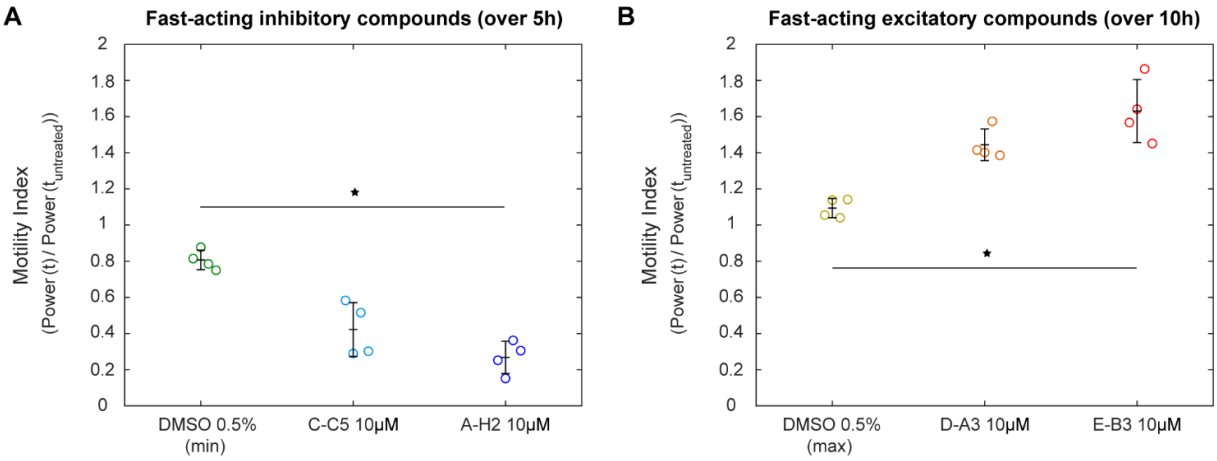

Figure S6. Analysis of fast-acting-drug-induced motility of schistosomula by using continuous impedance-based monitoring. **A** The plot shows the maximum transient impedance-based motility inhibition of the two most active compounds (C-C5 and A-H2) compared to the vehicle control (DMSO) during the first 5 hours of drug incubation. Each condition is represented as four replicates (circles) with bars indicating the mean value and corresponding standard deviation. To compare multiple groups, the Kruskal-Wallis test was used, followed by the Dunn-Sidák multiple-comparison test. The individual pair-wise test was conducted at a Sidák-corrected α value of 0.025. The black star indicates the p-value: * $p < 0.01$. **B** The same statistical evaluation was performed for fast-acting excitatory compounds (D-A3 and E-B3). A comparison of the maximum *in vitro* excitatory effect on NTS, treated with 10 µM of D-A3, E-B3 and 0.5% v/v DMSO (control), was made during the first 10 hours of exposure. Each circle represents one replicate for each condition, and mean and standard deviation bars are shown. The Sidák-corrected α value was 0.025, and the black star indicates the p-value: * $p < 0.01$.

Table S2. Assessment of drug-induced NTS viability at 72 hours using the HPI system. The parasite larvae were exposed to 57 compounds, selected by visual inspection from the Pandemic Response Box, at a single constant concentration of 10 µM for the entire assay. The impedance-based schistosomula viability was calculated by normalizing the motility index of each drug condition to the motility index of the vehicle control (0.5% v/v DMSO). The NTS viability is presented as the mean values of four analysis units along with the standard error of the mean. The five most active antischistosomal compounds, which showed a viability inhibition of more than 70%, are highlighted in red (for the MMV ID of each drug see Figure S5).

Drug code	Normalized NTS viability at 72h (Motility/ Motility $_{DMSO\ 0.5\%}$)
A-A10	0.58 ± 0.07
A-A5	0.81 ± 0.09
A-A9	0.84 ± 0.07
A-B11	0.45 ± 0.11
A-B3	0.86 ± 0.07
A-B4	0.90 ± 0.12
A-D2	0.59 ± 0.06
A-D5	0.80 ± 0.09
A-D8	0.02 ± 0.01
A-E2	0.89 ± 0.08
A-F10	0.81 ± 0.09
A-F6	0.87 ± 0.09
A-F7	0.93 ± 0.09
A-G10	0.90 ± 0.08
A-G2	0.72 ± 0.07
A-G6	0.79 ± 0.06
A-H2	0.04 ± 0.03
A-H3	0.71 ± 0.06
A-H5	0.68 ± 0.09
A-H6	0.52 ± 0.08
B-A11	0.89 ± 0.08
B-A3	0.94 ± 0.08
B-C7	0.57 ± 0.09
B-F7	0.90 ± 0.08
B-F9	0.92 ± 0.06
B-G9	0.56 ± 0.11
C-C5	0.05 ± 0.02
C-D11	0.79 ± 0.07
C-D6	0.53 ± 0.08
C-D9	0.89 ± 0.12
C-E10	0.93 ± 0.08
C-E5	0.74 ± 0.06
C-F4	0.70 ± 0.07
C-F5	0.72 ± 0.11
C-F9	0.55 ± 0.06

C-G11	0.90 ± 0.09
C-H2	0.79 ± 0.08
D-A3	0.97 ± 0.08
D-A4	0.24 ± 0.05
D-B11	0.87 ± 0.10
D-B7	0.62 ± 0.09
D-D11	0.81 ± 0.09
D-E4	0.95 ± 0.06
D-G2	0.97 ± 0.07
E-A11	0.72 ± 0.07
E-A6	0.69 ± 0.09
E-B3	1.00 ± 0.04
E-B8	0.67 ± 0.09
E-C4	0.79 ± 0.09
E-D2	0.87 ± 0.07
E-D5	0.03 ± 0.02
E-F8	0.79 ± 0.11
E-G4	0.72 ± 0.09
E-H11	0.87 ± 0.07
E-H7	0.90 ± 0.06
E-H8	0.83 ± 0.06
E-H9	0.73 ± 0.12

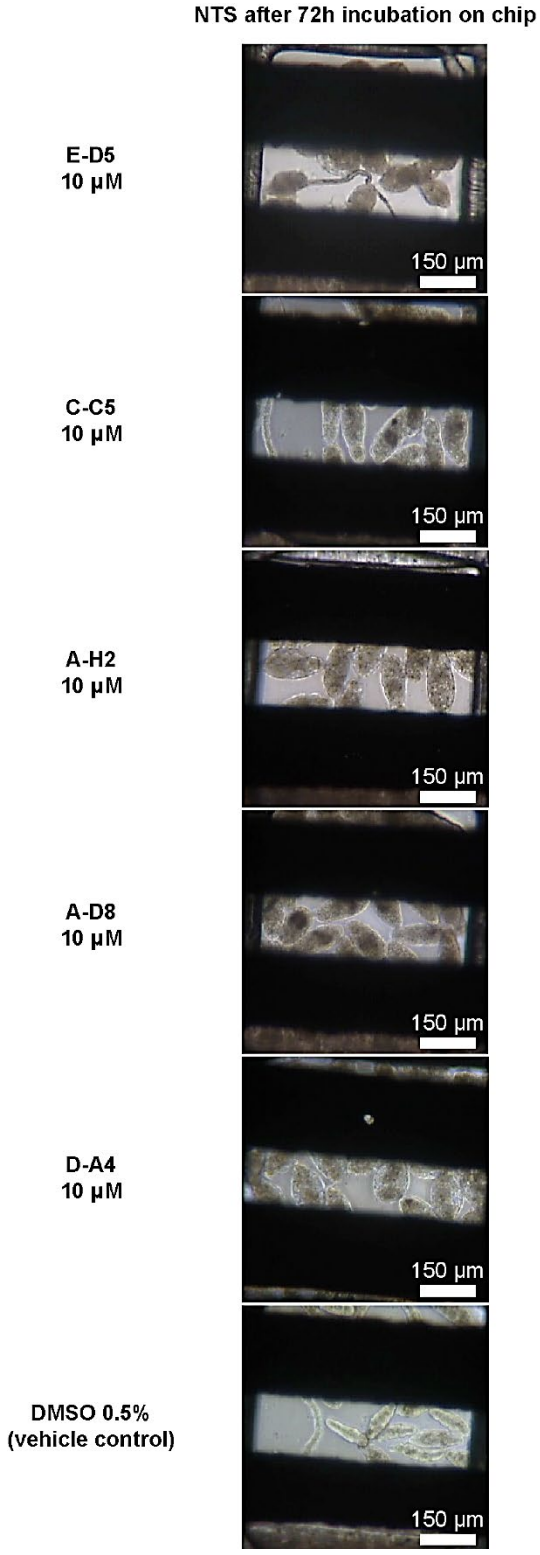

Figure S7. Images of larval phenotypes upon dosage of the five identified hit compounds in the PS chip. The bright-field images of NTS exposed to 10 µM of each compound and of the drug-vehicle condition (0.5% v/v DMSO) at 72 hours were captured with an inverted microscope. The pair of platinum electrodes at the bottom of each microwell (black horizontal bars) are clearly visible in the images. For all drugs, severe morphological alterations of the schistosomula were observed, which included increase in granularity, opacity and swelling (compared to alive control parasites).

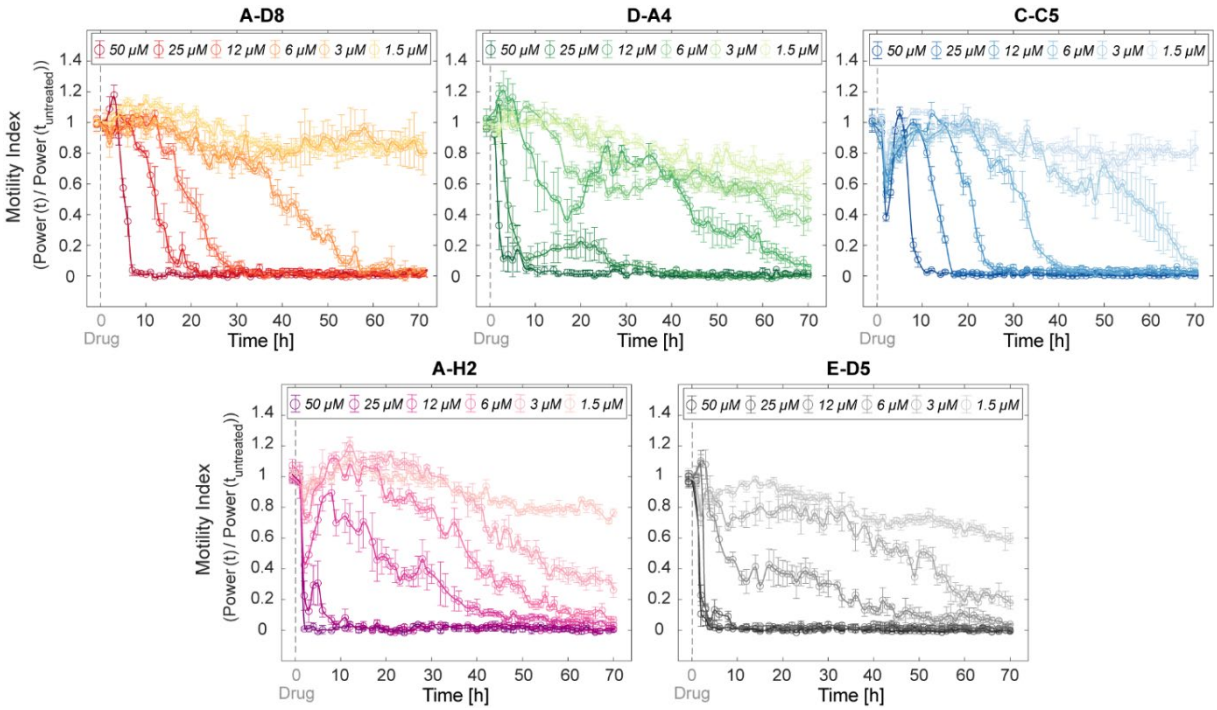

Figure S8. Measurement of drug-induced NTS motility using the HPI device. The motility values of the parasite larvae, exposed to six concentrations (1.5, 3, 6, 12, 25, and 50 µM) of the five-hit compounds (A-D8, D-A4, C-C5, A-H2, and E-D5), are plotted every hour during 3 days of recording. Each point represents the mean motility index of four analysis units, normalized to the NTS motility before drug loading ($t_{-1.5h}$), and the error bars indicate the standard error of the mean. Six trend lines are superimposed to the points for the different conditions to guide the eye.

Table S3. Cytotoxicity and measured *in vitro* potency of hit compounds, selected by impedance measurements, against *S. mansoni* larvae. The cytotoxic concentration (CC_{50}) of each compound against Chinese hamster ovary cells (CHO) was taken from the Pandemic Response Box screening of Reader et al.[2] The 50% inhibition concentration (IC_{50}) was extrapolated by a sigmoid fit of the NTS viability, measured using the impedance-based platforms, as a function of drug concentration at 48 hours. The ratio of CC_{50} and IC_{50} values serves as a selectivity parameter for *in vivo* drug testing applications (indication of potential side effects).

Drug code	MVV ID	Reported cytotoxicity on CHO - CC_{50} (µM) [2]	Impedance-based potency on S. mansoni larvae - IC_{50} (µM)	Ratio CC_{50}/IC_{50}
E-D5	MMV688991	> 20	2.7 ± 0.3	> 7.5
A-H2	MMV1634491	37.2 ± 6.5	4.0 ± 0.5	9.2
C-C5	MMV1578555	> 20	3.3 ± 0.3	> 6.2
A-D8	MMV1582497	> 20	5.2 ± 0.4	> 3.9
D-A4	MMV394033	1.4 ± 0.6	8.4 ± 1.7	0.2

Table S4. *In silico* analysis of hit compounds against NTS, selected by impedance measurements. All physicochemical properties were calculated using algorithms available in the RDKit software. The molecule lipophilicity, expressed as the logarithm of the octanol/water partition coefficient (logP), was predicted using an RDKit implementation of the Ghose-Crippen method.[3] The number of violations of Lipinski's "rule of 5" serves as an indicator of oral bioavailability.[4] Lipinski's rule of five is a rule of thumb to determine if a chemical compound with a certain pharmacological or biological activity has chemical and physical properties that would make it a likely orally active drug in humans.[4]

Drug code	MMV ID	ChEMBL ID	Name	Drug type	Molecular weight (g/mol)	H-bond acceptors	H-bond donors	AlogP	Lipinski's violations
E-D5	MMV688991	CHEMBL1401	Nitazoxanide	Antivirals	307.29	7	1	2.23	0
A-H2	MMV1634491	CHEMBL4576188	(Z)-1-(4-chlorophenyl)-3-(2,4-dichlorophenyl)-2-imidazol-1-ylprop-2-en-1-one	Antifungals	377.75	2	0	5.72	1
C-C5	MMV1578555	CHEMBL1504283	4-chloro-N-(4-fluorophenyl)-6-oxo-1-phenylpyridazine-3-carboxamide	Antibacterials	343.75	4	1	3.28	0
A-D8	MMV1582497	CHEMBL3394250	4-methylsulfinyl-2-oxo-6-[3-[(4-propan-2-ylphenyl) methoxy]phenyl]-1H-pyridine-3-carbonitrile	Antibacterials	406.51	4	1	4.35	0
D-A4	MMV394033	CHEMBL1185172	1-(2,4-dichlorophenoxy)-3-[2-imino-3-(2-piperidin-1-ylethyl)benzimidazol-1-yl]propan-2-ol	Antivirals	463.41	6	2	4.15	0

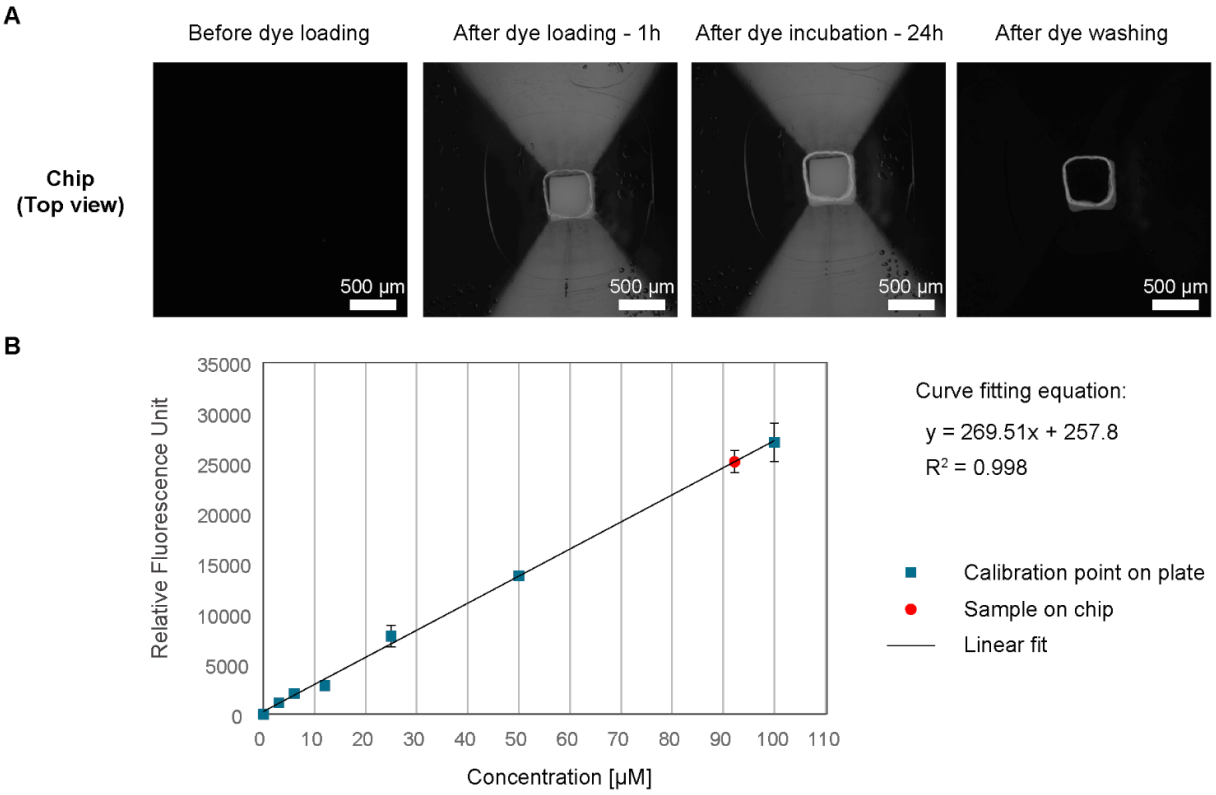

Figure S9. Characterization of polystyrene (PS) absorption of small hydrophobic molecules. **A** Rhodamine B uptake of the PS chip (100 µM in DI water) was evaluated during 24 hours. The fluorescence image series (top view) until 1 day of dye incubation and washing demonstrates that rhodamine B did not diffuse into PS, and a negligible amount of dye remained at the square edges of the laser-cut adhesive tape, located underneath the chip. **B** The graph shows the fluorescence intensity measurements of seven reference concentrations (1.5, 3, 6, 12, 25, 50, and 100 µM) of rhodamine B loaded in a 96 well-plate and the 100-µM condition incubated during 24 h on-chip. The points represent the mean relative fluorescence of four replicates, and the error bars indicate the corresponding standard deviations. A linear fitting curve, using the seven calibration values (blue squares), was superimposed to the points for concentration estimation. The 100-µM sample, after 1-day incubation on-chip, yielded fluorescence intensity values corresponding to a concentration of 92.22 ± 4.15 µM, which did only slightly differ from the 100 µM well-plate reference value.

3.9.2 Supplementary references

[1] J. Strovel, S. Sittampalam, N. P. Coussens, M. Hughes, J. Inglese, A. Kurtz, A. Andalibi, L. Patton, C. Austin, M. Baltezor, M. Beckloff, M. Weingarten, S. Weir, *Assay Guidance Manual*, National Institutes Of Health, **2004**.

[2] J. Reader, M. E. van der Watt, D. Taylor, C. Le Manach, N. Mittal, S. Ottilie, A. Theron, P. Moyo, E. Erlank, L. Nardini, N. Venter, S. Lauterbach, B. Bezuidenhout, A. Horatscheck, A. van Heerden, N. J. Spillman, A. N. Cowell, J. Connacher, D. Opperman, L. M. Orchard, M. Llinás, E. S. Istvan, D. E. Goldberg, G. A. Boyle, D. Calvo, D. Mancama, T. L. Coetzer, E. A. Winzeler, J. Duffy, L. L. Koekemoer, G. Basarab, K. Chibale, L. M. Birkholtz, *Nat. Commun.* **2021**, *12*, DOI 10.1038/s41467-020-20629-8.

[3] A. K. Ghose, G. M. Crippen, *J. Chem. Inf. Comput. Sci.* **1987**, *27*, 21.

[4] C. A. Lipinski, F. Lombardo, B. W. Dominy, P. J. Feeney, *Adv. Drug Deliv. Rev.* **2012**, *64*, 4.

4. CONCLUSION AND OUTLOOK

4.1 Conclusion

The integration of electrical impedance spectroscopy in the presented miniaturized test systems enables to record, in real-time, the activity of *S.mansoni* larvae exposed to potential active drugs. This thesis includes the design and development of automated and parallelized impedance-based platforms for (i) continuous long-term monitoring of parasite viability and (ii) for screening large antischistosomal drug libraries.

The second chapter of the thesis presented the implementation and characterization of a platform for long-term culturing and impedance detection of a larval-stage worm of genus *Schistosoma*. The platform relied on an electrical readout that provided an unbiased and automated estimation of parasite viability and continuous detection of parasite motility before and after drug exposure to obtain information on drug kinetics. The testing chip consisted of a PDMS structure featuring eight microwells with an inverted-pyramid shape, which were aligned to eight pairs of platinum electrodes with a 150 µm electrode-to-electrode distance. The spacing between electrodes was similar to the NTS dimensions and ensured that a large portion of medium volume between the electrodes was displaced upon NTS movements. To prevent drug absorption by PDMS during long-term compound incubation, the chip surface was coated with a parylene-C polymer. The micro-structured well design enabled a 10-fold reduction in drug and sample consumption, as only ~15 NTS per well were required to evaluate motility. In addition, the developed system adhered to standard microtiter-plate formats for compatibility with lab automation tools, which is a key requirement to achieve high throughput. The platform featured 32 independent units, which allowed for simultaneous characterization of parasite responses to multiple drug conditions during more than 48 h. To validate the platform, the real-time dose-dependent NTS responses to four antischistosomal compounds were measured, namely oxethazaine, praziquantel, mefloquine and methiothepine. Continuous monitoring of the parasite larvae via impedance-based detection enabled to reveal transient behavioral phenotypes of the schistosomula, which were different depending on the test compounds and their dosage. Furthermore, the continuous analysis also allowed to extract temporal characteristics of the dose-response curves, which provided additional information for the identification of antischistosomal drugs with high activity and fast kinetics of action. The dose-response results, which were achieved using the impedance-based detection, were in good agreement with those obtained from standard visual scoring of *S. mansoni* larvae. This

agreement demonstrates that the impedance-based approach constitutes a reliable alternative method to identify new antischistosomal candidates.

In the third chapter of the thesis, a new impedance-based plastic platform for higher-throughput quantitative measurements of NTS viability and its application for analyzing large compound collections is described. The chip microwell design, which had been previously realized in PDMS, was transferred to a standard laboratory plastic material, polystyrene (PS), to avoid compound ad/absorption in PDMS. The PS chips were fabricated using injection molding, which facilitated high-volume production and low costs per chip. Each chip included a top PS layer containing 8 analysis units, which was bonded via double-sided adhesive tape to a PET foil, patterned with 8 pairs of co-planar platinum electrodes. To further increase the throughput of the impedance-based measurements, the new system enabled to simultaneously record from up to 16 chips in parallel, which corresponded to 128 conditions in a single instrument run. The implemented device was then used to continuously monitor the activity of 57 compounds of the Pandemic Response Box library on NTS for more than 72 hours. From the initial impedance-based screening analysis at 10 µM, five compounds were identified to efficiently inhibit parasite viability after 3 days of exposure. The temporal characteristics of the dose-dependent responses of these most active drugs against NTS were then analyzed during 72 hours of continuous impedance-based measurement to obtain more insights into the drug kinetics in order to select the most promising compounds. The continuous evaluation of drug efficacy on *S. mansoni* larvae enabled to identify fast-acting and potent compounds, which would have been less efficient using the standard end-point analysis, as pharmacodynamics could not have been assessed. Moreover, the real-time recording of dose-response relations proved beneficial in comparison to other *in vitro* tests for the selection of active compounds for follow-up investigations. In our analysis, the high *in vitro* potency and low cytotoxicity of the four hits confirmed their suitability for additional preclinical testing on adult-stage parasites. Finally, the overall study showed the reliability of the new system as a tool for high-throughput antischistosomal drug screening application and the benefits of real-time impedance-based monitoring for the identification of novel candidate treatments against schistosomiasis.

In summary, in this thesis, I have shown the performance of two highly-parallelized platforms, which were specifically designed to obtain deeper insights into the drug-induced viability of NTS and could be operated with minimal experimental efforts and complexity. The implemented platforms were fully characterized and validated before they were adopted for addressing the needs in antischistosomal drug screening. Furthermore, the modular and flexible

nature of the platforms renders the presented approach widely applicable to other *in vitro* drug testing applications using different helminths.

4.2 Outlook

The presented EIS-based platforms offer a straightforward method for increasing the throughput and the objectivity of drug screening on NTS, which could boost the use of this screening technology in laboratories working on antischistosomal discovery. The developed chip design is suitable for high-volume production by means of injection-molding and is potentially reusable after washing, which renders this solution low-cost and easy to adopt in various research settings, including low-resource labs, a common scenario for neglected diseases. The real-time evaluation of NTS viability, facilitated by the implemented systems, can expedite the identification of fast-acting antischistosomal compounds.

Furthermore, the microwell chip can be readily adapted for viability studies of other relevant motile schistosome stages, such as juvenile and adult parasites, by simple modification of the sensing-area design, which would improve the selection of antischistosomal hit candidates before *in vivo* testing. The application of the developed chip could be also extended to other helminthic species, including non-spontaneously motile nematodes, such as *H. polygyrus*, a rodent worm widely used as parasitic infection model, after the integration of a reliable stimulation method. Recently, it has been shown that functional movements of the common nematode *C. elegans* can be stimulated using fluorescent light or electrical stimuli without harming the parasites.[1–3] Impedance analysis, as implemented for the NTS, could therefore be used to monitor the worm viability in an automated setting. This approach could be further adopted for studying non-spontaneous motile parasites like hookworm nematodes, which are currently stimulated by hot water for the evaluation of transient motility and viability during end-point *in vitro* drug testing.[4] Parameters that could be used to trigger the movement of *H. polygyrus* larvae, such as AC voltage-signal frequency, voltage amplitude, monochromatic light intensity and light exposure time were assessed in the current microwell chip design and yielded promising preliminary results (Figure 1). Furthermore, implementation of microelectrodes using indium-tin-oxide (ITO), which is a transparent, biocompatible and conductive material, may offer a viable solution for efficiently stimulating the parasites by light and/or electric sources (depending on the efficiency) and for continuously assessing via electric measurement the viability of non-motile nematodes upon drug exposure.[5] A device featuring a combination of reliable stimulation and motion-analysis techniques would help to obtain deeper insights in

the antagonist/agonist actions of compounds on nematode muscular receptors and would greatly contribute to improving anthelmintic drug screening.

Figure 1. Bright-field image of *H. polygyrus* larvae loaded on the PS chip for electrical- and light-based stimulation/analysis. The pair of platinum electrodes at the bottom of the microwell (black horizontal bars) is clearly visible in the image.

A current limitation of the standard antischistosomal screening procedure includes the constant drug exposure of the parasites during the entire *in vitro* assay, which does not represent realistic *in vivo* compound dynamics. Since scoring is regularly performed during exposure at a fixed concentration, any observed decrease in worm viability may not be permanent once the drug will be removed from the system, similar to *in vivo* conditions under which drugs are metabolized and excreted. Therefore, a more exhaustive and informative study may include the evaluation of parasite viability upon removal of the drug to identify permanent effects.[6] A drug wash-out assay early in the screening cascade would be advantageous for better *in vitro* selection prior to *in vivo* testing, which would reduce the use of laboratory animals for drug discovery.[7] Nevertheless, a manual wash-out procedure is tedious to perform and requires more experimental time, in terms of pipetting and scoring steps. Thus, a novel candidate chip for controlled wash-out assays should be developed that provides a sufficient throughput in the measurements, features reduced complexity of the assay and physiologically relevant concentration profiles, and improves the selection of hit compounds. A first tubing-free microfluidic chip for antischistosomal drug wash-out assays, which overcomes the limitations of manual procedures and drastically reduces operator efforts, has been recently prototyped (Figure 2). The time-scale for drug removal was determined through a statistical analysis of pharmacokinetic data from a library of potential candidates. The platform design, which featured two cylindrical reservoirs connected by a straight microfluidic channel, was optimized with the support of Comsol simulations. Rapid prototyping techniques were adopted for chip fabrication using thermoplastic polymers, such as PMMA for realizing medium reservoirs, and Flexdym^{TM} (Eden Microfluidics, Paris, France) for the microchannels. The chip was validated

in terms of flow profiles and a viability study was carried out to assess the condition of *S. mansoni* larvae on chip. Electrodes were not yet integrated and structures for spatial confinement of NTS for the continuous impedance-based viability evaluation of parasite responses during drug removal were not yet implemented.

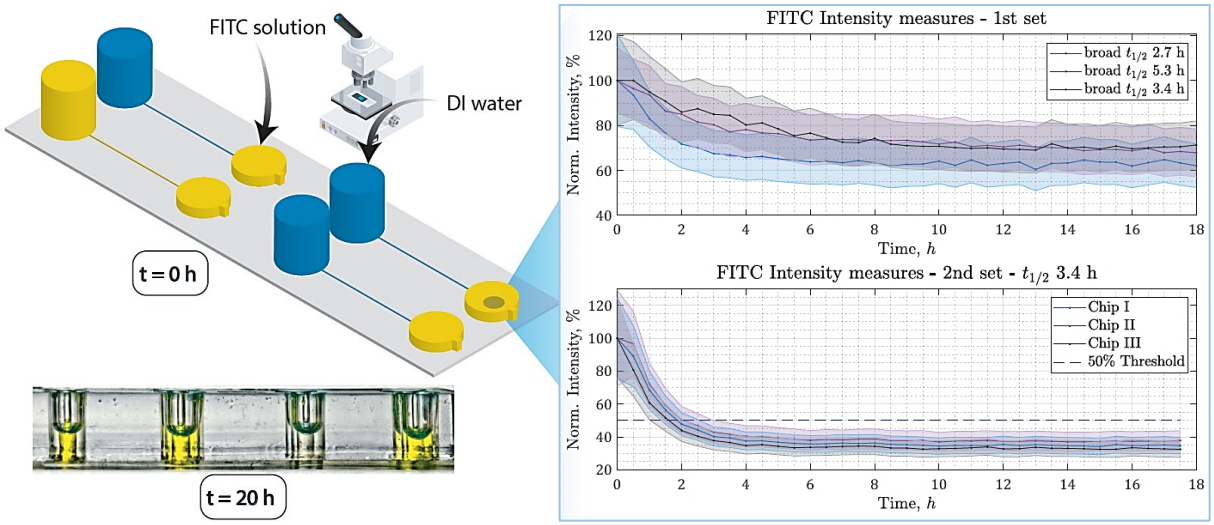

Figure 2. Schematic of the developed tubing-free mixing chip for concentration measurements with FITC-based water solutions; mean fluorescence intensity profiles over 18 hours. Dissolved FITC (0.1 mg/mL) was excited at 483 ± 25 nm, and the emission was observed at 524 ± 28 nm. The imaged region was a 443 x 443 μm^2 section at the center of the reservoir in each unit. Fluorescence images were acquired every 30 min with an exposure time of 100 ms.

Finally, several studies have shown that patients suffering from schistosomiasis have an increased risk of hepatocellular carcinoma, bladder cancer and cardiopulmonary disorders.[8,9] Therefore, a combination of multiple organotypic tissue models, such as liver and myocardial microtissues, could be used in co-culture with NTS to investigate potential cytotoxicity or liver-mediated drug (prodrug) biotransformation, which could ultimately affect drug efficacy on the parasite larvae.[10] The results of our collaborators at the Swiss Tropical Public Health Institute showed that liver spheroids can recapitulate liver-specific effects *in vitro* and that differences in IC_{50} values between standard *in vitro* testing and co-incubation with, e.g., liver microtissues could be observed.[11] Most currently applied parasite evaluation methods, such as the standard visual inspection, still limit the throughput, as they are laborious, subjective and slow. Moreover, the use of standard well-plate formats is not suitable for testing of multi-tissue arrangements. Hence, a microfluidic impedance-based system, which allows to electrically monitor the effects of the parent compounds and their metabolites, e.g., on cardiac beating and hepatic functions in parallel to NTS viability measurements and within the same microenvironment, could be implemented. For this application, the presented microwell chip could be easily adapted by fluidically interconnecting multiple units using laser-cut

microchannels realized on a double-sided adhesive tape at the bottom (Figure 3). Each well will be specifically designed to host a microtissue or NTS and the embedded coplanar electrodes will allow for evaluating each sample condition through automated and continuous EIS recordings. Such an integrated multi-tissue microsystem will simultaneously provide information on compound efficacy and toxicity in real-time and help to improve the selection of lead candidates for *in vivo* testing.

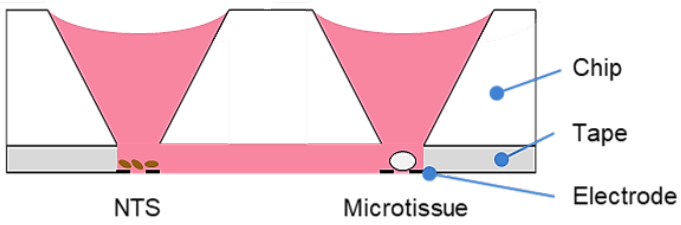

Figure 3. Schematic side view of the "infected body-on-a-chip" platform for drug efficacy tests on NTS and for toxicity and metabolic assays with different microtissues. NTS and spheroids will be cultured on top of the electrodes and the characteristic impedance variations will be measured in real-time during the drug experiment.

4.3 References

[1] M. D. Mathew, N. D. Mathew, P. R. Ebert, PLoS One **2012**, 7, 3.

[2] M. Hayasaki, J. Vet. Med. Sci. 2020, 82, 237.

[3] J. Tong, P. Rezai, S. Salam, P. R. Selvaganapathy, B. P. Gupta, J. Vis. Exp. **2013**, DOI 10.3791/50226.

[4] J. Keiser, G. Panic, R. Adelfio, N. Cowan, M. Vargas, I. Scandale, Parasites and Vectors **2016**, 9, 1.

[5] D. M. Lewis, N. Mavrogiannis, Z. Gagnon, S. Gerecht, Biomicrofluidics **2018**, 12, 1.

[6] P. McCusker, M. Y. Mian, G. Li, M. D. Olp, V. V. N. P. B. Tiruveedhula, F. Rashid, L. K. Golani, R. S. Verma, B. C. Smith, J. M. Cook, J. D. Chan, PLoS Negl. Trop. Dis. **2019**, 13, 1.

[7] L. K. Sharma, P. M. Cupit, T. Goronga, T. R. Webb, C. Cunningham, Bioorganic Med. Chem. Lett. **2014**, 24, 2469.

[8] D. G. Colley, A. L. Bustinduy, W. E. Secor, C. H. King, *Lancet* **2014**, *383*, 2253.

[9] M. S. Tucker, L. B. Karunaratne, F. A. Lewis, T. C. Freitas, Y. san Liang, Schistosomiasis, **2013**.

[10] O. Frey, P. M. Misun, D. A. Fluri, J. G. Hengstler, A. Hierlemann, Nat. Commun. **2014**, 5, DOI 10.1038/ncomms5250.

[11] F. C. Lombardo, P. S. Ravaynia, M. M. Modena, A. Hierlemann, J. Keiser, ACS Infect. Dis. **2020**, DOI 10.1021/acsinfecdis.0c00614.